1-1-2013

# Development Of Peptide Inhibitors Targeting Clostridium Difficile Toxins A/b And Characterizing The Regulatory Role Of A Putative Negative Regulator Tcdc In Clostridium Difficile Toxin Gene Expression

Sanofar Jainul Abdeen
*Wayne State University,*

# DEVELOPMENT OF PEPTIDE INHIBITORS TARGETING *CLOSTRIDIUM DIFFICILE* TOXINS A/B AND CHARACTERIZING THE REGULATORY ROLE OF A PUTATIVE NEGATIVE REGULATOR TCDC IN *CLOSTRIDIUM DIFFICILE* TOXIN GENE EXPRESSION

**by**

**SANOFAR J ABDEEN**

**DISSERTATION**

**Submitted to the Graduate School**

**of Wayne State University,**

**Detroit, Michigan**

**in partial fulfillment of the requirements**

**for the degree of**

**DOCTOR OF PHILOSOPHY**

**2013**

**Major: CHEMISTRY (Biochemistry)**

**Approved by:**

_____

**Advisor** **Date**

_____

_____

_____

## DEDICATION

Dedicated to

My parents

Saliha Abdeen and Jainul Abdeen

And also to my husband, daughter and my sister

Nilshad Salim, Nuha Salim and Ruzniya Abdeen

## ACKNOWLEDGEMENTS

I thank God for providing me courage, strength and guidance throughout my life. First of all I would like to express my greatest gratitude to my advisor Prof. Andrew Feig for providing tremendous guidance, knowledge and support in making me a better scientist and as a person. I am also grateful to my other committee members, Prof. Louis Romano, Prof. Matthew Allen and Prof. Jeffrey Withey for helping to make this thesis the best that it could be. I would like to thank my lab mates Dr. Amy Kerman, Dr. Nilshad Salim, Dr. Stephanie Kern, Mattie, Rebecca, Dandan and Amit for providing a wonderful environment for me to work and learn. My sincere gratitude also goes to Prof. Mary T. Rodgers and Yuan-wei Nei with whom we collaborated with mass spectroscopy work. I thank all my Sri Lankan friends in Wayne State University for being there for us as a family throughout all five years. Finally, I would like to thank my husband Nilshad Salim for all his great support and encouragements throughout theses years and also my parents and sister for everything they have done to support me throughout my student career.

# TABLE OF CONTENTS

# LIST OF TABLES

# LIST OF FIGURES

# LIST OF ABBREVIATIONS

CDI: *Clostridium difficile* associated infections

CDAD: *Clostridium difficile* associated diseases

CROP: C-terminal repetitive oligopeptide region

CDT: Binary actin ADP-ribosyltransferase toxin

CO-IP: Co-immunoprecipitation

ESI: Electrospray ionization

FTICR: Fourier transform ion cyclotron resonance

$His_6$: Hexahistidine tag

$IC_{50}$: Half maximal inhibitory concentration

IPTG: Isopropyl β-D-1-thiogalactopyranoside

$IP_6$: myo-inositol hexaphosphate

GTD: Glucosyltranferase domain

GT: Glucosyltranferase

GH: Glucosylhydrolase

GFP: Green fluorescent protein

GTPase: Guanosine triphosphate hydrolase proteins

HPLC: High performance liquid chromatography

MALDI: Matrix-assisted laser desorption/ionization

MLD: Membrane localization domain

MD: Molecular simulation

$OD_{600}$: optical density at 600 nm

PaLoc: Pathogenicity Locus

PBS: Phosphate-buffered saline

RMSD: Root-mean-square deviation

RNAP: RNA polymerase

SDS-PAGE: Sodium dodecyl sulfate polyacrylamide gel electrophoresis

TcdA: *Clostridium difficile* Toxin A

TcdB: *Clostridium difficile* Toxin B

TcdA/B: Toxin A and Toxin B

TcdC: Toixn C

TcdR: Toxin R

TcdE: Toxin E

UTP-Glc: UDP-glucose

UDP: Uridine diphosphate

# CHAPTER 1

## Managing *Clostridum difficile* associated diseases: Current and Novel therapeutic perspectives

### 1.1 Etiology of *C. difficile* infection

*Clostridium difficile* (*C. difficile*) is an obligate anaerobic, gram-positive, spore forming opportunistic pathogen and the main causative agent of toxin mediated antibiotic associated diarrhea (Figure 1.1A). The disease severity ranges from asymptomatic colonization to life threatening colonic inflammatory lesion, formation of pseudomembranes and can cause death in more severe immunosuppressed patients (Figure 1.1B) (1). The disease spreads mainly through spores. The spores are highly resistant to high temperatures, desiccation and disinfectants and remains viable for months outside of a host (2).

The main route of infection occurs via fecal-oral transmission by ingestion of spores or vegetative cells. However, the subsequent colonization and disease progression entirely depends on the host immune response causing extensive tissue damage as the body tries to ward off the infection (3). Although the stomach acidity reduces viability of the vegetative cell up to ~ 98% (4), highly resistance spores tend to survive in the acidic stomach environments and colonize in the intestinal area. Patients receiving acid-suppressive agents would be more susceptible to vegetative cells that mediate *C. difficile* colonization (5). Spore germination in the intestine is initiated by small molecules known as germinants (e.g. bile salts and glycine etc.) (6). Interestingly, asymptomatic colonization has been reported in ~4% of the adult population and 25% in infants (3,7). Therefore a relationship between antibiotic mediated alteration of normal intestinal microbiota, colonization and subsequent toxin production is proposed that occurs through a complex network of events (6). Accordingly, recent studies have shown broad-spectrum antibiotics impact on the progression of *C. difficile* associated diseases in two main

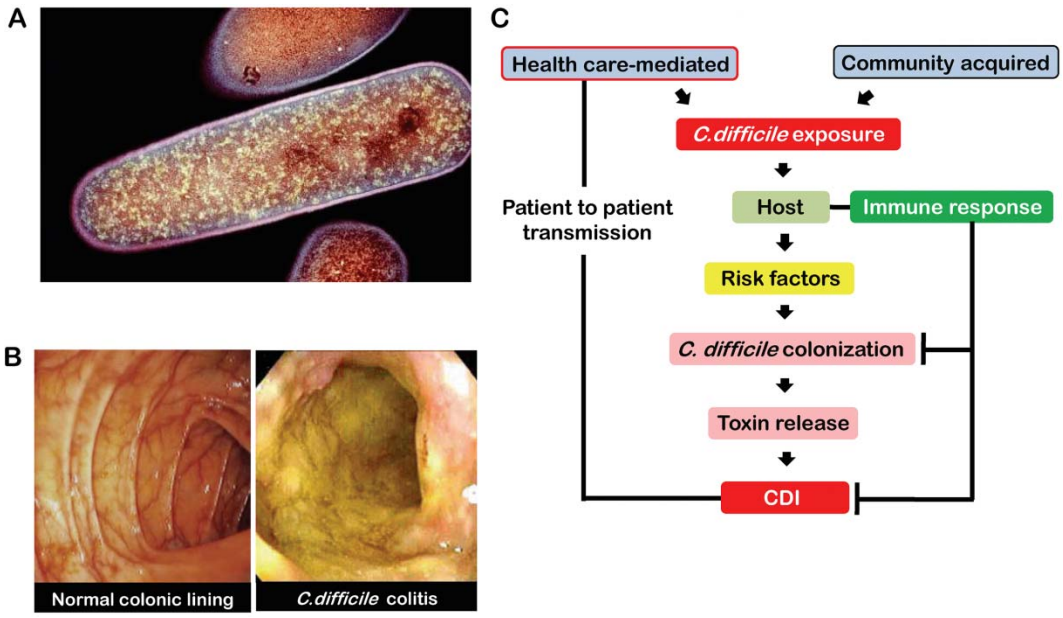


**Figure 1.1 Pathogenesis of *C. difficile* infections.** (A) Colored transmission electron micrograph (TEM) of *C. difficile*. Magnification: 35,000. Photo credit: Dr. Kari Lounatmaa / Science Source (March 2012, image number SL9520 sciencesourcenews.blogspot.com). (B) Comparison of endoscopic views of healthy colon vs. pseudomembranous colitis; characterized by scattered yellow plaques due to destroyed intestinal cells and inflammations. (Photo credit: Three Riverside Endoscopy center. PA, USA, accessed on www.gi.health.com). (C) Pathway of infection. Health care settings remain major reservoirs for *C. difficile* spores and vegetative cells. Upon exposure, subsequent colonization and disease progression depends on combination of multiple risk factors. But antibiotics-mediated destruction of colonic microbiota acts as a major risk factor. However asymptomatic colonization vs. disease progression is mainly determine by the host innate and adoptive immunity.

perspectives by disturbing the integrity of colonic microbiota as well as inducing expression of putative colonization factors and toxin production (8).

### 1.2 Pathogenesis of *C. difficile* infections

Main risk factors associated with *C. difficile* infections include broad spectrum antibiotic usage (cephalosporins, fluroquinolones and clindamycin) and a recent hospitalization as these-events provide opportunities for contact with bacterial spores and compromise protective microbiota that compete with *C. difficile* for nutrients in the GI tract (9,10). Other factors that affect clinical onset of *C. difficile* infections include: age ( >65 have ~10-fold greater susceptibility compared to a younger host) (11), recent gastrointestinal surgery (12) and individuals with compromised immune systems (13). However, recent changes in the epidemiology of *C. difficile* infections have shown an increased potential for additional risk factors for community acquisition of the disease, via food-born contamination (retail meat products, vegetables etc) (Figure 1.1C) (14,15).

*C. difficile* colonization resistance is mediated by gut microbiota and the host immune response (16). The proposed mechanism involves competition for nutrients, the ability of normal flora to convert host metabolites to compounds inhibitory to *C. difficile*, secretion of antimicrobial peptides toxic to *C. difficile* and the host's immunity (16). However, the extent of contribution by host factors and the microbiome on colonization resistance is not fully understood. Colonization, secretion of virulence factors and subsequent biofilm formation is initiated when the colonization barrier is distressed by combination of both primary and other risk factors.

Key disease symptoms are mediated by the activity of primary virulence factors, the two large cytotoxins Toxin A (TcdA) and Toxin B (TcdB). Both TcdA and TcdB bind to the apical

side of intestinal epithelial cells are taken up by host cells through endocytosis but the N-terminal region escapes the endosome during acidification (Figure 1.2) through an autocatalytic processing event mediated by its own internal cysteine protease activity (17); cleaving parent TcdA/B between amino acid residues (543/544)/(544/545) correspondingly and releasing the catalytic domain to the cytosol where it acts as a glucosyltransferase. Irreversible glucosylation the RhoA family of small GTPases (18) alters intracellular signaling, integrity of the cytoskeleton and thus results in the destruction of tight junctions and the epithelial cells barrier. Following the breach of intestinal epithelial cells, toxins induce the resident mucosal immune process including intestinal epithelial cells, mast cells and macrophages to release of proinflammatory cytokines ultimately resulting edema, influx of neutrophils, increased mucosal permeability, fluid secretion in to intestinal lumen and diarrhea (19,20). The acute severe inflammatory responses are the main cause of intestinal injury followed by pseudomembranous colitis. However, an exact mechanism by which both toxins trigger the immune system is yet to be determined (2,3,19,21).

### 1.3 Epidemiology of *C. difficile* infections

The epidemiology of *C. difficile* associated infections (CDI) has drastically changed over the past decade. This is associated with two main changes. The first was an increase in the incidence of *C. difficile* associated diseases (CDAD) (500,000/year in US), severity, mortality (14,000/year in US) (2,22), poor response to antibiotic treatments and high relapse rates; in North America there has been an approximately five-fold increase in the whole population (23). Similarly, higher frequencies of CDI have been observed in Canada, European countries (UK, Netherlands, Belgium, and France etc), New Zealand and Australia (24). In addition several incidences have identified in Asian and Middle Eastern countries which were not previously

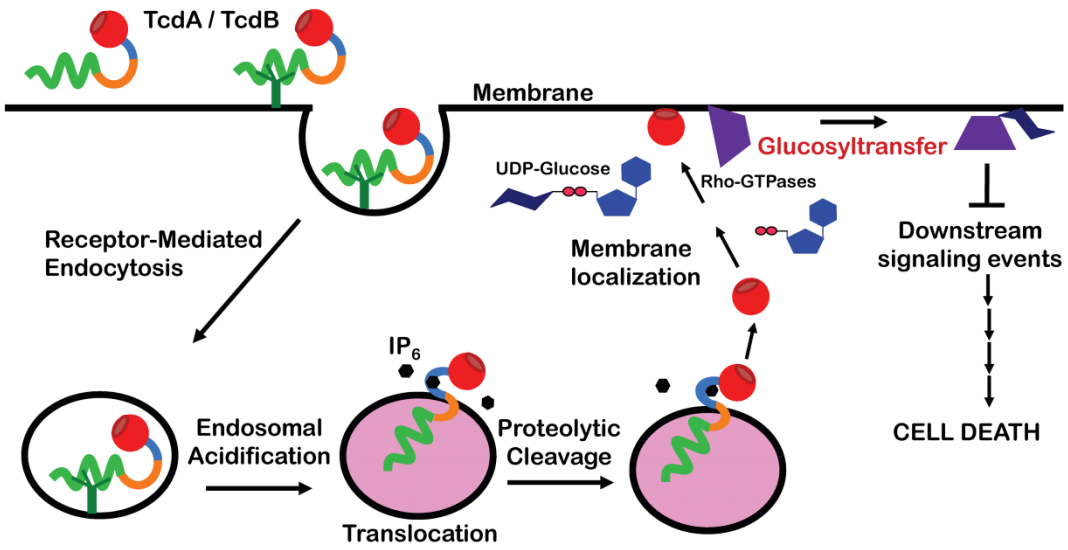


**Figure 1.2 Etiology of *C. difficile* infections.** (A) Etiology of TcdA/TcdB, The CROP region binds to receptors and get internalize via receptor-mediated endocytosis. Endosomal acidification triggers a conformational change and leads to membrane insertion. Binding of cytosolic myo-inositol hexaphosphate ($IP_6$) activates the auto processing activity of cystine protease domain and releases the enzymatic domain, where it catalyses glucosylation of Rho family GTPases and thereby resulting in cell death [Figure modified from (25)].

reported (26-30). Therefore *C. difficile* infection is becoming increasing burden to health care systems (e.g. $ 3 billion /year in extra health cost in US). The epidemic out-breaks and disease severity have been mainly associated with immergence of a fluoroquinolone resistant hypervirulent strain called ribotype 027 or NAP1 (24,31,32). In an *in vitro* study, the NAP1/027 strain has been reported to produce 16-fold higher concentrations of TcdA, 23-fold higher concentrations of TcdB than other non-toxinotype strains (33). The extreme virulence, high relapse rate and epidemic outbreaks of the NAP1/027 strain have been proposed due to combination of increased TcdA/B production, secretion of binary toxin, increased sporulation rates and mutations in a toxin negative regulatory protein TcdC etc. The second alarming change is associated with the increasing number of community-acquired infections without previous direct contact with a hospital setting as well as occurrence of CDI in populations that were previously considered to be low risk (34,35), such as infants, young children and pregnant women. Proposed community resources for CDI include soil, water, animals used for food (Calves, Piglets, and Chicken etc), retail meat and vegetables (potatoes, mushroom, tomatoes, cucumber and salad etc) (14). In addition to the ribotype 027/NAP1 strain another potentially important high-toxin producing strain found in community-acquired disease is ribotype 078 (36). Although the contaminated food animal and vegetables are the major public concern, the original source of *C. difficile* is still under debate in the field. Therefore to better control the spread of CDI and eliminate the overwhelming cost in health care systems; improved guidelines for diagnosis, efficient health care hygienic managements and development in wide range of new effective therapeutic options are crucial in the near future.

### 1.4 Pathogenicity Locus (PaLoc) - mediated *tox* gene regulation

Toxins TcdA/B are encoded on the same 19.6 kb chromosomal pathogenicity locus (PaLoc) together with three other proteins TcdR, TcdE and TcdC, (Figure1.3) (37) involved in toxin regulation, production and release into the extracellular environment. *tcdR* lies upstream to the major virulence factor encoded for an alternative sigma factor for RNA polymerase. Proteins homologous to TcdR have been identified in other gram-positive pathogenic bacteria such as *Clostridium tetani* (TetR), *Clostridium perfringens* (UviA) and *Clostridium botulinum* (BotR) (38). In both *in vivo* and *in vitro* studies TcdR have shown to activate its own promoter as well as gene specific activation of *toxin* gene promoters (38,39).

The *tcdC* gene is oriented in the opposite direction relative to the rest of the PaLoc genes and encodes a negative regulatory protein lacking the common helix-loop-helix DNA binding motif. It is a membrane associated dimmeric protein with no helix-loop-helix motif for DNA binding. In contrast to other genes encoded within the PaLoc, *tcdC* expression is highly expressed during early exponential phase and is repressed when cells enter stationary phase (37). This inverse pattern of expression has initially led to the hypothesis that TcdC may act as a putative negative regulator during exponential phase. Although its negative regulatory role has been probed *in vivo* using reporter fusion studies the exact mechanism by which it perform the regulatory role is currently unknown.

TcdE shows homology with phage holin proteins (40). During the phage lytic cycle, bacterial cell wall degradation enzymes endolysin are released through the cell membrane by holin oligomerization and pore formation (41). Recently Revadi Govind et al., reported TcdE oligomers facilitates the release of *C. difficile* toxins to the extracellular environment, however

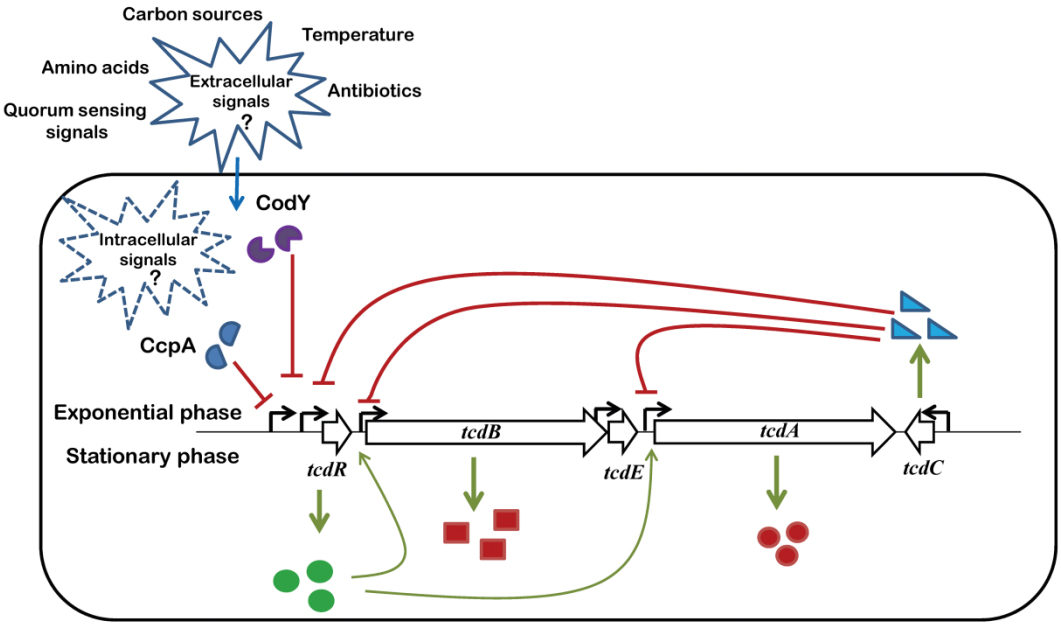


**Figure 1.3 Schematic representation of PaLoc gene regulation.** During the exponential phase, TcdC may inhibit *tox* genes transcription either by inhibiting *tcdR* transcription alone or it may target multiple promoter regions (*tcdR*, *tcdB* and *tcdA*) and maintains tightly regulated expression of virulence factors. In addition to that additional layer of inhibition also reported by global negative regulator CodY and catabolic control protein CcpA. However environmental cues governing the PaLoc gene expression are not known to date.

unlike the phage holing-mediated pathway, expression of TcdE does not cause destruction of the entire cell wall (42).

PaLoc genes are regulated in a highly complex manner. Under normal growth conditions, toxin synthesis increases as cells enter stationary phase and is stimulated by addition of certain amino acids, antibiotics, biotin and is inhibited by rapidly metabolizable carbon sources, etc (43-45). It has been reported that upstream genes of PaLoc (*tcdR, tcdB, tcdE, tcdA*) are transcribed from their own promoter, as well as by read through transcription from promoter *tcdR (37,46).* (38,47). During the transition from exponential phase to stationary phase, TcdR activates *tcdB, tcdE* and *tcdA* as well as its own promoter and therefore plays a crucial role in expression of virulence factors**.** Due to its positive feedback loop activity on its own promoter, very low level of TcdR accumulation inside the cell will amplify its regulatory role. Therefore very tight regulation of *tcdR* is essential during exponential phase of growth for the invasion of host by *C. difficile*. Based on this concept, several regulatory circuits have been identified to act upon TcdR expression such as TcdC, CodY and CcpA. CodY, the global negative regulator of gram positive bacteria, has been shown to mediate growth dependent toxin gene regulation by repressing toxin genes during the exponential phase via binding to promoter *tcdR* (43). The catabolic control protein CcpA, a regulatory protein mediates catabolic repression based on rapidly catabolizable carbon sugars was found to bind to both *tcdA* and *tcdB* promoter regions (45) as well as *tcdR* and *tcdC* regulatory regions. However, the complex regulatory network in terms of proteins and environmental cues governing the PaLoc gene expression is not fully clarified to date.

### 1.5 Virulence Factors

*C. difficile* associated diseases are mediated through a combination of virulence factors. The large clostridial glucosyltransferases, TcdA/B are the major disease causative agents and are

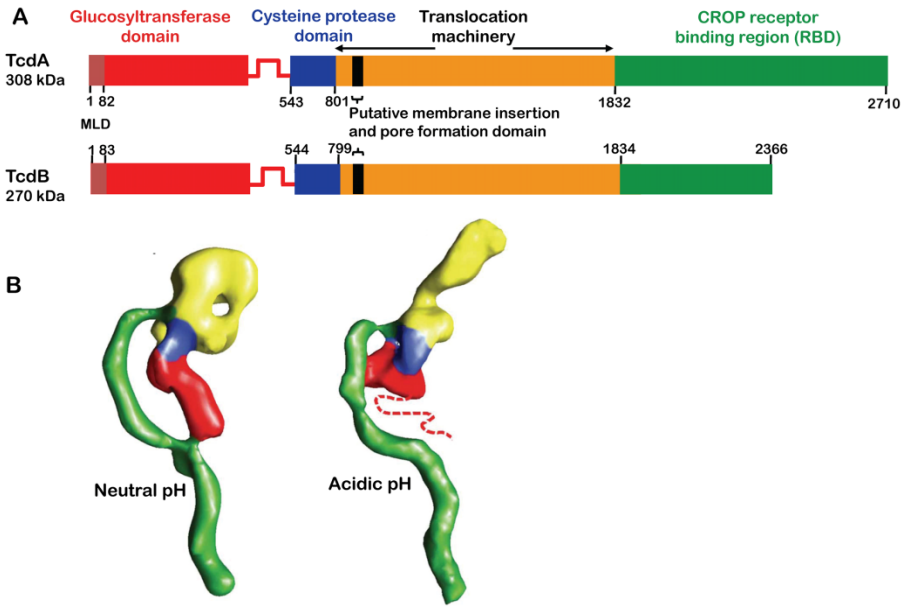


**Figure 1.4 Structural organization of *C. difficile* toxin A (TcdA) and B (TcdB).** (A) Both proteins consist of four functional domains. An enzymatic domain (GTD), an intrinsic cysteine protease domain (CPD), translocation machinery with central hydrophobic patch and the receptor binding region known as CROP (C-terminal repetitive oligopeptide). (B) TcdA holotoxin 3D model build based on a 25Å low resolution negative stain EM structure (48). In neutral pH it is known to exist as a bi-lobed structure with two protrusions. The shorter protrusion (Red) is proposed as GTD domain whereas the longer curve region (Green) as CROP. Upon exposure to lower pH "pincher-like" head region (Yellow: central translocation machinery) rearranges to form an elongated appendage for membrane insertion and delivery of GTD. Region colored in blue indicates the CPD.

discussed in detail below. The other characterized minor virulence factors include a binary actin ADP-ribosyltransferase toxin (CDT) (49,50), the surface layer protein (SLP) (51,52), two flagella proteins (53), a fibronectin binding protein (Fbp68) (54), cell wall adhesion Cwp66 and cell wall protease Cwp84 etc (55). These factors function in pathogenesis by promoting efficient adherence and colonization in hosts.

TcdA/B belong to the family of single-chain large clostridial toxins (LCT, > 250 kDa) that includes *Clostridium novyi* alpha toxin (TcnA), *Clostridium sordidellii* hemorrhagic toxin (TcsH) and lethal toxin (TcsL) (56). These toxins are grouped together on the basis of their primary structural organization and function (57). They are also known as A-B type toxins based on their mechanism of activity in hosts, where the B-moiety mediates host receptor recognition binding and internalization whereas the A-moiety contains an enzymatic domain harboring glycosyltransferase activity to covalently modify host Rho- and Ras-GTPases (56,57). Both TcdA (308 kDa) and TcdB (270 kDa) are encoded within the 19.6 kb pathogenicity locus, share 47% sequence identity, 63% similarity and found to have similar native structures according to a recent negative stain electron microscopy image (Figure 1.4) (20,48,58). The major regions of homology between TcdA and TcdB are found within the receptor binding and enzymatic domains of both toxins (59). Despite of their structural and functional similarity there have been controversies over the relative importance of each toxin towards disease progression.

A number of variations in activity of purified TcdA and TcdB have been observed in cells and animal models. In cultured cells both TcdA and TcdB have reported to induce cytotoxicity but TcdB has shown to be ~1000 times more potent than TcdA (20,60). TcdA was initially identified as an enterotoxin while TcdB failed to provide enterotoxin activity unless it is combined with TcdA, thereof known to be a cytotoxin (61). However with the isolation of TcdA$^-$

/TcdB$^+$ strain in nosocomial outbreak of ***Clostridium difficile***-associated diarrhea (62,63) and with most recent findings on isogenic mutants of *C. difficile* producing either TcdA or TcdB alone can cause fulminant disease in a hamster model (64,65), provided more evidence that TcdA/B are potent enterotoxins and both can play important roles in pathogenesis. Both toxins harbors a multidomain organization with an enzymatic domain, an intrinsic cysteine protease domain (CPD), translocation machinery with a central hydrophobic patch and the receptor binding region known as CROP (C-terminal repetitive oligopeptide) (Figure 1.4).

### 1.5.1 Receptor binding domain

Toxin internalization is initiated by the binding of the C-terminal CROP receptor binding region to intestinal epithelial cells. The CROP regions are composed of 19-24 short amino acid repeats (SR) and 31 amino acid long repeats (LR) (66). The CROP domain of TcdB (532 amino acids) is considerably shorter than that of TcdA (878 amino acids). The TcdA CROP domain composes of 32 SRs and 7 LRs (Figure 1.5A), whereas TcdB possesses 19 SRs and 4 LRs (66). Based on a model derived from a crystal structure of the short fragment of TcdA (127 amino acid fragment), toxins composed of antiparallel β-hairpins formed with SRs that are interrupted by the kinks introduced by LRs to form a flexible β-solenoid helix (Figure 1.5A) (67). The kinks in the β-solenoid structure of TcdA was initially shown to bind various glycans such as α-Gal-(1,3)-β-Gal-(1,4)-β-GlcNAc (PDB: 2G7C) (68), however the specific α-galactosyltransferases involved in the formation of α-galactosyl bond on such sugars are not found in humans (69). A glycoprotein sucrose-isomaltase in rabbit ileum was found to bind TcdA (70), followed by this a recent study employing co-immunoprecipitation and mass spectrometric methods identified a human sucrose-isomaltase colonocyte plasma membrane protein gp96, binds to TcdA (71). But the nature of the carbohydrate modification involved in the binding events is yet to be

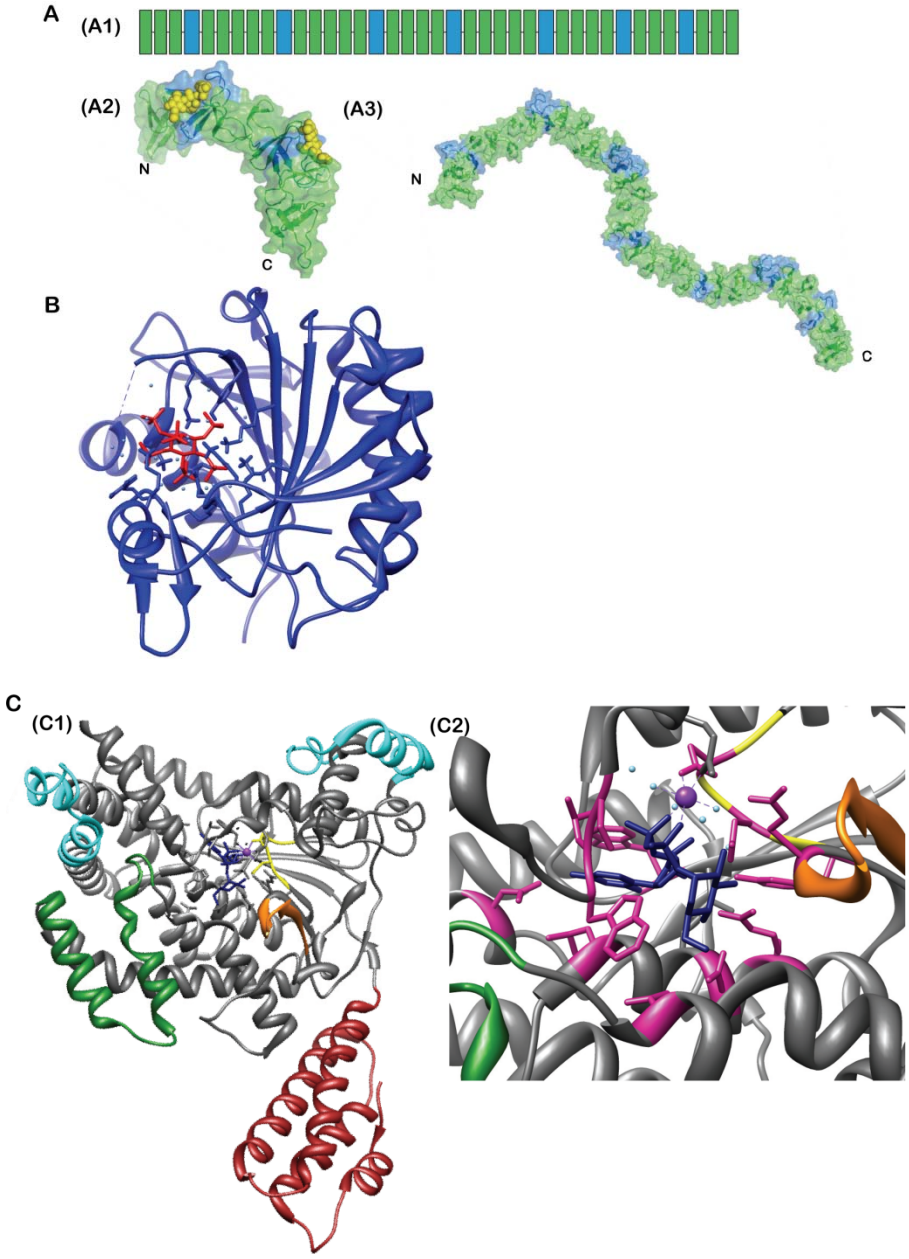

**Figure 1.5 Crystal structures-based in detail view of CROP, CPD and GT domains of TcdA.** (A) Structural organization of TcdA CROP region. (A1) CROP is made out of alternative arrangements of short amino acid repeats (SR) and 31 amino acid long repeats (LR). TcdA consists of 32 short repeats (green) and 7 long repeats (blue) [Adopted from (72)], (A2) crystal structure of a 127 fragment of C-terminal repetitive (PDB: 2G7C) peptide region, kinks regions were bound with liposaccharide α-Gal-(1,3)-β-Gal-(1,4)-β-GlcNAc, (A3) β-solenoid-like entire model of the CROP binding domain is build based on a crystal structure PDB: 2G7C.(B) $InsP_6$ (red) bound, CPD is shown (PDB: 3HO6). $InsP_6$ binds to a basic lysine-rich cleft separated from active site by 3-stranded-β-hairpin structures. (C) Crystal structures are shown for the UDP-glucose bound glucosyltransferase domain of TcdA (PDB: 3SRZ) [Modified based on (73)]. (C1) In detail structural analysis provides, well defined regional organization for substrate recognition, binding and catalysis. The membrane localization four helix bundles are shown in brown. Consists upper promontories (cyan), substrate recognition region (green), UDP-glucose binding (yellow) and catalysis moieties (orange), (C2) A close-up view of active site, amino acids highlighted in violet indicates, residues involved in $Mn^{2+}$ (purple), UDP-glucose (dark blue) binding and catalysis. Coordinating water molecules are shown in blue.

investigated. Although TcdB is known to be toxic for a wide range of cells, the receptor involved in TcdB-host cell interactions are not known to date.

Previously it was believed the receptor-mediated endocytosis was exclusively dependent on the CROP-binding region, however Olling et al., 2011 reported a truncated form of TcdA lacking the CROP region retained cytotoxicity but was 5 to 10-fold less potent than wild type TcdA (74). This finding was further confirmed by Genisyuereketal et al., 2011 (75), showing an additional binding activity is contributed by a ~350 amino acid segment preceding the C-terminal region (75). However due its lectin-like structural repeats, CROP region is considered a major immunogenic region of *C. difficile* toxins and plays important roles in the field of vaccine development (76-78).

**1.5.2 Central translocation machinery**

After binding to membrane receptors, toxins are endocytosed through the clathrin-mediated pathway (79). The membrane localization domain lays between the cysteine protease and receptor binding domain, spaning around ~1000 amino acids (66,80). It is known to play a number of roles in membrane insertion, pore formation and delivery (81-83). Although the other domains are structurally well characterized, the membrane translocation domain has to date not been characterized. Recent low resolution negative-stain electron microscopy data provide more evidence on the structural changes within the translocation domain associated with pH changes (Figure 1.4B) (48). Further deletion studies by Genisyuerek et al., revealed both toxins harbors a ~160 amino acid containing two hydrophobic transmembrane region (Figure 1.4A) flanking a negatively charged loop region and neutralization of above negatively charged region by endosomal acidity is prerequisites of membrane insertion and pore formation activity of the central translocation machinery (75).

### 1.5.3 Cysteine protease domain

Cysteine protease domain (CPD) lies in between the N-terminal glucosyltransferase domain and the central translocation machinery and is involved in the release of the N-terminal region into the cytosol by its auto-proteolysis. Both TcdA CPD and TcdB CPD exhibit 56% sequence similarity (84) (Figure 1.5B). Cysteine protease activity is mediated through a catalytic triad mechanism, involving cysteine histidine and aspartate residues. Eukaryotic intracellular metabolite inositol hexakisphosphate ($InsP_6$) and the reducing environment of the cytosol are required to activation an allosteric circuit and subsequent cleavage (85). According to recent crystal structures, it has been revealed that negatively charged $InsP_6$ binds to a basic, lysine-rich cleft separated from that active site by a 3-stranded-β-hairpin structure denoted as the β-flap (Figure 1.5B) (17,86,87). However systematic mutational and disulfide bond engineering studies further identified both regions contain an interconnected network of amino acid interactions that are involved in transmitting $InsP_6$-induced structural changes to the active site (86).

### 1.5.4 Glucosyltransferase domain (GT)

The autoproteolytic cleavage leads to the delivery of the N-glucosyltransferase bearing 543 amino acid region of TcdA/544 amino acid of TcdB into the cytosol (20). The catalytic domain uses cellular UDP-glucose as a co-substrate, irreversibly glucosylating the RhoA family of small GTPases (Figure 1.5C) (18), and induces subsequent apoptosis and epithelial cell destruction (88). According to the crystal structures of the N-terminal region of TcdA and TcdB, they share 74% structural homology and similarity have been preserved within catalytic core involved in UDP-glucose binding and glucose transfer, however GTPase-binding surfaces vary greatly (89). The above difference has been proposed to be associated with their substrate specificity. The enzymatic domain possesses several structural elements important for its

function (Figure 1.5C). It has a central catalytic core surrounded by three helical structures that includes an N-terminal four helix bundle later named as the membrane localization domain (MLD); identified by analyzing several GT-A family of glycosyltransferase protein toxins (90). It is known to localize the catalytic domain towards the membrane and thereby mediates the interaction with GDP-bound small Rho/Ras family GTP-ases. The two lateral helical structures are known as "upper promontories'' (73). A recent MD simulation study identified that the above helix regions undergo scissoring motion and proposed to function in substrate accommodation (73). The mobile loop region shown in yellow includes another typical feature of GT-A family glucosyltranferases, the DXD motif (Asp-X-Asp) (91). It coordinates with the catalytic $Mn^{2+}$ and thereby indirectly involves in precise positioning of UDP-glucose for catalysis (Figure 1.5C). The hairpin loop [Figure 1.5C (orange)] known as active site flap region was postulated to be involved in catalysis and substrate recognition (92). The green region has been reported to be involved in substrate recognition (92).

Substrate small Rho family GTP-ases are molecular switches that plays a crucial function in intracellular signal transduction pathways. Both TcdA and TcdB are reported to mono-glucosylate small Rho family GTP-ase RhoA, RhoB, RhoC, RhoG, RacI and CdC42 (20). A recent study identified TcdA also modifies Ras family GTPases Rap1A and Rap2A (89). Rho/Ras family GTP-ases are master regulators in actin cytoskeletal integrity (89), beside this they also play vital roles in a large variety of other cellular functions such as cell adhesion, cell migration, cell cycle progression, phagocytosis, modulation of epithelial and endothelial cell junctions, apoptosis etc (93). Small GTP-ases cycle between an inactive GDP-bound and an active GTP-bound state to regulate activity (93,94). Mono-glucosylation occurs at Thr-37 in RhoA and at Thr-35 in Rac1/CdC42 in an effector loop region and stabilizes Rho proteins in

GDP-bound inactive state (95,96). Glucosylation thus prevents Rho activation by guanine nucleotide exchange factors and its coupling to downstream effector proteins and cytosol-membrane cycling of Rho protein. Ultimately glucosylation leads to the complete shutdown of Rho-dependent signaling pathway and induces cell death via apoptosis (97). Due to its crucial role in epithelial cell destruction, the enzymatic domain has been considered as an attractive target towards the development of small molecule inhibitors, immunotherapeutics and vaccines.

**1.5.5 Binary toxins**

In addition to major protein toxins TcdA and TcdB, some *C. difficile* isolates (< 10%) produce a third toxin known as binary toxin (CDT) (98). It is characterized as the family of actin-ADP-ribosylating toxins produced by many pathogenic species such as *C. botulinum* (C2 toxin), *C. perfringens* (iota toxin) etc. CDT is positioned within a 6.2 kb CdtLoc locus separate from the PaLoc (99). CdtLoc encodes three genes, the two-component ADP ribosyltransferase encoded by the genes *cdtA* (enzymatic component) and *cdtB* (binding component) and cdtR encodes for a transcriptional activator (98). CDT is characterized as an AB type binary toxin made up of two independent components: 48 kDa actin-modifying ADP-ribosyltransferase (CDTa) and a 74 kDa transport component. Both components act synergistically to transport the enzymatic component into the cytosol of target cells (98,100). In the cytosol, the enzymatic region ADP-ribosylates G-actin at arginin-117 thereby prevents actin polymerization (101). However the role of CDT as a virulence factor is not clear so far. A more recent study showed that CDT induces the formation of microtubule-based protrusions leading to a dense meshwork at the cell surface (102). The meshwork increases the surface area for adherence of clostridia to the intestinal epithelium. Accordingly, Carsten Schwan et al., showed that CDT induces a ~5 fold increase in adherence of *C. difficile* under anaerobic conditions (100). In animal model studies, *C. difficile* $A^-B^-CDT^+$

strain caused fluid accumulation in rabbit ileal loops but no diarrhea or death in hamsters (103). The above experimental evidence on CDT shows that in the early phase of infection CTD-induced adherence of vegetative cells to epithelia may be more involved in enhancing colonization than direct cytotoxicity.

### 1.6 *C. difficile* associated diseases preventive and therapeutic view

In terms of CDI management the old saying "prevention is better than cure" could be more appropriate. There are three challenges associated with CDI management (a) control of disease transmission, (b) management of fulminant or severe complicated disease symptoms and (c) controlling of multiple recurrences. Preventing transmission of *C. difficile* solely relies on use of consistent standard precaution techniques by health care settings and on time accurate diagnosis of patients with CDAD. From the year of 2000 to the present, recurrence after the first episode have been reported to be ~33-45% (104). Up to 20-50% of recurrence is mediated through re-infection due to a new antibiotic resistance *C. difficile* strain or re-colonization due incomplete irradication of the resistant original strain (105,106). Therefore the most successful way to treat such patients is to taper antibiotic usage, minimize the activity of toxins to subdue the symptoms and replenish the normal gut flora to promote better competition with *C. difficile*. Furthermore there are no promising treatment strategies for severe and complicated CDI (107), where in most cases medical managements fails, patients are subjected to subtotal or total colectomy. However it is related with high risk of mortality. Thus newer agents and strategies are desperately needed for CDI.

If we look at the strategies used for combating *C. difficile* associated diseases, it can be divided into two main categories, involving infection control and treatments (Figure 1.6). Treatments can be directed towards the elimination of the microbe by means of classical

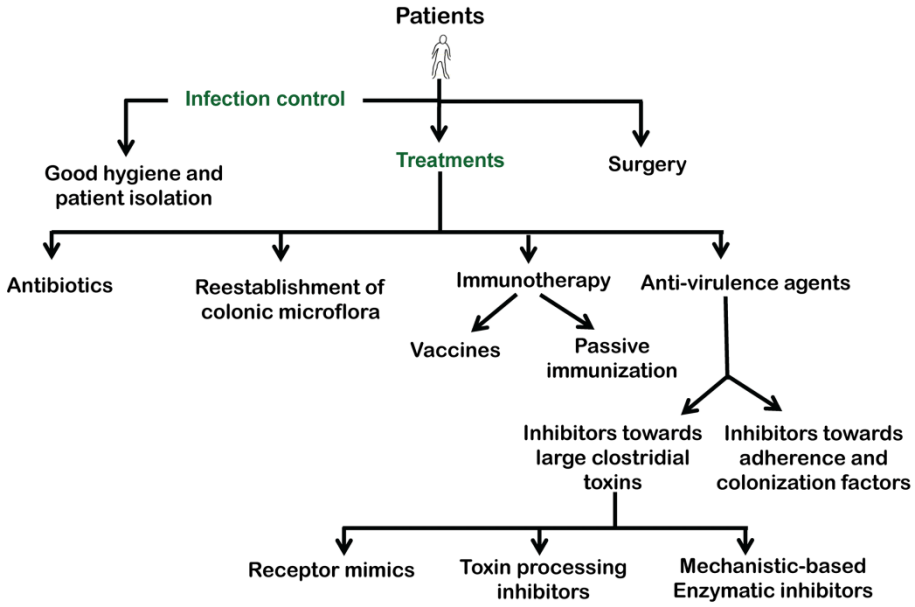


**Figure 1. 6 Overview of classical and novel approaches towards combating *C. difficile* associated diseases.**

antibiotics, establishing colonization barriers and reduce the disease progression and symptoms by hampering the major virulence factors.

**1.6.1 Preventive measures of CDI**

The main sources of *C. difficile* are colonized/infected individuals and contaminated environment. Therefore there are two types of control measures that have to be considered in health care settings; those including barrier methods and environmental hygiene. Barrier methods control healthcare workers-to-patient and patients-to-patients transmission, whereas environmental hygiene prevents the encounter of contaminated environment-to-individuals (108).

Barrier methods mainly rely on clinical isolation of patients with diarrhea to prevent transmission and consistent hygiene practices (hand washing, decontamination of surfaces, etc). Patient isolation and restrictions in patient transfer are the most important way to prevent environmental contamination with *C. difficile* spores. Prompt isolation of patients with confirmed CDI or suspected CDI in a separate room with appropriate sanitization facilities are essential in hospital environments, in addition, movement and transport of such patients should be restricted unless required due to severe health conditions (109). Health care workers are often the primary vectors of transmission (110), therefore hand hygiene and preventive cloths such as disposable gloves and disposable gowns have to be strictly maintained in handling such patients. Since the alcohol-based hand rubs and gels are not effective against removing *C. difficle* spores, traditional hand washing with antimicrobial soap and water is preferred (111).

Studies performed to correlate infection rates with hospital environment shows that, in hospital conditions with poor infection control practices; the rate of contamination is

proportional to the number of patients (112). Therefore environmental and equipment hygiene is critical. The major drawback associated with *C. difficile* spore eradication is the traditional detergents and ammonium-based agents that do not show any sporicidal activity and actually enhances sporulation of vegetative cells (113,114). Hypochlorite-based disinfectant (at least 5000 ppm) was shown to significantly reduce spores (115). Significant attention towards cleaning and decontamination should be maintained patients frequently touched surfaces such as toilet areas, bedrails, call bells, TV remote controls and linens etc. Further medical devices (e.g. thermometers) need to be decontaminated properly or where possible disposable items can be used. Combination of education on disease management among health care workers and expanded-infection control measures can be utilized to reduce the spread of *C. difficile* infections.

**1.6.2 Antibiotics**

Although many new therapeutic approaches for CDAD have been studied, to date antibiotic treatments still remains as standard treatments. The main goal of any antibiotic is clearance or prevention of infection within the context of the host. One of the most important risk factor associated with CDI is with the use of broad spectrum antibiotics such as clindamycine, cephalosporin, quinolones and fluoroquinolones, etc (116). As a first line of disease management, in younger patients with mild diarrhea; withdrawal of the predisposing antibiotic and the use of supportive care with hydration is effective enough for the recovery. However for the individuals with moderate-to-severe infections; along with the removal of primary antibiotics, specific antibiotic therapy is recommended (32).

The two antibiotics (Metronidazole and Vancomycin) have been in use against CDAD for more than 30 years. Metronidazole is generally prescribed as the first-line treatment for *C.*

*difficile* infection due its low cost. It disturbs the DNA structure, leading to the inhibition of DNA replication (117). Standard initial oral dose has been shown to successfully resolve symptoms in >90% patients within 10 days (32). Although MIC (minimum inhibitory concentration) of metronidazole was shown to differ between strains, it is highly active against many pathogenic strains of *C. difficile* (118,119). However, prolonged use of Metronidazole can lead to resistance and decreased susceptibility over time (120). Therefore Metronidazole has been found ineffective in recurrent infections (104).

Vancomycin is often considered as a second-line for treating moderate-to-severe CDI (121). It is a glycopetide known to have broad activity against the gram-positive bacterial cell wall synthesis (122). Because of its low systemic absorption, higher colonic concentrations can be achieved. Therefore vancomycin provides a better response rate compared to metronidazole (121). It is highly active against all pathogenic strains of *C. difficile* (123). However, its usage is limited due to its high cost and emergence of vancomycin-resistant enterococci and *Staphylococcus aureus* (121). But both vancomycin and metronidazole have been shown to suppress *Bacteroids spp* in the fecal flora, which are considered helpful as a colonization barrier (121). Although *C. difficile* is sensitive to both antibiotics, with the recent change in epidemiology they have been associated with treatment failures and ineffective in recurring infections. Fidaxomicin is a macrocyclic narrow-spectrum antibiotic approved by the FDA in 2011 for the treatment of CDI. It is minimally absorbed from the bowel into the bloodstream and reported to be with more active than vancomycin against *C. difficile* (124). Its minimal activity against normal gut flora and *Bacteroids spp* makes it as a promising candidate to treat recurrent CDI (125).

Even though antibiotics have been the preferred treatment strategy, long-term usage applies enormous evolutionary pressure and leads to the emergence of resistant strains. For *C. difficile* infections, the main is the alteration of colonic micro-flora. Although antibiotics provide some respite, it increases the risk of recurrence due to the disruption of the colonization barrier normal microbiota provides. In this case very narrower spectrum antibiotics with high potency would be more effective (126). Since the disease symptoms are mainly mediated due to the toxins, anti-virulence agents that targets the toxins in combination with antibiotics are crucial to obtain effective therapeutic outcomes in patients with severe diarrhea.

### 1.6.3 Reestablishment of colonic microflora

The development of diarrhea (AAD: antibiotic associated diarrhea) following antibiotic administration is common. In general the disease is mild and no specific pathogens are isolated. AAD is mainly due to the disruption of the colonic mucosal integrity and basal micro biota (127). However, upon C. *difficile* exposure, the antibiotic-mediated destruction of colonic microbiome becomes a major risk factor in CDI initiation. Therefore it is believed that reconstruction of colonic microbiota-mediated homeostasis would provide *C. difficile* colonization barrier (16). Two methods are employed to reestablish colonic microbiota including probiotics and fecal-source microbial repopulation. In addition to this, a new approach indicates that colonization with nontoxigeneic strains of *C. difficile* is effective in preventing toxigenic *C. difficile* colonization in hamsters (128). In future, recent developments in human microbiome projects will be tremendously helpful in-depth identity on gut normal flora, impact on antibiotics in such systems and will lead to develop carefully defined therapeutic approaches (116,129).

#### 1.6.3.1 Probiotics

Probotics are defined as live or live-attenuated microbes that are administered to the patient to repopulate gut microbiota in order to prevent and treat infectious diarrhea (130). A large variety of organisms have been studied including, *Saccharomyces boulardii*, *Lactobacillus acidophilus*, *Bifidobacterium bifidum*. However, most probiotics consist of single or mixed formulations of certain bacteria (130,131). Although many probiotic-mediated studies were conducted, a smaller number of studies have shown a modest therapeutic benefit from probiotics towards treatments of *C. difficile* diarrhea (132). Difficulties in interpreting these studies were mainly due to variability of the type of probiotics used and differences in specified indications (e.g usage in mild diarrhea vs. severe diarrhea / acute disease vs. recurrence) (133). However the draw backs in the development of standard probiotics are due to lack of standardized preparations (the exact composition of individual microbe is typically not known) and most probiotics are not evaluated or approved by the Food and Drug Administration (FDA) (134). Despite the disparate results in the field, probiotics remains a safe and reasonable way to provide an initial colonization barrier to patients under long-term antibiotic therapy and possibly a treatment for recurrence infections. Studies with carefully defined and widely available probiotic preps are underway to optimize the type of organism and usage in moderate-to-recurrence CDI.

#### 1.6.3.2 Fecal transplantation

The widespread interest in the field of "fecal source-based microbial repopulation" has its own contradictions due to poor patient acceptability and possible transmission of other infectious diseases (bacteraimia, fundaemia) (135). However with increased disease severity and recurrence of *C. diffile* associated diseases scientists have revisited this form of therapy as an option. In this case the donor fecal product is administered using nasouodenal, nasogastric and enema infusions via colonoscopy. Although many preliminary studies provide ~90% beneficial results after one

or two treatments (136,137), there are many issues associated with dosage, mechanism of collection, processing, selection of donor individuals etc. Leading to the lack of well-controled studies published in the field. However preliminary animal studies comparing this mode of treatment with standard antibiotics for recurrent CDI are ongoing.

### 1.6.4 Immunotherapy

The clinical outcome of *C. difficile* mediated diseases ranges from asymptomatic carriers to severe pseudomembranous colitis. Serum and colonic antibody responses to *C. difficile* virulence factors have been reported in ~60% of the general population (138,139). Therefore in most cases the clinical *C. difficile* disease presentation and recurrence have been believed to link with host factors rather than bacterial. Warny et al., reported serum levels of IgG antibody against toxin A and fecal levels of IgA antibody against toxin A were higher in patients with mild CDI compared to severe CDI (140). Followed by this another study further confirmed increased serum levels of IgG antibody against tcdA were found in asymptomatic carriage of *C. difficile* (141). Information gathered from *in vivo*, animals and clinical studies show that immune system-based toxin neutralization approaches are feasible to prevent and treat CDI. Since both toxins play crucial role in disease symptoms, antibodies to both TcdA and TcdB are required to provide therapeutically effective protection. There are two immune system-based approaches that have been in progress; active immunization/vaccine and passive intravenous immunoglobulin infusion therapy.

#### 1.6.4.1 Active immunization (Vaccines)

Active immunization can be used prophylactically against CDI symptoms but also used in recurrent infection along with other non-antibiotic approaches such as probiotics. Vaccines are mainly designed to target major virulence factors TcdA and TcdB (142). Non-toxic

immunogenic determinants are generated by two main approaches: (a) chemically inactivated purified TcdA/TcdB and (b) recombinant chimeric units with the combination of both TcdA and TcdB regions. Formalin-inactivated toxoids A and B (ACAM-CDIFF$^{TM}$- Sanofi Pasteur) where the toxins have been purified from *C. difficile* bacterial cultures was shown to be safe and immunogenic in healthy volunteers (142). Although it is still in Phase 2 clinical trails, it has been granted fast track designation by the FDA in 2010, for urgent or life-threatening medical need. The other two most promising vaccines which entered for Phase 1 clinical trials include: a fusion protein containing the receptor binding domains of *C. difficile* TcdA and TcdB (C-TAB.G5-Intercell) (78) and a chimeric vaccine (cTxAB) by switching the receptor binding domain of TcdB with that of TcdA (143). cTxAB has been shown to be effective in treating spore-induced disease relapse (143).

#### 1.6.4.2 Passive immunization

While there has been significant development in the field of vaccines over past few years, the protective effect obtained by passive immunization will be useful in treating immunocompromised patients with CDI. A variety of antibodies (e.g., IgY, IgG, IgA) targeting *C. difficile* toxins have been produced from immunized animals (144). Many studies have been reported that the administration of pooled human IgG containing anti-toxin antibodies improved the diseases severity of patients with severe CDI (145). In *C. difficile* infections, antibodies targeting toxins have been designed for oral and systemic administration. For systematic therapeutic usage, antibodies should be humanized or human origin to suppress potential immunogenicity. However this should not be a concern in the oral approach. In this case antibodies have to be further formulated to survive harsh gastrointestinal environments. Babcock et al., reported the first humanized monoclonal antibody in 2006 (146) and now fully human

monoclonal anti-TcdA (CD-1) and TcdB (CD-2) antibodies targeting the receptor binding region are in phase III clinical trials for the treatment of CDI ( Massachusetts Biologic Laboratories in partnership with Medarex, Inc) (147).

### 1.6.5 Anti-virulent strategies

Managing multiple recurrences and disease progression into more severe infections are the two most pressing challenges in treating *C. difficile* associated diseases. Although antibiotics are useful in clearing pathogenic bacteria during infections, their uses increases the risk of emergence of antibiotic resistant strains and high relapse rates that renders this line of treatments less effective in the *long run* in eliminating CDI. Alternative ways to combat *C. difficile infections* stems from the mechanistic insights where targeting specific virulence factors such as the "*toxins*" that plays a pivotal role in disease pathogenesis. This line of strategy serves a two-fold advantage where on one hand it provides a specific and direct response to disrupt the infection while on the other hand having no effect on normal flora that helps maintain the equilibrium of bacterial populations (148,149). Newer strategies utilize the mechanistic details of virulence factors in pathogenesis to develop effective anti-virulent agents. In terms of *C. difficile* toxin agents can be designed to inhibit uptake, processing and enzymatic activity essential for ultimate host cell destruction (Figure 1.6).

#### 1.6.5.1 Toxin-binding agents

Initiation of toxin internalization begins with the binding of toxin to appropriate receptors. Receptor mimics/toxin-binding agents have been a longstanding interest in the field (150,151). These compounds can be orally administered and readily excreted without any systemic absorption. The main advantages of using such agents are that they act in the lumen of the intestine, do not require cellular uptake and prophylactically higher concentrations can be

achieved to efficiently inhibit toxin activity (151). A variety of toxin-binding agents have been reported such as cholestyramine- an anionic exchange resin (151), Tolevamer - an anionic styrene-based polymer (152,153), Synsorb 90- inert silica-based resin coated with trisaccharide to enhance binding of receptor binding region (Synsorb Biotech; Calgary, Alberta, Canada) etc (154). However these compounds failed in clinical trials due to cross-reactivity with of standard antibiotics, poor tolerability and reduced availability due to aggregation issues (151). While there is still hope in this area with newer compounds with improved properties would clinically useful.

**1.6.5.2 Auto processing activators / inhibitors**

Both toxins require cysteine protease (CPD) mediated autocatalytic cleavage to release the enzymatic domain into the cytosol. Although many specific inhibitors for *C. difficile* CDP have been reported (87), they may not be therapeutically successful since the catalytically active N-terminal region is already poised for cellular damage. But specific CPD activators that induce premature cleavage of CPD before toxin internalization would be more appropriate. A recent study has shown that one of the host-mediated endogenous mechanisms to protect from clostridial toxin is by nitrosylation of the active site cysteine (S-NO) of CPD (155). Above observations opens up a new therapeutic scenario for CPD inhibitors, if inhibitors were specifically designed to irreversibly bind catalytic cysteine in the GI tract, the inhibitors will remain intact even when the toxin gets internalized and there by prevent release of N-terminal catalytic domain.

**1.6.5.3 Enzymatic domain inhibitors**

Mechanistic-based enzymatic domain inhibitors remain as the most promising area regarding reduction of symptoms associated with CDI. As explained in CPD, although catalytic activity occurs intracellularly the inactivation could be targeted in the GI tract (Explained in

detail in Chapter 2 and Chapter 3). Toxin etiology indicates that two main approaches can be used to develop GTD inhibitors (148). A homolog that mimics UDP-glucose and small molecules or peptides that mimic the RhoA substrate might provide a greater interaction surface with GTD. Sugar analogs bind poorly and make poor drug candidates (156). A polyhydroxylated indolizidine alkaloid, castanospermine was found to inhibit *in vitro* glucosyltransfer of TcdA and TcdB via transition state mimicry (157). However it showed poor *in vivo* binding properties and tissue micro injection was required for its protection.

#### 1.6.5.4 Inhibitors towards potential virulence factors

These factors function in pathogenesis by promoting efficient adherence and colonization in host. Therefore inhibitors targeting potential virulence factors interfere with colonization initiation. In recent years an array of studies have provided detailed understanding on mechanisms of spore formation, germination and colonization that has set the stage towards identification of novel clinically potential targets. The recent research interests in this field have mainly focused on two areas: germination inhibitors (158) and inhibitors for surface layer-mediated host cell adherence (159). These non-absorbable agents appear to be amenable for oral administration and may act prophylactically to prevent colonization.

## 1.7 Conclusions

According to a recent report by the CDC (Centers of Disease Control and Prevention), *C. difficile* infection has known to be the most costly healthcare-associated infection. Despite the incontestable success of antibiotics in treating *C. difficile* infections, with the emergence of high toxin producing epidemic strains, high recurrence rates, potential emergence as a community-acquired pathogen and increased morbidity and mortality of disease have increased the need of

more reinforced infection control procedures in healthcare settings and novel effective therapeutic approaches.

### 1.8 Thesis Statement

The major pathophysiology associated with numerous epidemic life-threatening bacterial infections such as anthrax (*Bacillus anthracs),* cholera (*Vibrio cholera),* antibiotic-associated diarrhea (*C. difficile*), hemolytic-uremic syndrome (*Enterohemorrhagic Escherichia coli*) are mainly caused by the secretion of virulence factors categorized as "protein toxins". Although antibiotics are broadly used as the treatment strategy, the main challenge has been the development of resistance strains and toxins that continue to cause symptoms even when bacteria are cleared form the system. Alternative ways to combat such diseases are from targeting specific virulence factors. Our lab has been interested in exploring the mechanistic details of *C. difficile* virulence factors and anti-virulent treatment strategies over past 10 years. This body of work centered on two main areas focusing on pathogenesis of *C. difficile*. (I) Identification and characterization of peptide-based anti-virulence agents specifically target glucosyltrasferase domain of *C. difficile* Toxins A and B. (II) Detailed understanding on regulatory networks that govern expression of virulence factors.

(1) Towards development of mechanistic-based anti-toxin agent, phage display was used to identify peptides that bind to the catalytic domain of *C. difficile* Toxin A. Characterization of the binding and inhibitory activity revealed that the lack of parent peptide ability to inhibit the cells *in vivo*. Further derivatization of above parent peptides in to irreversible binders lead to protects cells *in vivo*. Mass spectroscopy approaches revealed the peptide inhibition was mainly due to cross-linking of modified peptide in to key catalytic residues in active site. While there are still several steps required to further explore in terms of the stability of these compounds that

could withstand harsh gastrointestinal environments, formulation, administration etc, before these candidates can be taken to the clinic, our results can be viewed in broader perspective in which it shows for the first time a pathway towards the systematic construction and proof of an active site binding peptide that can irreversibly inactivate an enzymatic domain of bacterial A-B type toxins and protect cells from its activity. Agents like these could be potentially used prophylactically to avoid extensive cellular damage during treatment with broad spectrum antibiotics or in populations prone to CDI.

(2) In addition to development of an anti-virulent agent, we are interested in gaining better understanding on toxin gene expression by a negative regulatory protein TcdC. Here we have employed both biochemical and genetic approaches to characterize the role of TcdC. Together our *in vitro* and *in vivo* studies illustrate that TcdC is not a repressor rather it could act as an anti-sigma factor. We have first time provided evidence that TcdC harbors a putative N-terminal signal peptide region and it undergoes cleavage *in vivo*. *In vivo* fusion studies revealed that the removal signal peptide leads to loss of function of TcdC. Fusion studies together with co-immunoprecipitation provided evidence on a direct interaction between TcdC and RNA polymerase *in vivo*. Above observations based on biochemical and genetic studies lead us to propose that TcdC, may function as a ECF class anti-sigma factor with regulated transmembrane proteolysis (RIP) pathway. In addition to that our data further verified that the truncated mutation leads to the activation of toxin promoters and thus play an important role in high toxin producing epidemic strains. Further our GFP-based reporter system system has a potential to be an adaptable tool for investigating fine details on PaLoc gene tunings, such as promoter specificities etc. Being able to adopt in host environment is vital for survival and propagation of a pathogenic

bacteria. Thus, exploring the regulatory nodes on PaLoc gene expression can be lead to exploit potential therapeutic opportunities hidden within such systems.

# CHAPTER 2[#]

## Peptide Inhibitors Targeting *Clostridium difficile* Toxins A and B

### 2.1 Abstract

*Clostridium difficile* causes severe hospital-acquired antibiotic associated diarrhea due to the activity of two large protein toxins. Current treatments suffer from a high relapse rate and are generating resistant strains, thus new methods of dealing with these infections that target the virulence factors directly are of interest. Phage display was used to identify peptides that bind to the catalytic domain of *C. difficile* Toxin A. Library screening and subsequent quantitative binding and inhibition studies showed that several of these peptides are potent inhibitors. Fragment based computational docking of these peptides elucidated the binding modes within the active site. These anti-toxin peptides will serve as potential lead compounds to further engineer peptidomimetic inhibitors of the clostridial toxins.

### 2.2 Introduction

*Clostridium difficile* infections cause one of the most common and vital hospital-acquired diseases often associated with broad-spectrum antibiotic usage (20). Disease severity ranges from asymptomatic colonization to life threatening colitis including toxic megacolon and colonic perforation (161). The emergence of hyper-virulent strains that are both more resistant to current antibiotics and produce dramatically more toxin during infection have lead to epidemic outbreaks in clinics around the world (162). Although elderly hospitalized patients still remain as the most susceptible entity for infection, recent reports indicate an increased prevalence of CDAD (*Clostridium difficile* associated diseases) in pediatric and adult population (163,164). An

[#] A part of this work is published in ACS Chemical Biology 160. Abdeen, S.J., Swett, R.J. and Feig, A.L. (2010) Peptide inhibitors targeting Clostridium difficile toxins A and B. *ACS chemical biology*, **5**, 1097-1103.

alarming rise in the incidence of community acquisition of CDAD has also been observed indicating new strains that may have serious health consequences for the general population if left unchecked.

While standard antibiotics such as metronidazole or oral vancomycin (165,166) provide some respite, due to the development of antibiotic-resistance, high relapse rates and more severe disease presentation caused by the epidemic strains, this line of treatment alone has often proven to be suboptimal. Therefore an increased demand for new, non-antimicrobial therapeutics has been born. Development in this area has focused on two basic strategies, one involving the active reconstitution of normal colonic micro flora with the idea that native microbiota provide significant protection from pathogens like *C. difficile* (16). The second area involves design of agents that target virulence factors assisted by the array of studies that have provided detailed understanding of the structure and function of these toxins (148,167). Recent therapeutic advances have focused on immunotherapy (168), vaccinations (78), toxin binding agents (158), and mechanistic-based inhibitors that targets toxin function(87,157,160). The above therapeutic strategies have an additional advantage that they minimally impact normal gut micro flora which should reduce risk of developing secondary *C. difficile* infections.

The N-terminal glucosyltransferase domain (GTD) binds to cellular UDP-glucose and irreversibly glucosylates small Rho family GTPases leading to the main pathophysiological effects (88,97). Mutations of key catalytic residues of the glucosyltransferase (GTD) completely inactivate the toxins (92), showing that inhibition of the GTD would be an effective route of preventing disease progression. Two main approaches can be used to develop GTD inhibitors. A homolog that mimics UDP-glucose without interfering with cellular glycobiology could be effective, but typical sugar analogs bind poorly and make poor drug candidates (156).

Alternatively, small molecules or peptides that mimic the RhoA substrate might provide greater interaction surface with GTD and thus make a more attractive starting point to develop drug candidates.

Phage display is a proven method for selecting peptides/proteins from large libraries where random short peptides/proteins are expressed as fusion proteins on bacteriophage coat proteins (169-171). This concept was first introduced by George Smith in 1985 (172). The rapid identification of specific ligands by phage display has been successfully used in many applications including antibody-epitope mapping, identification of peptide mimics of non-peptide ligands, selection of DNA binding proteins, drug discovery, used in enzymology to determine substrate specificity and to identify modulators/inhibitors etc (170,173-179). Phage display-based inhibitory peptide selection was effectively employed against the anthrax toxin (174,180). In phage display, exogenous peptides/proteins of interest are expressed and presented on non-lytic filamentous phages (M13, f1, fd) or lytic phages (T7, T4, lambda), where filamentous phage are employed for displaying short peptides where as lytic phage are commonly used for cDNA expressing larger proteins (169,171,181). Filamentous phage M13 is the most frequently used vector to generate random peptide-display libraries. In M13-based display, protein or peptide of interest is fused N-terminally to pIII or pVIII coat proteins (Figure 2.1A). pIII is present at 5 copies per phage of which all five can be fused to peptides without interfering with infectivity. But pVIII coat protein is present as ~2700 copies per virion but only about ~ 10 % of the pVIII can be fused with peptide/protein of interest. Peptide libraries based on pVIII coat proteins suffers from "avidity effect" and generally results identification of low-affinity binders for target (169,182,183). The most common screening method is based on enrichment of phage clones that bind to the target, by a process called biopanning (Figure 2.1B).

The biopanning includes; introduction of phage library to an immobilized target, washing away unbound phages, elution of bound phages and amplification in host bacteria. This process was continued until the desired sequence enrichment is achieved and then the displayed peptides were identified by DNA sequencing.

## 2.3 Results and Discussion

### 2.3.1 Biopanning of M13 Ph.D.- 7 library indentified TcdA binding peptide families

We selected a commercially available M13 Ph.D. -7 (NEB) phage display library with random heptapeptides fused to the N-terminal of pIII coat proteins. Compared to the other longer peptide libraries, the heptapeptide library is useful in identifying tighter binding peptide sequences instead the selection of multiple weak binding contacts. Biopanning was performed using an affinity capture method. The direct immobilization of target (toxin) to plastic support will potentially lead to partial denaturation of proteins and alter protein confirmation that is required for ligand binding. Therefore we used the affinity capture method to overcome these issues. The biopanning protocol (Figure 2.2A) was specifically designed to identify phage that bind toxin within the substrate binding pocket by requiring direct competition with RhoA. Therefore as the target, instead of holo Toxin A, a recombinant form of Toxin A, previously constructed in our lab with the minimal catalytic domain ($rTcdA^{540}$) was used. The $rTcdA^{540}$ was immobilized to Ni- NTA resin using its 6x his tag. In order to overcome the problem of selection of $Ni^{2+}$ binding phages, during the biopanning a pre-clearance step was carried out by introducing the phage pool to the resin in the absence of $rTcdA^{540}$. Initially the library was pre-cleared three times to remove $Ni^{2+}$ binding phage. This step was reiterated at the beginning of each round of selection. During the first round of biopanning, bound phage were recovered non-

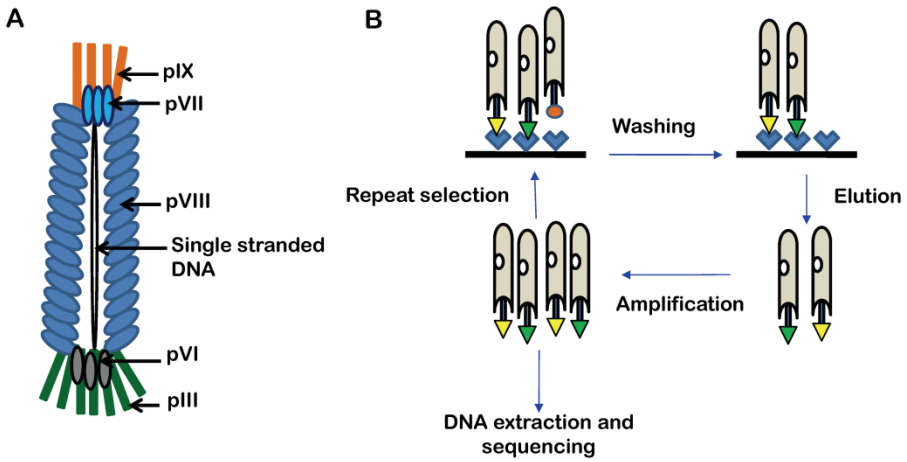


**Figure 2. 1 Overview of M13-based phage display screening.** (A) Schematic representation of M13 phage with major coat proteins. Exogenous peptides/ proteins are displayed on pIII or PVIII coat proteins. (B) Representative image of biopanning. The phage library is introduced to immobilized target, and unbound phages are removed by washing. Bound phages are eluted, amplified in *E. coli*, and subjected to the next cycle of biopanning. The cycle is repeated several times to enrich target-specific phages. Individual enriched phages are isolated and sequenced.

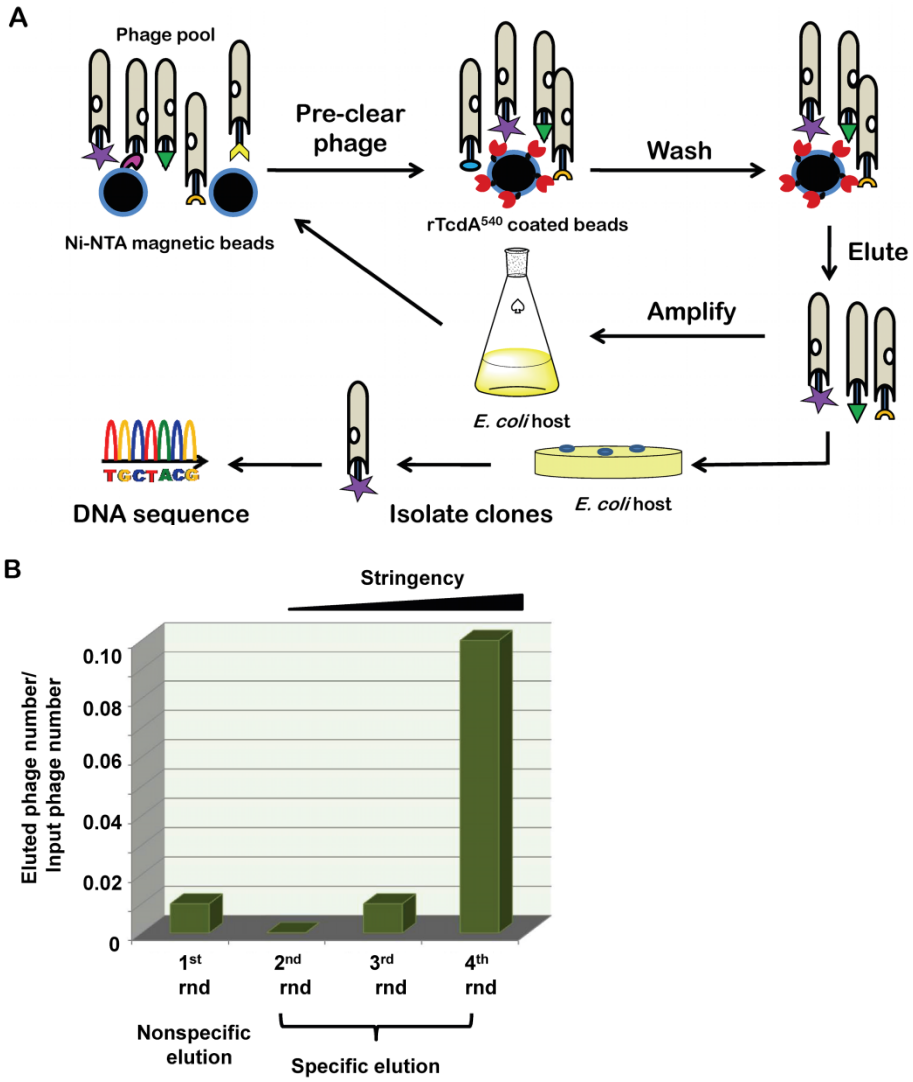


**Figure 2. 2 Overview of biopanning strategy and progression of selection.** (A) Schematic diagram of the phage display protocol. A pre-clearance step was carried out to remove nonspecifically binding phages from Ph.D-7 library. In the first round non-specific elution was performed with EDTA to elute his-tagged rTcdA$^{540}$ from Ni-NTA magnetic beads along with bound phage. During other three subsequent rounds, specific elutions were carried with RhoA, such that the eluted phages are those competitively released from the RhoA-rTcdA$^{540}$. (B) Histogram showing the progress of biopanning over the course of the selection process indicating the fraction of the phage recovered during each round. Identical numbers ($10^{10}$pfu/ml) of phage were introduced in all four rounds.

specifically by releasing with EDTA. In the next three rounds, the bound phage was eluted competitively with RhoA while increasing the stringency of the washing to improve the overall affinity of the surviving phage. As shown in Figure 2.2B, despite an equal number of phage being introduced during each round of selection, the number of eluted phage decreased in the second round. This result indicates that by switching from non-specific to competitive elution, non-specific peptides that survived the first round were removed from the pool. During rounds 2 - 4, phage recovery increased continuously and at the end of the fourth round, 10% of all input phage were captured. The above pattern represents a strong selection of $rTcdA^{540}$-interacting peptide sequences at this step. The consensus sequences obtained by sequencing 200 phages at the end of the $4^{th}$ round (Figure 2.3A) further confirmed that strong selection of target binding peptides. Analysis of 200 peptides sequences revealed 36 unique peptides, many of which were identified multiple times (Figure 2.3A). These peptides were divided into five distinct families based on their sequence similarity (Families A - E) and highly structured subfamilies, suggesting that these peptides are not random but have been preferentially selected.

### 2.3.2 ELISA-based screen revealed 17 potential $rTcdA^{540}$ binders

Individual phages were tested in isolation to measure their affinity for $TcdA^{540}$. First, a rapid ELISA screen was used employing a single concentration of $rTcdA^{540}$ (Figure 2.3A), identifying 17 individual peptides (shown in red) with the tightest toxin binding. Hit scores reflected the binding capacities of each phage (described in detail in materials and methods). The preliminary binding study indicated within each family the binding affinities of phage varied. Subfamilies $C_2$ and $B_2$ consist of mostly very weak binders (Figure 2.3A). Thereby indicating, binding affinities were distributed based on specific peptide sequence preferences. A more quantitative ELISA assay was then used to measure affinities ($K_d$) for phage-bound peptides. A

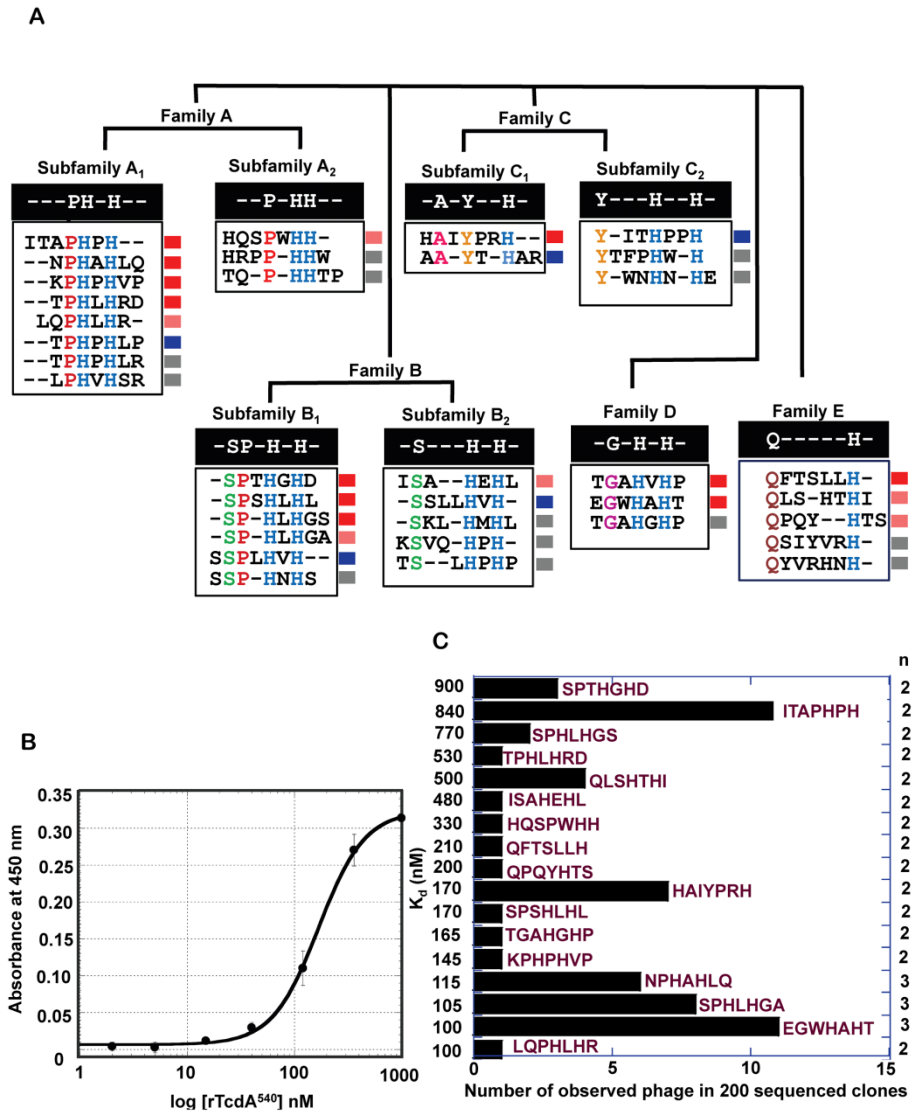


**Figure 2.3 Binding affinities of phage displaying inhibitory peptides.** (A) Families of peptide sequences identified from the analysis of 200 independent phage sequences and their apparent affinities. The binding affinities were obtained by a phage-based preliminary ELISA. Those marked in red exhibited binding affinities < 200 nM, blue: 200 – 1000 nM, and grey: > 1 µM. (B) Representative binding plot showing the interaction of phage HAIYPRH binding rTcdA$^{540}$ with $K_d$ of 170 ± 10 nM and cooperativity factor of 3. (C) Histogram showing the frequency with which each of the 17 tight binding peptides was observed among the 200 phage sequenced. Peptides are ordered based on their affinities for rTcdA$^{540}$ and cooperativity values (n) are shown at the far right. All $K_d$ values are the mean of four independent measurements.

quantitative ELISA assay was then used to measure affinities ($K_d$) for the phage-bound peptides by titrating the amount of $rTcdA^{540}$ immobilized in each well (Figure 2.3B). For the quantitative binding studies the tightest binders (Red) from preliminary ELISA was chosen. Overall, peptides exhibited cooperative binding with Hill coefficients of 2-3 and with $K_d$ values ranging from mid-nanomolar to low micromolar (Figure 2.3C). The majority of the tightest binders presented with the coorperativity factor of 3. All 14 out of 17 peptides exhibited $K_d$ of below 500 nM. In a polyvalent phage display, multiple binding events can give rise to chelate or avidity effects leading to over-representation of lower affinity peptides during the selection process. Since the natural substrate RhoA has poor affinity ($K_M$ >300 μM) to TcdA (184), the peptides exhibit tight binding relative to the natural substrate.

### 2.3.3 Selected TcdA binding phages inhibit toxin glucosyltransferase activity *in vitro*

Two phage sequences were selected for detailed inhibition analysis. Phage displaying the peptide EGWHAHT is a tight binder from family D ($K_d$~100 nM) and was among the tightest interactions from the initial screen. HQSPWHH from Family A2 binds toxin with modest affinity ($K_d$~330 nM) but showed the highest affinity in computational docking studies (section 2.2.6). (A fragment-based computational docking approach was used to observe the binding modes within the active site. The docking analysis was performed by our lab member Rebecca J. Swett). Inhibition activity was tested using a filter plate assay (184). UDP-[$^{14}$C]-glucose, $rTcdA^{540}$ and phage were incubated with RhoA in glucosylation buffer. Aliquots were removed at desired time points, quenched, and applied to a protein binding membrane to capture the radiolabeled product (Figure 2.4A). Control experiments in the absence of RhoA verified that the TcdA was incapable of glucosylating phage proteins. Typical data from a kinetic time course, measured as a function of phage concentration, are shown in (Figures 2.4B and 2.4C). Both peptides HQSPWHH and

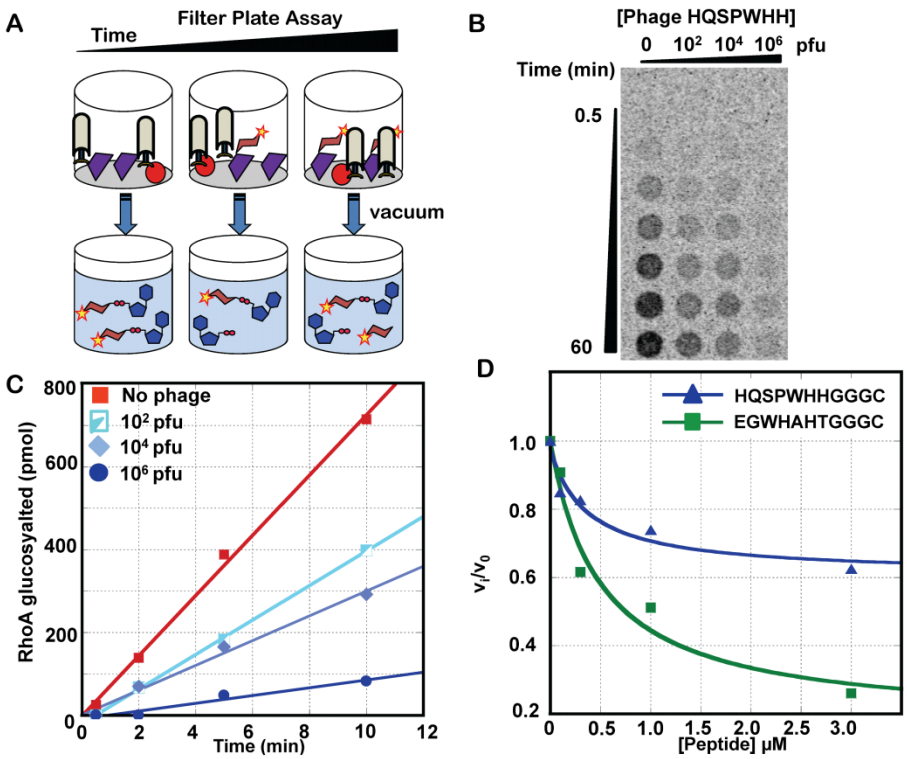


**Figure 2.4 Phage and peptide-based *in vitro* glucosyltransferase inhibition.** (A) Schematic of filter plate assay. Phage/peptide at varying concentration was titrated against constant rTcdA$^{540}$ concentration. At appropriate time points aliquots were removed and quenched and applied on membrane (B) Phosphorimage of an inhibition assay time course involving phage displaying the peptide HQSPWHH. Each column is an independent 60 minute time course. (C) GT inhibition progress curve at initial time points for Phage HQSPWHH. Glucosylated RhoA at each time point was calculated using a standard curve methodology. (D) Representative glucosyltransferase inhibition plot for synthetic peptides HQSPWHHGGGC and EGWHAHTGGGC showing the relative rate ($v_i/v_0$ where $v_i$ is the rate in the presence of inhibitor and $v_0$ is the rate in the absence of inhibitor) as a function of peptide concentration.

**Table 2. 1 Comparison of $K_d$ and $K_i$ values of peptides**

| Sequence | $K_d$ (nM)[a] | $K_i$ (pfu)[a] | $K_i$ (peptide) nM[b] | |
|---|---|---|---|---|
| | | | rTcdA$^{540}$ | rTcdB |
| EGWHAHT | 100 ± 5 | $10^5$ | 500 ± 200 | 54 ± 20 |
| HQSPWHH | 330 ± 40 | $10^2$ | 300 ± 200 | 18 ± 9 |

[a] *Values were obtained from phage-based TcdA540 binding and GT inhibition experiments.*
[b] *Obtained from peptide-based GT inhibition experiments.*
*TcdA$^{540}$- recombinant form of TcdA consists of only glucosyltransferase domain.*
*rTcdB - recombinant form of holotoxin TcdB*

EGWHAHT effectively inhibit glucosyltransfer activity (GT) *in vitro*. In the context of the phage, HQSPWHH was 100-fold more effective as an inhibitor than EGWHAHT (Table 2.1), despite the fact that EGWHAHT has a tighter binding affinity. Thus, the phages that bind more tightly to TcdA are not necessarily the best glucosylation inhibitors. This can be explained by the fact that the weaker binders may comprise an appropriate binding geometry in the active site of TcdA so that they efficiently interfere with RhoA binding and glucosylation.

**2.3.4 Synthetic peptides inhibit both TcdA and TcdB *in vitro***

A recent study indicates isogenic mutants of *C. difficile* producing either toxin A or toxin B alone can cause fulminant disease in a hamster model (64). Thus it's important to classify inhibitory activities of peptides with respect to both toxins A and B. In phage display the peptides were fused in a polyvalent context with phage. This may affect target binding and inhibition potencies of peptides. Therefore following the phage-based analysis intact peptides-based binding affinities and inhibition efficiencies were characterized. The synthetic peptides were designed with the following features, since the C-terminal of displayed peptides were fused to the phage, the C-terminal carboxylate residue of the synthetic peptides were amidated to block the negative charge. The Ph.D.-7 phage display library consists of randomized linear heptapeptide fused to the coat protein pIII via a flexible linker Gly-Gly-Gly-Ser, our synthetic peptides were designed to have a Gly-Gly-Gly linker to the C-terminal but we replaced the Ser with Cys. The free thiol group of cysteine can be easily employed for peptide labeling purposes. Consequently, synthetic peptides with the sequence EGWHAHTGGGC and HQSPWHHGGGC were tested for GT inhibition activity with both TcdA and TcdB and a non-specific 7-mer peptide from a different phage display experiment employing the PhD-7 library showed no inhibition. These data were fit to a partial competitive inhibition model to obtain the apparent $K_i$. Consistent

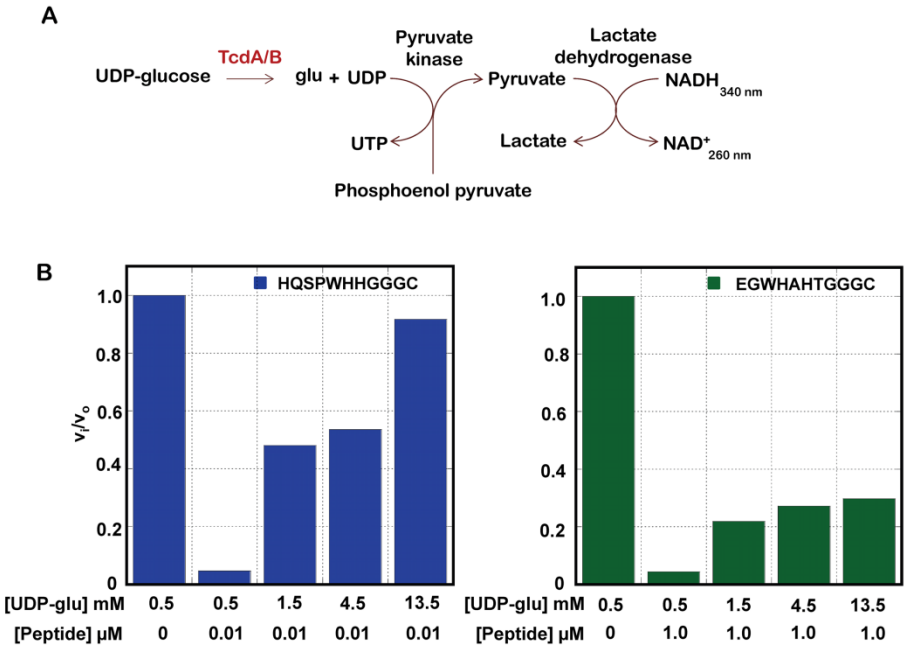


**Figure 2.5 Schematic representation of optical enzyme coupled glucosylhydrolase (GH) assay and competitive UDP-glucose mediated GH inhibition recovery.** (A) The generation of UDP by TcdA/TcdB mediated UDP-glucose hydrolysis was quantified through the coupled-enzyme system of pyruvate kinase (PK) and lactate dehydrogenase (LDH). The turnover rate of PK and LDH were much faster than GH activity of TcdA/TcdB, allowing accurate rate determination of UDP production. The oxidation of NADH is monitored by the loss of absorbance at 340 nm. (B) At constant maximal GH inhibitory peptide concentration UDP-glucose (UDP-Glc) was titrated from 0.5 to 13.5 mM. The relative GH rate was calculated using the ratio of initial GH rate in the presence ($v_i$) and absence of peptide ($v_0$). HQSPWHHGGGC-UDP-Glc titration is indicated in blue and EGWHAHTGGGC-UDP-glc titration in green. At 0.5 mM UDP-Glc concentration ~ 95% inhibition was observed in the presence of 10 nM HQSPWHHGGGC and 1 µM EGWHAHTGGGC and recovery in inhibition was observed with increase in UDP-glc concentrations.

with the phage-based inhibition studies, (Figure 2.4D and Table 2.1) HQSPWHHGGGC had a lower $K_i$ (300 ± 200 nM) compared to EGWHAHTGGGC (500 ± 200 nM), but a lower overall extent of inhibition. Whereas in the case of rTcdB apparent inhibition constants ($K_i$) of 18 ± 9 nM for HQSPWHHGGGC and 54 ± 20 nM for EGWHAHTGGGC was obtained. Promisingly, the peptides effectively inhibit both TcdA and TcdB in the low micomolar range. The differences in $K_i$ in the presence of $rTcdA^{540}$ and rTcdB can be largely explained by the fact that truncated TcdA/TcdB harboring only glucosyltransferase domains posses enhanced (~ 800 fold) glucosyltransferase catalytic activity over the holotoxins A and B *in vitro(89)* and observed RhoA modifying rate is higher in TcdA compared to TcdB (89). Thus leads to lower inhibitory potential of peptides towards $rTcdA^{540}$ compared to rTcdB.

**2.3.5 Peptides act as reversible competitive inhibitors**

In addition to the GT activity, in the absence of suitable protein substrates, toxins catalyze UDP-glucose hydrolysis (GH activity). Although GH activity is thought to be irrelevant in vivo, it is useful in an enzymology perspective to identify and characterize the properties of inhibitors. Both peptides EGWHAHTGGGC and HQSPWHHHGGGC effectively inhibited $TcdA^{540}$ GH activity at low (0.5 mM) UDP-glucose concentrations (Figure 2.5C and 2.5D), and inhibition behavior was competitive with respect to UDP-glucose. But in contrast to EGWHAHTGGGC, in the presence of HQSPWHHHGGGC, the inhibition was ~90% recovered with increasing UDP-glucose concentration. The above observation validates the fact that both peptides having different binding modes within the active site. In addition to that the partial competitive inhibition observed in GT inhibition assays thus results from the high UDP-Glc concentrations used in the enzyme assays to ensure rapid GT activity and may be less important in a cellular context where UDP-Glc concentrations are relatively low (185).

### 2.3.6 Docking studies elucidated the peptides binding modes within the TcdB active site

*[In sillico studies were performed by Rebecca J. Swett]*

To better understand how the peptides bind to *C. difficile* toxins, a computational approach was used. Molecular models of the selected peptides were created and flexibly docked into N-terminal catalytic domain of TcdB (96). The crystal structure of the N-terminal catalytic domain of TcdB was used as the catalytic domain as TcdA has not been crystallographically resolved by that time. Both TcdA and TcdB target Rho proteins, Rac1 and Cdc42 and have identical substrate specificities. Furthermore, the catalytic domains of TcdA and TcdB exhibit 74% sequence homology (20) making it a suitable substitute for these studies. The docked structures were then validated using molecular dynamics under full solvation. Over a 10 ns time course, no major rearrangements were observed.

Peptides EGWHAHT and HQSPWHH both bind with their N-terminal residue occupying the active site (Figure 2.6). Binding conformations exhibit backbone coordination of the catalytic metal ion and electrostatic interactions with the highly charged active site region. HQSPWHH adopts a more curled conformation (Figure 2.6A) in order to facilitate interaction of the C-terminal histidines with the charged loop region comprised of residues 513-526, a known mobile loop within the active site critical for GT activity (83,186). These two histidines form close contacts with a methionine and an asparagine respectively (Figure 2.6C). The curled conformation directs the backbone segment between the serine and the proline to the coordination sites of the magnesium (Figure 2.6C), while allowing the N-terminal histidine to contact a pocket comprised of an Asn-Asp pair. EGWHAHT adopts an extended conformation (Figure 2.6B and 2.6D) inserting His-4 in an Asn-Gln-Lys pocket just above the metal center (Figure 2.6D) while His-7 occupies a Glu-Asn-Glu pocket. Interestingly the docking studies in

good correlation with out *in vitro* inhibition studies, clarify the fact of moderate binder HQSPWHH being the strongest inhibitor is mainly due to its binding confirmation in the active site, where it interacts with a mobile loop within the active site critical for substrate recognition region required for glucosytransferase activity of *C. difficile* toxins.

### 2.3.6 Synthetic peptide-TcdA$^{540}$ binding

In order to identify the binding interaction of EGWHAHTGGGC and HQSPWHHHGGGC with toxin, isothermal titration calorimetry (ITC) was used. It will provide a better understanding on the binding affinities ($K_d$), stoichiometry and the cooperative binding nature of intact peptides to rTcdA$^{540}$. We did not observe any significant binding energy, once 2.5 µM of TcdA$^{540}$ (titrate) was titrated with 30 µM of EGWHAHTGGGC and HQSPWHHHGGGC. This may predominantly due to insufficient heat of binding associated with peptide-TcdA$^{540}$ interaction. Our previous binding studies were carried out with pentavalently displayed peptides in context with the phage. Compared to the size of the fused peptides and its targets, the M13 phage size itself very large (65 Å diameter and 9300 Å length). Therefore the large surface and polyvalency may assist structural constrains on displayed peptides, thereby leading to increased affinity and cooperative effects on target binding compare to intact peptides. It is possible; to increase the biological activity of weakly binding peptides by presenting multiple copies of it, on the same molecule (polyvalent inhibitors) therefore in future presenting the peptide in a polymer backbone may enhance the binding affinities (187) and may result in detectable binding energies in ITC experiment.

### 2.3.7 Characterization of selected peptides

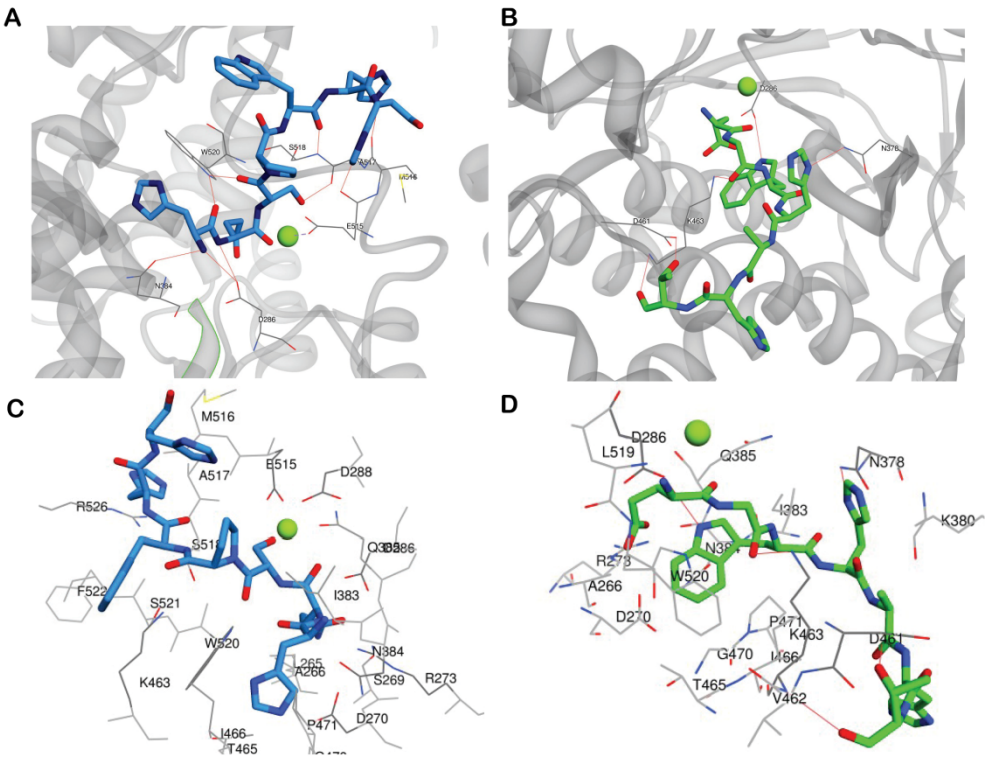


**Figure 2.6 Binding modes of peptides HQSPWHH (blue) and EGWHAHT (green) derived from computational docking.** (A) HQSPWHH in the TcdB active site. (B) EGWHAHT in the TcdB active site. Catalytic magnesium is indicated as a green sphere. (C) A stick diagram showing close up view of HQSPWHH in the TcdB active site. All TcdB residues within 3 Å of the peptide are shown and labeled. The curled conformation and backbone coordination of the catalytic manganese are more readily apparent when viewed in stereo. (D) A stick diagram showing close up view of EGWHAHT in the TcdB active site. All TcdB residues within 3 Å of the peptide are shown and labeled. Ring stacking of the peptide tryptophan on Trp520 of TcdB is apparent, as are the numerous electrostatic interactions.

Toxin inhibitory activity was initially characterized with two peptides HQSPWHH and EGWHAHT. However, the analysis has to be expanded to other potential binders in our library in order to establish their usefulness as inhibitors. As a cost-effective approach, peptides were recombinantly expressed as fusion proteins. Green fluorescent protein was used as a scaffold for presentation of peptides (188,189). The light emitting properties of fusion constructs allow easy purification of our small hepta-peptides and detection on binding studies.

cloning, characterization of binding and inhibition activity of peptide fusion constructs was carried out by Stephanie Kern (Former graduate student in our lab). The LC-ESI mass spectroscopy data confirmed the purified protein have expected product but the N-terminal methionine remained intact in the purified protein even though it was expected to be cleaved from expressed protein in *E. coli*.

The ELISA based binding assay and a gel shift binding assays did not reveal any significant binding of pep-GFP fusion to $TcdA^{540}$. This may be due to two main reasons; the displayed peptides on GFP may not be in a preferred orientation so that it can interact with $TcdA^{540}$ or the N-terminal methionine may interfere with the peptide-$TcdA^{540}$ binding. According to computational based docking data, the N-terminal residues in peptides were crucial for favorable peptide-toxin interactions. Thus, introducing an additional amino acid residue may have hindered the favorable contact of the peptide with the active site. This requires an expression system to produce peptides without additional N-terminal residues.

Alternatively, we used cyanogen bromide (CNBr) treatment for the removal of N-terminal methionine. This protocol included TEV protease treatment on purified peptide-EmGFP to release of fused peptide, followed by cyanogen bromide cleavage. This methodology led to a poor yield of peptide which was insufficient to carry out inhibition studies. In addition, there

were issues with separation of un-cleaved methionine from the cleavage products. While considering the time requirement for all above steps, the amount of starting material required and final yield, it is more cost efficient to proceed with synthetic peptides. But due the financial limitations we could not progress with the analysis of the remaining 15 peptides.

**2.4 Conclusions**

We used a random heptapetide phage display library to identify peptide inhibitors that target *C. difficile* toxin. The consensus peptide sequences obtained at the end of the 4$^{th}$ round of biopanning, suggested that these peptides are not just random peptides but have been preferentially selected over other sequences. Subsequent qualitative and quantitative binding studies provided, 17 potent rTcdA$_{540}$ binders with affinities varying from high nanomolar to the low micromolar range. The phage-based and peptide-based GT inhibition assays revealed the possible notion of strong binders may not be the strongest inhibitors. Above peptides inhibit both TcdA and TcdB activity *in vitro.* The UDP-glucose competition analysis on GH activity presented that both peptides bind with TcdA$^{540}$ competitively with respect to UDP-glucose. The peptide-based inhibition analysis revealed that both peptide EHWHAHTGGGC and HQSPWHHGGGC inhibits TcdA and TcdB. The UDP-glucose competition analysis on GH activity presented that both peptides bind with TcdA$^{540}$ competitive with respect to UDP-glucose. In sillico studies provides evidence that both peptides bind to the active site of TcdB, albeit with different geometries. This finding clarifies the fact the strong binders may not be the strongest inhibitors. The binding study based of peptide-EmGFP fusion constructs provides that incorporation of an extra amino acid at N-terminal may abolish peptide-toxin binding. Binding and inhibition activity of the remaining 15 peptides have to be further characterized using synthetic peptides as well as alanine scanning of inhibitory peptides can be carried out to identify

the amino acid residues that required in making favorable contact with active site. This information can be utilized to build small molecules with better in vivo stability and potency.

## 2.5 Materials and Methods

### 2.5.1 rTcdA$^{540}$ purification

All procedures with rTcdA$^{540}$ DNA were carried out in Biosafety Level 2 lab (BL2) following standard operating procedures. The N-terminal minimal catalytic domain of *C. difficile* Toxin A comprised of residues 1-540 (rTcdA$^{540}$) was successfully cloned and catalytic activity was confirmed (184). *E. coli* BL21 (DE3) cells (Stratagene) harboring a rTcdA$^{540}$ plasmid was used for protein expression. Cells were lysed by sonication in 50 mM sodium phosphate, 300 mM NaCl, 10 mM imidazole, at pH 8.0, supplemented with EDTA-free complete protease inhibitor cocktail (Roche). The cell lysate was clarified by centrifugation and sterile filtered (0.22µm filter). The protein was purified using a nickel-chelated HiTrap column (GE Healthcare) and eluted with 250 mM imidazole. It was further purified over a HiLoad 16/60 Superdex 200 gel filtration column (GE Healthcare). Size exclusion column fractions were reapplied to the nickel-chelated HiTrap column to concentrate the protein and eluted in a small volume of buffer containing 250 mM imidazole. The purified protein was dialyzed into storage buffer (50 mM HEPES-K, 100 mM KCl and 1 mM $MgCl_2$, at pH 7.5) and stored at 4 °C.

### 2.5.2 RhoA purification

The Glutathione-S-transferase (GST)-tagged RhoA was purified using *E. coli* Rosetta2 (DE3) cells (Invitrogen) harboring pGEX-2T-RhoA-GST, courtesy of the Richard A. Cerione lab (190). Cells were lysed by sonication in PBS, supplemented with EDTA-free complete protease inhibitor cocktail (Roche). The clarified cell lysate was loaded onto immobilized Glutathione resin (Thermo Scientific) and incubated for 1 hour at 4 °C on a rotating platform. After the

incubation period, the slurry was transferred to a disposable plastic column (Thermo Scientific). Bound protein was eluted in 50 mM Tris.HCl, containing 10 mM reduced glutathione at pH 8.

*E. coli* Rosetta2 (DE3) cells (Invitrogen) containing pET28a vector with $His_6$-tagged human RhoA were also utilized for protein expression (184). Cells were lysed by sonication in lysis buffer (50 mM HEPES, 300 mM NaCl, 1mM $MgCl_2$ pH 8.0), supplemented with protease inhibitors. Proteins were purified using an imidazole gradient from a nickel-chelated HiTrap column. Both the purified GST-tagged and $His_6$-tagged protein were dialyzed into storage buffer and stored at 4 °C.

**2.5.3 Phage display**

M13 phage-based 7-mer linear peptide library (Ph.D-7 peptide library from New England Biolabs) was used as the initial phage display library. Magnetic Ni-NTA bead-based affinity capture was used to immobilize $rTcdA^{540}$. Therefore a pre-clearance step was performed prior to each round of panning to remove plastic and $Ni^{2+}$ binders from the phage pool. Ni-NTA (250 µg capacity) magnetic agarose beads (QIAGEN) were washed 5 times with TBST buffer (50 mM Tris.HCl, 150 mM NaCl, 0.1 % [v/v] Tween-20, pH 7.5). TBST buffer containing $10^{10}$ pfu/ml of the phage library was incubated with washed Ni-NTA magnetic agarose beads at room temperature for 1 hour with continuous rotation. The supernatant of this solution provided the pre-cleared phage pool. For target immobilization, 20 µl of washed Ni-NTA magnetic agarose beads (50 µg capacity) were coated for 1 hour at room temperature with 100 µg of purified his-tagged $rTcdA^{540}$ with continuous rotation. After the incubation period, unbound toxin was washed away with storage buffer. The pre-cleared phage pool was added to the $rTcdA^{540}$ coated Ni-NTA beads, and incubated at room temperature for 1 hour with continuous rotation. Unbound phage were removed by washing 20 times with 200 µl TBST buffer. Four rounds of elution were

performed under the following conditions: TBST buffer supplemented with 50 mM EDTA for round 1, 25 µg of purified Glutathione S transferase-tagged RhoA in round 2, and 50 µg of purified GST-tagged RhoA for rounds 3 and 4.

At the end of each round of selection, eluted phage were amplified in *E.coli* ER2738 cells (NEB) and phage were counted. After the fourth round, 200 phage colonies were selected randomly. Phage DNA was purified using the manufacturers protocol (NEB) and sequenced (Beckman-Coulter CEQ8000 sequencer).

### 2.5.4 Preliminary ELISA to identify rTcdA$^{540}$ binding peptides

A 96-well flat-bottom black assay plate (Fisher) was incubated with TBS (50 mM Tris.HCl, 150 mM NaCl, pH 7.5) buffer containing $10^{10}$ pfu from each of 36 phage colonies overnight at 4 °C. (Note: all colonies were plated in duplicate, allowing one well to serve as a negative control). After the incubation period, the wells were washed 6 times with TBS and then blocked with 2% bovine serum albumin (Sigma) in TBS for 2 hours at room temperature. Wells were then washed 6 times with TBS. Storage buffer (negative control), or storage buffer supplemented with 2 µM rTcdA$^{540}$ was added to each well. The plate was incubated at room temperature for 1 hour with shaking and then washed 3 times with TBS buffer. To each well 1µg/ml His Probe-HRP [a nickel ($Ni^{2+}$) activated derivative of horseradish peroxidase (Thermo Scientific)] was added and incubated at room temperature for 1 hour. Wells were washed 4 times with TBS. To each well 200 µl of 1:1 mixture of Luminol/Enhancer Solution with Stable Peroxide Solution (Thermo Scientific) was added and after 5 minutes chemiluminesence was measured on a luminometer (Tecan GENios Plus multi label reader). Sample readings were compared to their corresponding negative control to obtain a hit score using equation 1 where $A_0$ is the chemiluminescence of the sample and $B_0$ is the intensity of the negative control.

$$\text{Hit score} = \log (A_0\text{-}B_0) / \log B_0 \quad (1)$$

### 2.5.5 Quantitative phage-rTcdA$^{540}$ binding assay

Purified rTcdA$^{540}$ (2 nM to 1000 nM in storage buffer) was coated overnight at 4 °C to 96-well flat-bottom transparent assay plates (Fisher). After the coating step, unbound toxin was removed and wells were washed with storage buffer. Plates were blocked for 2 hours at room temperature with a solution of 2% non-fat dry milk in storage buffer and then washed again. Approximately 40 µl solution containing 1x10$^{10}$ phages were added to wells and incubated for 3 hours at room temperature with shaking. After washing 6 times with storage buffer, the plates were incubated for an additional 1 hour with anti-M13 monoclonal antibody coupled to horseradish peroxidase (GE healthcare) (1:10,000 dilution into storage buffer). Unbound antibodies were removed and the wells were washed 10 times with storage buffer. The enzymatic activity was assayed by addition of 1 Step Turbo TMB-ELISA (Thermo Scientific). The reaction was terminated with 100µl of 1M $H_2SO_4$. Color intensity was quantified at 450 nm using a Tecan GENios Plus multi label plate reader and compared to control reactions using milk-coated wells. Data were plotted as the mean ± SD of four independent experiments. Binding data were fit using nonlinear least square analysis (Kaleidagraph, Synergy Software) to a cooperative binding model (191).

### 2.5.6 Phage based glucosyltransfer inhibition assay

Glucosyltransferase activity in the presence or absence of inhibitory phage was measured by pre-incubating 2 nM rTcdA$^{540}$ with 10$^{10}$ pfu phage for 1 hour at 37 °C. Reaction was initiated by addition of pre-incubated toxin-phage mixture to glucosylation buffer (50 mM HEPES-K, 100 mM KCl, 2 mM $MgCl_2$, 2 mM MnCl2, pH 7.5) containing 2 µM RhoA, 15 µM UDP-glucose (Sigma) and 15 µM UDP-[$^{14}$C]-glucose (Perkin Elmer). At desired time points, 8 µL aliquots

were removed and quenched into 40 µL 10 mM EDTA at pH 8.0. Quenched sample points were loaded onto a Biodyne-B high-protein binding 96-well filter plate (Nunc) and aspirated into a collection plate in a MultiScreen Vacuum Manifold (Millipore). The filter membrane was washed extensively with wash buffer (50 mM HEPES-K, 100 mM KCl, pH 7.5), dried and imaged overnight in a phosphorimage cassette. A Typhoon phosphorimager (GE Healthcare) and ImageQuant software were used to quantify the pixel intensities.

Pixel intensities were converted to moles of [$^{14}$C]-glucosylated RhoA by using a standard curve(184). A GT reaction containing 20 µM RhoA, 163 nM rTcdA$^{540}$ and 30 µM UDP-[$^{14}$C]-glucose (Perkin Elmer) was incubated at 37 °C for 5 hrs to achieve quantitative modification of RhoA. The reaction mixture was then dialyzed using a 3500 MWCO Slide-A-Lyzer Cassette (Pierce) to remove all unincorporated label. Serially diluted dialyzed reaction mixture was applied to Biodyne-B high-protein binding 96-well filter plate (Nunc), while duplicate samples were analyzed by liquid scintillation counter (Beckman Coulter). Radioactivity was then directly related to amount of $^{14}$C-labeled RhoA retained on the filter membrane, which provides the conversion factor to moles of $^{14}$C retained on the membrane. The standard curve membrane is exposed on the same PI plate with all experimental data to account for differential exposure.

Apparent inhibition constants ($K_i$) were obtained by fitting the ratio of initial rate of the GT assay, in the presence ($v_i$) and absence ($v_0$) of peptide using nonlinear linear least square analysis to a reversible partial competitive inhibition model (192)(equation 2) where $I$ = phage or peptide inhibitor concentration, $K_M$ = Michaelis-Menten constant for RhoA, $K_i$ is the inhibition constant, S is the substrate concentration (RhoA) and $X_0$ is the coefficient of maximum inhibition under the experimental conditions.

$$v_i/v_o = [K_M / (((K_M*(1+I/K_i)) + S)] + X_0 \qquad (2)$$

### 2.5.7 Peptide inhibition of glucosyltransferase assay

Synthetic peptides EGWHAHTGGGC and HQSPWHHGGGC with C-terminal amide-modification were purchased from American Peptide Company, Inc. Sunnyvale, CA. Peptides were purified by reverse-phase HPLC over a C18 column (Beckman Coulter)], using a gradient of 0 – 100% acetonitrile containing 0.1% trifluoroacetic acid and monitored by UV absorption. After purification, the peptide was lyophilized and redissolved in water. The identity of each product was confirmed by electrospray mass spectrometry.

GT inhibition assays contained 10 μM RhoA, 15 μM UDP-glucose (Sigma) and 15 μM UDP-[$^{14}$C]-glucose (Perkin Elmer) in glucosylation buffer as described above, as well as 0 - 3000 nM peptide. Reactions were initiated by addition of 2 nM rTcdA$^{540}$ or TcdB (courtesy of the Prof. Hanping Feng (192)). $K_i$ values were obtained by fitting the data to a partial competitive reversible inhibition model as described for the phage-based GT inhibition assays**.**

### 2.5.8 Glucosylhydrolysis (GH) assay

This an optical coupled assay, UDP released from hydrolysis is coupled to the oxidation of NADH(193) using pyruvate kinase (PK) and lactate dehydrogenase (LDH). The reaction was carried out using an Agilent 8453 UV-VIS spectrophotometer equipped with a circulating water bath to maintain the temperature at $37^{0}$ $^{\circ}$C. Reaction was monitored by adding 200 nM rTcdA$^{540}$ to glucosylation buffer supplemented with UDP-glucose, 0.2 mM NADH, 1 mM phosphoenolpyruvate (PEP), 3 units of pyruvate kinase and 6 units of lactate dehydrogenase. The initial GH rate was measured at 0.5 mM UDP-glucose (standard saturation conditions) in the absence or at constant maximal peptide inhibitory concentrations of 10 nM HQSPWHHGGGC or 1μM EGWHAHTGGGC while varying UDP-glucose from 0.5 to 13.5 mM to monitor the effect of increased substrate concentration on the inhibition behavior. The relative rate ($v_i/v_0$)

was calculated by the ratio of the initial rate of the GH assay, in the presence and absence of peptide.

**2.5.9 Peptide docking**

Molecular models of selected peptides were built using Spartan '02(181), minimizing at the AM1 level of theory. Models were saved in Sybyl mol2 format and catenated into a library for docking. Flexible docking was performed using FlexX 3.1.0(194). Crystal structure 2BVL(96) was retrieved from the RCSB database for use as the docking receptor. Crystallographic phasing markers and counter ions were removed, retaining crystallographic water molecules. The active site for docking was defined by 20Å spheres around each atom of the crystallographically observed UDP. The crystallographic catalytic manganese was replaced with a magnesium ion for ease of calculation. A docking pharmacophore with two optional constraints was constructed utilizing the two octahedral coordination sites of the magnesium occupied by the crystallographic UDP molecule. Water molecules within the active site were included in the docking, designated as fully rotatable and displaceable. Dockings were ranked using the FlexX internal scoring protocol (195). Results were viewed and all images were generated using the UCSF Chimera visualization program (196) version 1.4.1. The docked structures were then simulated for 10ns to determine the stability of the docked conformation. The complete protein/peptide complex was solvated and ionized to 0.5mm NaCl and simulated using the CHARMM27 force field under NAMD(20) on the WSU Grid supercomputer. A timestep of one femtosecond was used, periodic boundary conditions applied, and Langevin dynamics were utilized to maintain constant temperature at 300K. A scaled cutoff was employed in the calculation of the long range electrostatics.

### 2.5.10 Isothermal titration calorimetry (ITC)

A VP-ITC titration calorimeter (MicroCal, Inc.) was used for all measurements. Samples were prepared by diluting a small volume of stock into $TcdA^{540}$ storage buffer. The syringe and sample cell components were prepared in matched buffers to minimize background heats of dilution. All buffers were prepared from stock solutions on the day of use and extensively degassed under vacuum. After an initial 2 $\mu$L injection to counteract backlash in the auto-titrator, ITC experiment consisted of 40 injections (at 7 $\mu$L per injection) of a 30 $\mu$M peptide EGWHAHTGGGC and HQSPWHHGGGC into 1.4 mL of the $TcdA^{540}$ at 2.5 $\mu$M. Sample stirring was set at 280 rpm for all measurements and temperature was maintained at 15 ºC.

### 2.5.11 Expression of peptide-EmGFP

[Fusion constructs were cloned and charecterized by Stephanie S. Kern]

For expression purposes, pRSET/EmGFP vector was selected as the parent vector and further manipulations were carried out to generate peptide fusions. Peptide-EmGFP was 6xHis tagged at C-terminal for purification purposes. Classical cloning, expression and purification protocols were followed to purify the fusion construct. The purity of the peptide was ensured by SDS-PAGE.

# CHAPTER 3

## Rational design of an irreversible peptide inhibitor targeting the major *Clostridium difficile* virulence factors

### 3.1 Abstract

*Clostridium difficile* infections cause one of the most common hospital-acquired diseases, often associated with broad-spectrum antibiotic usage. Recent increases in infection rates, disease severity and recurrence have spawned renewed efforts to develop more effective therapeutics against this pathogen. The previous chapter described a family of peptides that bound the active sites of TcdA and TcdB, the primary virulence factors that cause cellular damage during infection. However, the parent peptides failed to protect cells from intoxication as they were displaced from the toxins during translocation due to their reversible binding and poor cell permeability. In this chapter, the peptides have been re-engineered to bind the toxins irreversibly. Modified in this way, one of the derivatized peptides provides ~95% cell protection from *Clostridium difficile* toxin induced cytotoxicity in cell culture assays. Mass spectrometry studies further confirm that the derivatized peptide cross-links within the active site of *Clostridium difficile* toxin A (TcdA). These peptides, or derivatives thereof, might provide an alternative approach to treating these infections that avoids traditional antibiotics by directly targeting bacterial virulence factors. In so doing, they provide a therapeutic modality that provides less evolutionary pressure toward the emergence of resistant strains.

### 3.2 Introduction

Managing multiple recurrences and disease progression into more severe infections are the two challenges in treating *C. difficile* associated diseases. Although antibiotics are useful in clearing pathogenic bacteria during infection they increase the risk of generating antibiotic

resistance. Furthermore, high relapse rates render such treatments less effective in the *long run*. Alternative ways to combat *C. difficile* infections stem from targeting specific virulence factors such as the "*toxins*" that plays a pivotal role in pathogenesis. This strategy serves a two-fold advantage; on one hand it provides a specific and direct response to disrupt the infections, whereas on the other hand it has little impact on normal microflora that helps maintain the equilibrium of bacterial populations and thus indirectly helps minimize CDI (*C. difficile* associated infections) in the first place. However to date a rationally designed drug that targets the "toxins" is yet to be used as a therapeutic.

The successful design of small molecule inhibitors for bacterial toxins depends on better *in vivo* inhibitory activities. In the previous chapter we discussed a collection of peptides that inhibited both TcdA and TcdB *in vitro*. Cellular protection studies performed with these peptides, however, revealed that they lacked the ability to protect cells from intoxication. It was hypothesized that this failure was likely due to the reversible nature of peptide binding. Because the clostidial toxins are endocytosed into cells, the conformational changes may accompany the dissociation of peptide-toxin interaction. This finding explains the poor performance of the parent as an *in vivo* inhibitor. Here we set out a goal that if these peptides could be derivatized with an appropriate electrophile in a reactive geometry relative to potential nucleophilic side chains near their binding site, a covalent adduct would form, such that inhibitory peptide would remain permanently bound in the active site and thus inhibit toxicity *in vivo*. This approach provides an added advantage in that the therapeutic molecules need not enter the cell, but rather could inactivate the toxins in the intestinal lumen avoiding numerous complications and minimizing the likelihood of serious toxicity through off-target interactions.

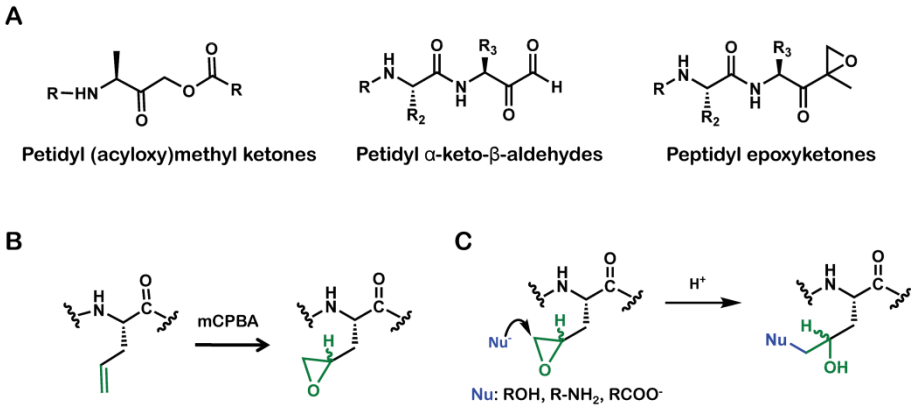


**Figure 3. 1 Examples of peptides modified to be irreversible inhibitors through covalent crosslinking with their targets.** Outline of synthesis and mechanism of action of epoxy peptide inhibitors. (A) Amino acid derivatives that can be incorporated into synthetic peptides to facilitate spontaneous covalent cross linking with targets. (B) Epoxide "war head" can be incorporated into the peptide by oxidation of allylglycine residue with meta-chloroperoxybenzoic acid. In this case the oxidation leads to a mixture of (R) and (S) epoxy peptides stereoisomes for the epoxide-containing side chain. Alternative synthetic transformations can be used that are stereospecific. (C) Nucelophilic ring opening of epoxide leads to covalent attachment of the peptide with its bindig partner.

A variety of electrophilic moieties, such as the acyloxymethyl ketone (AOMK) (197), α-keto-β-aldehyde, peptide epoxy ketone, O-aryloxycarbonyl hydroxamates, epoxy peptides, pyridones, 2-pyrrolidone (87,198-203).etc (Figure 3.1A), can be introduced into synthetic peptides to facilitate spontaneous crosslinking to its protein partner. We opted for an epoxide modification for the proof of concept as it could be incorporated in high yield in a single step with great selectivity from a synthetic peptide containing an allylglycine at the appropriate site of modification (Figure 3.1B and 3.1C).

Enzymatic domains of bacterial A-B type toxins produced by *C.difficile* (TcdA/TcdB), *Bacillus anthracis* (anthrax toxin), *Vibrio cholera* (cholerae) toxin are all attractive targets for non-antibiotic treatments plans, the design of inhibitors is challenging since small molecules that resemble the natural substrates have the potential to interfere with other cellular activities and must has to be bind to their targets before cellular internalization. In this work, we show that epoxy-based peptide inhibitors can act as attractive therapeutic molecules, due to their ability to irreversibly bind *C. difficile* toxins before internalization.

### 3.3 Results and Discussion

#### 3.3.1 Parent peptides failed to protect cells *in vivo*

First we characterized our parent peptides ability to obstruct TcdA induced cytotoxicity *in cellulo*. Toxin levels were set to induce > 60 % cell death during the incubation period in the absence of peptide. Then, the toxin was challenged with various concentrations of parent peptide HQSPWHH/EGWHAHT. Control cells were incubated with PBS/peptides/ TcdA. Cells were imaged after 24 hrs (Figure 3.2A). However, both parent peptides EGWHAHT and HQSPWHH failed to protect cells from TcdA. It was hypothesized that the lack of protection could be due to the reversible binding nature of peptides to toxins where the interaction may not have been

sufficient to withstand toxin internalization. This led to the hypothesis of two possible remedies. First, we could find a way to allow cellular uptake of the peptides, potentially by fusing them to cell penetrating peptide sequences. Alternatively, we could derivative the peptides to make their interaction with the toxin irreversible so that the inhibitor would not be left behind in the endosome during internalization. We therefore opted to pursue derivatization approach.

### 3.3.2 Peptide cross-linked TcdA by means of a heterobifunctional cross linker, posses less cellular toxicity

As a proof of concept experiment to validate the use of irreversible inhibitors and to clarify their applicability in *C. difficle* toxin inactivation *in cellulo*, we initially used a photo activatable-thiol reactive heterobifunctional cross-linker benzophenone-4-iodoacetamide (BPIA). This was completed in two steps, first parent peptide EGWHAHTGGGC (Cys) was allowed to react with iodoacetamide (204-207) (Figure 3.2B). Next BPIA labeled peptide was cross-linked to holo Toxin A via UV irradiation (365 nm) (Figure 3.2B). At this wave length protein damage is minimized. The photo activation forms a covalent adduct between benzophenone moiety and bound toxin. Next the activity of above cross-linked rTcdA was tested *in cellulo*. Cell viability was imaged after 2 hrs (Figure 3.2C). The peptide cross-linked rTcdA provided ~ 70 % cell protection showing that irreversibly linked peptide can be transported along with toxin and permanently inactivates toxin activity. Control experiments performed with UV exposed rTcdA confirmed, UV exposure itself does not affect rTcdA activity. This experiment provided sufficient evidence that covalent attachment of a peptide into the active site inactivates the toxin to justify moving forward this approach.

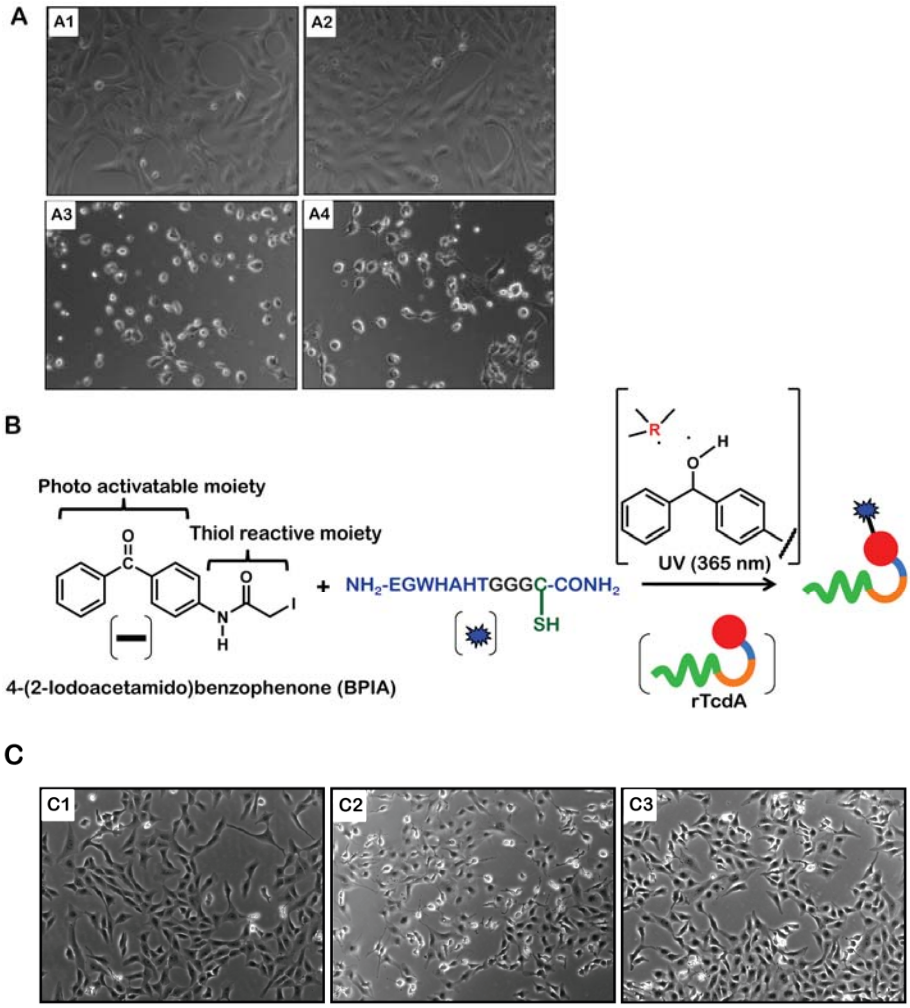


**Figure 3.2 In cellulo viability assays with parent peptide HQSPWHHGGGC and cellular toxicity of rTcdA cross-linked to EGWHAHTGGGC via heterobifunctional cross linker.** (A) Images showing the morphology of Vero cells obtained from cell viability assay performed with parent peptide HQSPWHHGGGC (A1) PBS-treated healthy Vero cells (A2) HQSPWHHGGGC treated cells showing that the peptide is non-toxic to cells (A3) Rounded and detached cells observed after rTcdA treatment (A4) rTcdA/HQSPWHHGGGC (0.6 mM) indicates that the parent peptide is unable to provide protection from rTcdA induced cytotoxicity. (B) Scheme showing the reactivity of photo activatable-thiol reactive heterobifunctional cross-linker BPIA with parent peptide EGWHAHTGGGC and rTcdA. The cartoon represents the cross-linking of peptide with catatytic domain of TcdA. (C) Images showing the morphology of Vero cells obtained with treatment of EGWHAHTGGGC cross-linked rTcdA after 2 hrs. (C1) PBS-treated healthy Vero cells (C2) Rounded cells observed after rTcdA treatment (0.2 nM) (C3) Cells treated with peptide cross-linked rTcdA (0.2 nM) showing a significant reduction in cell rounding.

### 3.3.3 In sillico epoxy screening provided information on optimal site for modification

[In silico studies were performed by Rebecca J. Swett]

Proper placement of the epoxide residue within the peptide sequence is critical for this mode of inhibition, such that the derivatized peptide could still bind to the toxin active site and inhibit toxin activity while also able to confer appropriate chemistry to form a covalent bond with the toxin. Possible amino acid candidates within the peptide for derivatization can be selected based on two methods where screening modified synthetic peptide libraries or computer-based virtual screening approaches are equally useful. The latter is a time saving and cost-effective method, which can be utilized to screen, enhance selectivity and specificity of the ligand of interest with its target (208,209). Virtual screening has been successfully utilized in discovery and modification of pharmacophores where this approach was used to identify inhibitors to a variety of protein systems, including inhibitors of HIV-1-proteases (210) and influenza hemagglutinin (211,212) among others. Here we utilized flexible protein-ligand docking to screen the epoxy peptide library.

Accordingly, HQSPWHH, the inhibitor shown to have the best *in vitro* activity was selected for further derivatization. In silico scanning was performed to determine the optimal site for modification based on docking energies to TcdB (PDB: 2BVL). This optimization was done in several steps. The first step involved incorporation of an alanine at each position to determine the relative contribution of the parent side chain at that site. Then, the peptides were re-docked, but this time in the presence of the R- and S-isomers of the epoxide-derivative of allylglycine (Table 3.1). In all of these experiments the overall parent peptide binding site was retained as was the overall backbone conformation, since all members of the docked library had RMSD <1 Å relative to the parent, unmodified peptide. Due to the nature of the docking

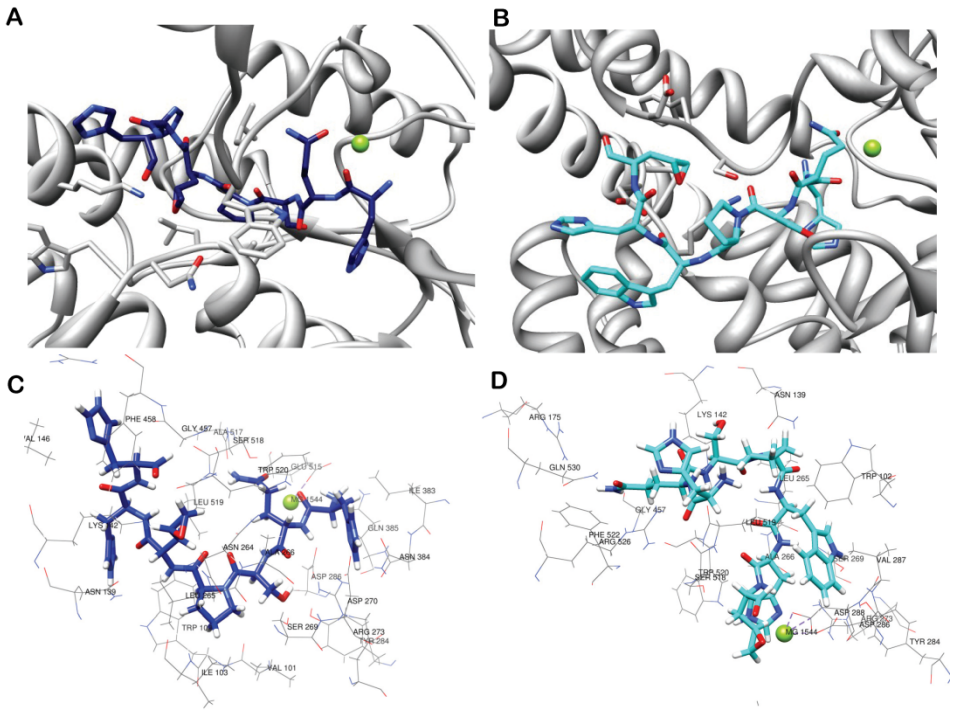


**Figure 3.3 Close-up view of ribbon structures and stereoimages of the TcdB active site, showing binding modes of highest scoring structures of HQSPGepoxyHH and HQSPWHGepoxy respectively.** Peptides are shown with all TcdB residues within 3Å. Coordinates were derived from computational docking as described in the Materials and Methods. (A) Ribbon diagram of the TcdB active site showing the lowest energy binding conformations of peptides HQSPGepoxyHH (dark blue) and (B) HQSPWHGepoxy (cyan) in the active site of TcdB. The epoxide residue of H-epoxy-7 is in close proximity to more polar amino acids when compared to H-epoxy-5. The catalytic magnesium ion is indicated as a green sphere in both images. Stereoimages of the (C) The epoxide of HQSPGepoxyHH has close contact with Lys142, Leu 265 and Asn 139. (D) The epoxide of HQSPWHGepoxy is within reach of Lys 452, Asp 523, Asp 461 and Ser 518.

**Table 3. 1 Indicates docking scores of parent peptide and family of peptides obtained by substitution of each amino acid with alanine and R- or S- epoxy derivative of allylglycine.**

| | WT | H-1-X | Q-2-X | S-3-X | P-4-X | W-5-X | H-6-X | H-7-X |
|---|---|---|---|---|---|---|---|---|
| Alanine | -36.01 | -38.84 | -31.93 | -29.86 | -35.18 | -34.74 | -35.47 | -39.12 |
| Epoxide R | -35.58 | -32.53 | -15.74 | -24.94 | -40.76 | -32.04 | -37.50 | -43.38 |
| Epoxide S | -36.04 | -29.04 | -2.06 | -35.34 | -20.89 | -52.85 | -33.01 | -24.26 |

*WT: Parent peptide HQSPWHH*

*X- Represent alanine/ (-R) or (-S) epoxy substitute*

algorithm, slight fluctuations in scores occur as a consequence of sub-angstrom variations in the docked conformation, predominantly through rotation around bonds in the flexible side chains (Table 3.1). While not on an absolute energy scale, this procedure provides reliable relative binding affinities to assess positions where the epoxide might be accepted. A docking score of greater magnitude than the parent's was considered an advantageous modification, while a docking score lower than the parent's was considered disadvantageous. For example, the substitution of an S-epoxidated allyl glycine at the fifth position (Table 3.1) leads to significant improvement in the docking score. The addition of an R or S-epoxidation at the second position causes a major decrease in the favorability of binding. For derivatization, peptides were selected based on two caveats, where either epoxy modified peptides with tighter binding affinity but with few reactive nucleophiles near its binding site or with moderate binding affinity but with larger number of surrounding nucleophiles could be used. Two peptides derivatized at different residues were subsequently selected for the synthesis (Figure 3.3), both with docking scores more favorable than the parent peptide (parent docking score, -35.58): HQSPGepoxyHH (H-epoxy-5) (Figure 3.3A and 3.3C) and HQSPWHGepoxy (H-epoxy-7) (Figure 3.3B and 3.3D). One reason for selecting H-epoxy-5 was that it displayed the overall tightest docking score (-52.85) (Table 3.1), while the rationale for selecting H-epoxy-7, despite a more modest docking score of -43.38 (Table 3.1), was due to the large number of potential nucleophiles in its vicinity that might facilitate rapid crosslinking.

### 3.3.4 Epoxy peptide derivatization

Allylglycine incorporated peptides (H-allyl-5) and (H-allyl-7) were purchased from American Peptide Company (Sunnyvale, California). Both peptides were modified with a GGGC tail at the C-terminus which has been shown previously to have no unfavorable effects on

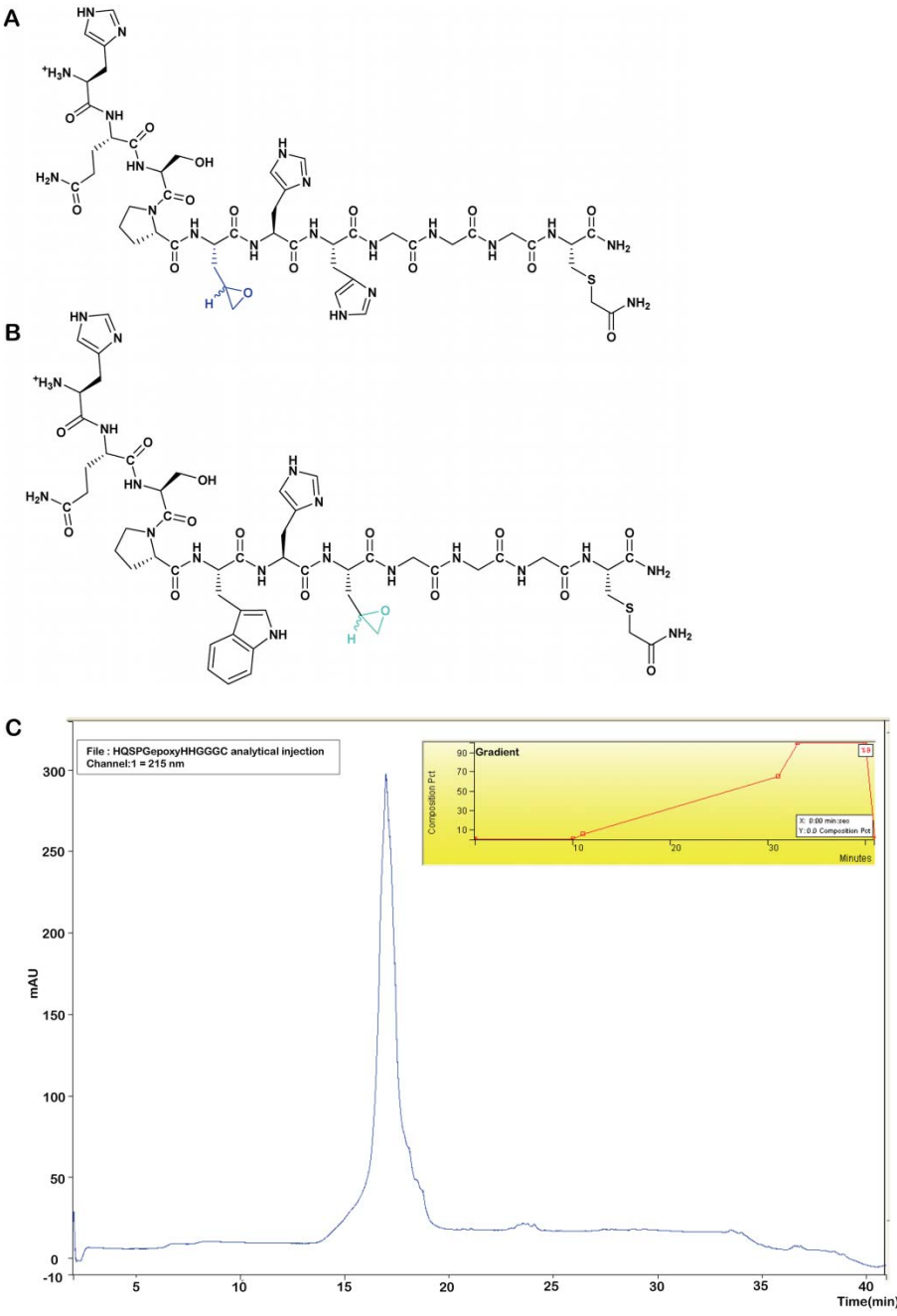


**Figure 3.4 Showing structures of derivatized epoxy-peptides and purity of H-epoxy-5 peptide.** (A) Structure of peptide HQSPGepoxyHHGGGC (H-epoxy-5), in which W5 of the parent peptide was replaced with the non-natural epoxide-containing amino acid and (B) Peptide HQSPWHGepoxyGGGC (H-epoxy-7), where H7 of the parent peptide was substituted. The free thiol of cysteine was protected with an acetamide group. (C) HPLC trace showing purity of H-epoxy-5 peptide obtained by an analytical injection. The gradient program is shown as an inset.

peptide binding or inhibition but provides a handle for labeling and other derivatizations in the future (160). The free C-terminus cysteine was protected with iodoacetamide (Figure 3.4A and Figure 3.4B) in order to avoid thiol mediated epoxide ring opening and to prevent non specific oxidation of free thiol by m-chloroperbenzoic acid. Thiol-protected, purified peptides were then converted to a racemic mixture of their corresponding epoxide by treatment with m-chloroperbenzoic acid (199,213) in a well-buffered reaction to prevent non-specific nucleophilic epoxide ring opening during the synthesis. HPLC purification (Figure 3.3C) was carried out after each step and the desired product was confirmed by LC/ESI-MS (Method and Materials).

### 3.3.5 Derivatized H-epoxy-5 peptide exhibits ~95% cell protection *in cellulo*

The ability of H-epoxy-5 and H-epoxy-7 peptides to block TcdA induced intoxication was tested *in cellulo*. Vero cells were challenged with TcdA in the presence of various concentrations of peptides H-epoxy-5 and H-epoxy-7 as well as the parent peptide HQSPWHH to observe any protection over the period of 48 hrs. Cell viability was qualitatively assessed by light microscopy, observing the number of rounded cells visible per field and quantitatively measured using the measured using a luminescent ATP-based (CellTiter-Glo) assay (Figure 3.5B). Interestingly, H-epoxy-5 showed concentration-dependent cell protection (Figure 3.5A and 3.5C). It provided ~95% cell protection at 600 μM and yielded an $IC_{50}$ of ~100 μM. Cell protection studies revealed that the H-epoxy-5-toxin complex remained intact during translocation while H-epoxy-7 was unable to protect cells from TcdA intoxication. Although computationally it was predicted to bind in a manner that would present more nucleophilic groups nearby, the activity assay indicating that the binding affinity governs the overall inhibition potential. Further it demonstrates that proper selection and placement of the epoxied

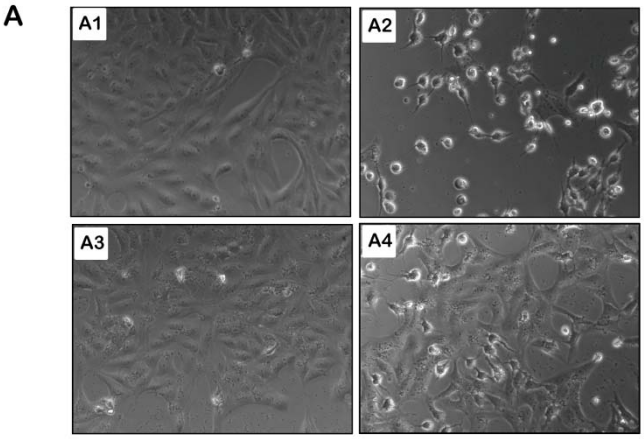


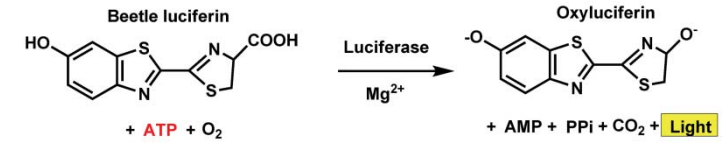


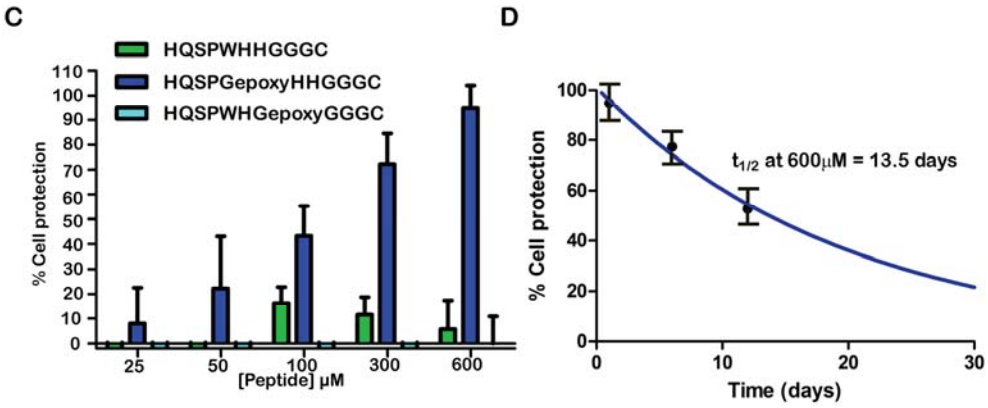

**Figure 3.5 *In cellulo* protection of vero cells from TcdA using epoxide-derivatized peptide inhibitors.** (A) Morphology of vero cells obtained from cell viability assay with parent peptide HQSPWHH and H-epoxy-5 (A1) Adherent, elongated, healthy cells after PBS treatment (A2) Rounded detached cells observed upon treatment of TcdA (A3) Control cells treated with only 0.6 mM H-epoxy-5, indicating the derivatized peptides were non-toxic to cells (A4) Cells treated with 0.6 mM H-epoxy-5 and TcdA showing a significant reduction in cell rounding in the presence of inhibitor. (B) CellTiter-Glo® Luminecent assay (Promega) is based on luciferase reaction. Mono-oxygenation of luciferin is catalyzed by luciferase in the presence of $Mg^{2+}$, ATP and molecular oxygen. The number of metabolically active (viable) cells in the culture is based on measurement of ATP levels. (C) Quantitative measurement of vero cell viability using CellTiter-GLO assay. The peptide concentrations were titrated at constant TcdA (0.4 nM) level. Parent peptide HQSPWHHGGGC did not show any protection against TcdA. Whereas H-epoxy-5 shows increased cell protection in a concentration-dependent manner with ~95% protection at 600 µM. Peptide H-epoxy-7 did not exhibit any protection against TcdA.(D) Indicates the half life of 0.6 mM H-epoxy-5 peptide monitored over two weeks period.

moiety within the parent peptide was essential for effective inhibition. The activity of H-epoxy-5 was monitored over a 2-week period revealing that the activity of the derivatized peptide reduces; yielding a half-life of approximately 13 days (Figure 3.5D). The loss of activity is most likely mainly due to the non-specific opening of the epoxide during the repeated freeze thaw cycles and thus indicates the necessity of optimization of storage conditions for long term usage.

### 3.3.6 Mass spectrometry studies confirm that the derivatized peptide cross-links within the active site of TcdA

[Mass spectroscopy was carried out in collaboration with Prof. Mary T. Rodgers lab (Yuan-wei Nei) Department of Chemistry, Wayne State University]

To confirm the selectivity and specificity of H-epoxy-5 peptide-toxin interactions, mass spectrometry was used. Modern cross-linking mass spectrometry and bottom-up proteomics techniques have significantly increased the scope of mapping proteins-proteins interfaces to supplement X-ray crystallography and NMR methods, due to its sensitivity and rapid analysis of complex mixtures where the size of the protein complexes is not a limiting factor since the proteolytic peptides are analyzed (214-216). Here we employed the ICR methodology because of its high mass accuracy that provides an invaluable prerequisite for the precise assignment of cross-linker containing species (217-219).

We mapped the binding site by bottom-up proteomic profiling using nano-high-performance liquid chromatography (HPLC)/ nano-electrospray FTICR (Fourier transform ion cyclotron resonance) mass spectrometry. In-gel trypsin digestion was performed on both $TcdA^{540}$ (catalytically active fragment of TcdA consisting of residues 1-540) (160) and $TcdA^{540}$ treated with H-epoxy-5. The resultant fragment libraries were compared to allow rapid identification of

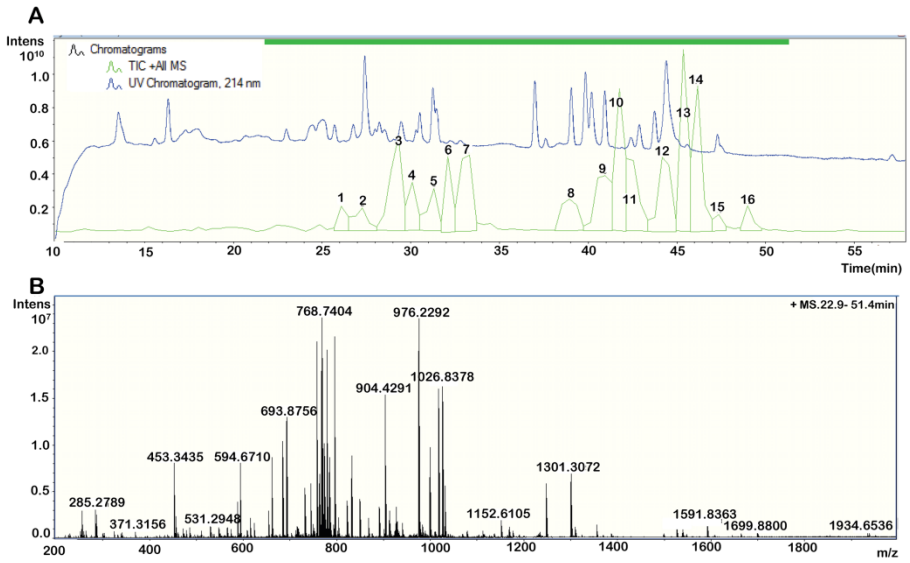


**C**

TcdA$^{540}$-*Clostridium difficile*; Average mass:65634.622 Da; Calculated pI:6.5; Peptide sequence coverage:70.76%

```
                                                                    60
MGSSHHHHHH SSGLVPRGSH MGLISKEELI KLAYSIRPRE NEYKTILTNL DEYNKLTTNN

                                                                   120
NENKYLQLKK LNESIDVFMN KYKTSSRNRA LSNLKKDILK EVILIKNSNT SPVEKNLHFV

                                                                   180
WIGGEVSDIA LEYIKQWADI NAEYNIKLWY DSEAFLVNTL KKAIVESSTT EALQLLEEEI

                                                                   240
QNPQFDNMKF YKKRMEFIYD RQKRFINYYK SQINKPTVPT IDDIIKSHLV SEYNRDETVL

                                                                   300
ESYRTNSLRK INSNHGIDIR ANSLFTEQEL LNIYSQELLN RGNLAAASDI VRLLALKNFG

                                                                   360
GVYLDVDMLP GIHSDLFKTI SRPSSIGLDR WEMIKLEAIM KYKKYINNYT SENFDKLDQQ

                                                                   420
LKDNFKLIIE SKSEKSEIFS KLENLNVSDL EIKIAFALGS VINQALISKQ GSYLTNLVIE

                                                                   480
QVKNRYQFLN QHLNPAIESD NNFTDTTKIF HDSLFNSATA ENSMFLTKIA PYLQVGFMPE

                                                                   540
ARSTISLSGP GAYASAYYDF INLQENTIEK TLKASDLIEF KFPENNLSQL TEQEINSLWS

                    560
FDQASAKYQF EKYVRDYTGG THHHHHH
```

**Figure 3.6 Representative mass spectra from the Nano-HPLC/Nano-ESI-FTICR mass spectrometry data of H-epoxy-5 treated TcdA$^{540}$ tryptic digest and TcdA$^{540}$ sequence coverage obtained from deconvoluted ESI-FTICR mass spectrum of the tryptic digestion of H-epoxy-5 treated TcdA$^{540}$.** (A) Shows overlapped chromatograms containing UV trace of separated peptides at 214 nm (Blue) and corresponding total ion count (TIC-green). For data analysis purpose the TIC trace was separated to 16 individual peaks and ions in each peaks were deconvoluted. (B) Representation of the total number of peaks containing sequence coverage information obtained after deconvoluting all 16 peaks of LC run. The peaks were obtained in the m/z range of 200-2,000 over the period of 22.9 min to 51.4 min. (C) TcdA$^{540}$ sequence coverage obtained from deconvoluted ESI-FTICR mass spectrum of the tryptic digestion of H-epoxy-5 treated TcdA$^{540}$. The data was obtained using Buker Daltonics Biotools software 3.2. Sequences highlighted in grey indicate the corresponding peptides observed in the data set. The amino acids marked in red specify the residues involved in glucosyltransferase activity. Diamonds (◆) denote every typtic cleavage sites identified from the mass spectra. The arrow (blue) indicates the peptide to which H-epoxy-5 covalently attaches to TcdA$^{540}$**.**

cross-linked fragments. In this approach maximal sequence coverage should be achieved to allow precise identification of the interaction site. Our data analysis revealed ~ 70% $TcdA^{540}$ sequence coverage (Figure 3.6), leading towards unbiased mapping of H-epoxy-5 and $TcdA^{540}$ cross-linked regions. Based on signals in the mass spectra of H-epoxy-5 and $TcdA^{540}$ cross-linked mixture, but not those of control samples from non cross-linked $TcdA^{540}$, the H-epoxy-5 interaction surface was indentified. Further in peak 4 (Figure 3.7 and Table 3.2), the signal at m/z 757.6962 can be assigned as $[M+ \text{ H-epoxy-5 } +H]^{3+}$ charged state of H-epoxy-5 cross-linked $TcdA^{540}$ fragment GNLAAASDIVR (residues 282-292 of TcdA) (Figure 3.7). The calculated monoisotopic mass of the respective cross-linked product is 22771.0801 (Table 3.2), which deviates by -3 ppm from the experimentally obtained monoisotopic mass. The overlap of theoretically obtained $[M+ \text{ H-epoxy-5 } +H]^{3+}$ isotopic distribution profile with experimental profile (Figure 3.7C) provides more agreement on assignment of the (+3) charge state.

The peptide GNLAAASDIVR lies in the core of the catalytic site including two residues (Asp-289 and Arg-292) (92) known to be involved in glucosyltransferase activity (Figure 3.8A and Figure 3.6). This further confirmed that H-epoxy-5 mediated cell protection (Figure 3.5B and 3.5C) is achieved due to the irreversible crosslink between TcdA and the derivatized peptide within the active site. Mass spectroscopy data, in agreement with computational docking studies revealed that the peptides covalently cross linked within the active site of TcdA exactly where the parent peptide was predicted to bind. In addition to the GNLAAASDIVR-H-epoxy-5 crosss-linked fragment, we also found SHLVSEYNR peptide region on $TcdA^{540}$ as another point of H-epoxy-5 cross-linking (Figure 3.8B and Table 3.2). The peptide SHLVSEYNR is located within the "upper promontories" (73). According to MD simulation studies (73), the "upper promontories" are the one of the highly flexible regions involved in a scissoring motion which in

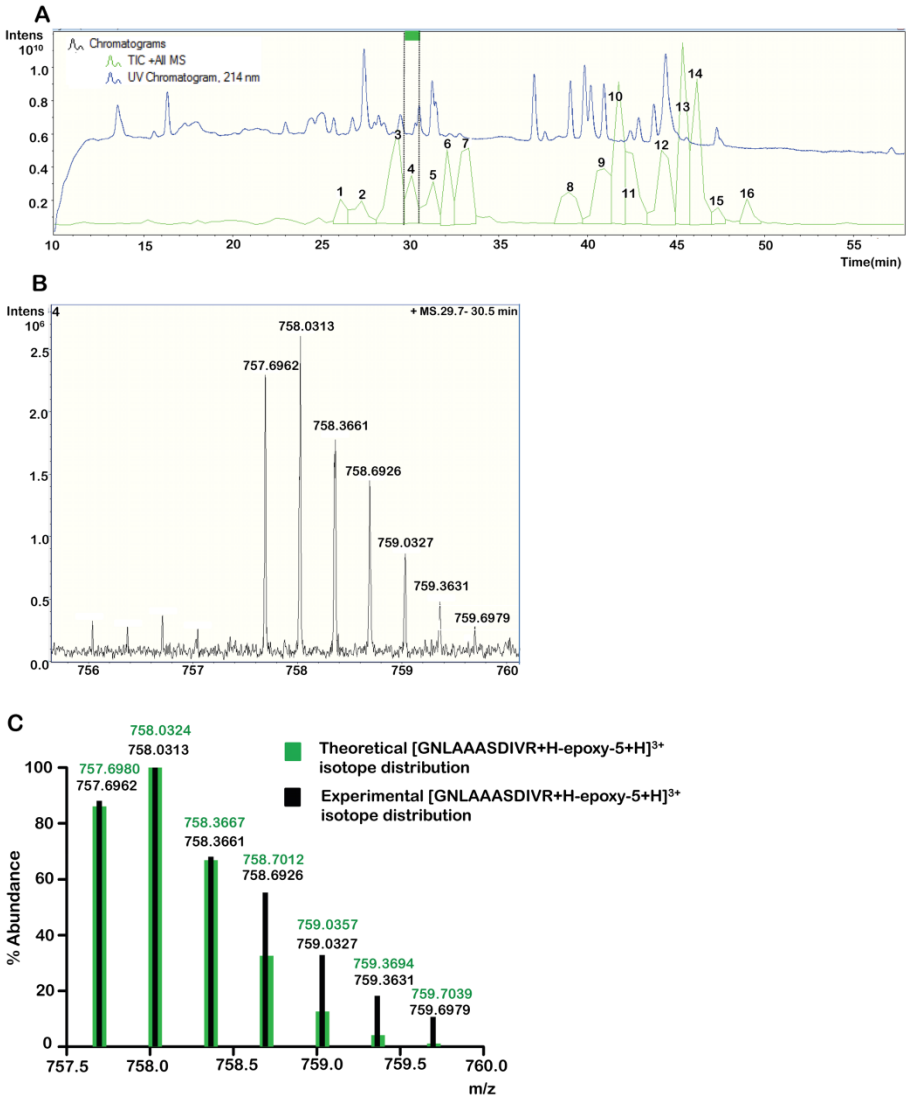


**Figure 3.7 Mass spectra from tryptic digestion of TcdA$^{540}$ after treatment with H-epoxy-5 obtained from Nano HPLC/ nano ESI-FTICR mass spectroscopy.** (A) Indicates overlapped chromatograms, consist UV trace of separated peptides at 214 nm (Blue) and corresponding total ion count (TIC, green). For data analysis purposes, the TIC trace was separated to 16 individual peaks and ions in each peak were deconvoluted. Peak 4 contained the H-epoxy-5 crosslinked-TcdA$^{540}$ peptide fragment (B) Intensity of the isotopic distribution pattern of [M+ H-epoxy-5 +H]$^{3+}$charge state of H-epoxy-5 cross-linked GNLAAASDIVR (282-292) TcdA$^{540}$ peptide fragment.(C) Illustration showing the overlap of theoretically obtained isotopic distribution profile for [GNLAAASDIVR+ H-epoxy-5 +H] $^{3+}$ and experimentally obtained charge distribution profile. The theoretical profile was obtained from Bruker Daltonics Data Analysis software version 4.0. The experimental profile was calculated using the individual peak intensities.

**Table 3. 2 H-epoxy-5 cross-linked to TcdA$^{540}$ peptide fragment GNLAAASDIVR and SHLVSEYNR peptide identified using deconvoluted ESI-FTICR mass spectra of H-epoxy-5 treated TcdA$^{540}$ tryptic digest.**

| | Observed charge state | Observed m/z | Experimental monoisotopic mass | Theoretical monoisotopic mass | Peak intensity | Deviation ± ppm | TcdA sequence range | TcdA Sequence |
|---|---|---|---|---|---|---|---|---|
| $[M_a+I]$ | $[M_a+I+H]^{3}_{+}$ | 757.6962 | 2271.0740 | 2271.0801 | $2.3 \times 10^6$ | - 0.27 | 282-292 | GNLAAASDIVR |
| $[M_b+I]$ | $[M_b+H]^{2+}$ | 1145.0212 | 2289.0351 | 2289.0332 | $3 \times 10^6$ | 0.83 | 227-235 | SHLVSEYNR |

*I: Represent H-epoxy-5 peptide*
*M: Predicted TcdA$^{540}$ peptide fragment*

turn affects the conformation of the active site of  toxin, and is predicted to be involved in substrate accommodation. Therefore, it is logical that the high flexibility of this region may thus lead to non-specific interactions with the epoxy peptide. Alternatively, binding of H-epoxy-5 to GNLAAASDIVR may lock the $TcdA^{540}$ confirmation in such that providing SHLVSEYNR peptide region as a secondary H-epoxy-5 binding site. However the specificity of the interaction has to be further clarified. This will provide more in sight on exact site of interaction and reactive nucleophile etc.

### 3.3.7 Epoxy-peptide derivatives towards therapeutic applications in future

Irreversible inhibitors are preferred lead compounds in pharmaceutics due to the requirement of clinically relevant low nano molar inhibitory constants ($IC_{50}$). In terms of therapeutic approaches for the treatment of CDAD, agents that act extracellularly would be advantageous, as higher concentrations can be achieved in the intestinal lumen compared to the systemic administrations.

During *C. difficile* infection, maintaining sufficiently high concentration of therapeutics in the gut due to the diarrhea is challenging. In this scenario effective therapeutic activity can be obtained by increasing the affinity of such compounds and formulating those that withstands the environmental conditions and proper release. Even though 95% cell protection was achieved by our epoxy-derivatized peptide, several concerns associated with its therapeutic application remain. The current compounds have high micromolar (~100 μM) $IC_{50}$ and the stability of these compounds in the GI track is as of yet untested. Although the purity of epoxy-peptide derivatives have been confirmed by analytical HPLC analysis, we have used an isomeric mixture of both (R)-and (S)-epoxides. These species can be easily resolved in the future if necessary. However it is not known which form of isomer is more potent and percentage of the specific active isomer

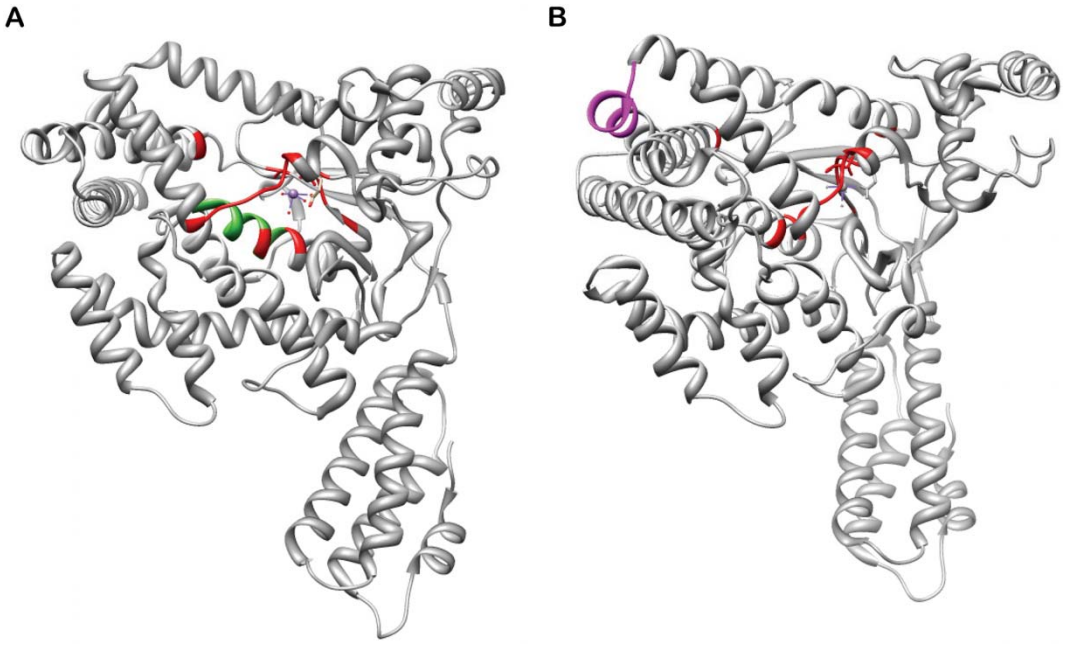


**Figure 3. 8 Ribbon structure of TcdA$^{540}$ (PDB: 2SS1) showing GNLAAASDIVR (green) and SHLVSEYNR (purple) peptide regions to which H-epoxy-5 is crosslinked. Residues marked in red are critical amino acids involved in glucosyltransferase chemistry where mutations lead to loss of activity.** (A) Showing GNLAAASDIVR peptide region where it resides amino acids (Asp-289 and Arg-292) that harbors key catalytic residues involved in glucosyltransferase activity. (B) Showing SHLVSEYNR peptide region in periphery of TcdA$^{540}$.

generated during synthesis, may lead to overall reduction in efficacy (activity/mg) of the derivatized peptides. Therefore in the future, stereo specific separation of each isomer may increase the apparent potency of the epoxy peptide. In addition to that, to further optimize our derivatives in terms of stability and potencies other electrophilic modification such as epoxy ketones/petidyl (acyloxy) methyl ketone/α-keto-β-aldehydes/a 2-pyridone/2-pyrrolidone (section 3.2) etc., can be screened in combination with *in silico* approaches.

Several other epoxide/epoxy derivatives containing drugs are FDA (U. S. Food and Drug Administration) approved or in advanced clinical trials (Table 3.3). Thus provides evidence on possibility of utilizing our epoxy peptides as potential therapeutic leads; however the key challenge in our case is to package the epoxy peptides for GI stabilization and colonic release. Several oral formulation strategies are known for compounds like the epoxypeptides. Examples include; liposomal medicated encapsulation, solid nano particle encapsulation, soft gelatin coated capsules, azo-polymers, microspheres, emulsions, mucoadhesive polymeric system and mesoporous silica-based materials etc (220-230). Ongoing work in collaboration with Prof. Joshua Reineke, Department of Pharmaceutical Sciences, Wayne State University is addressing the formulation challenges of these peptide inhibitors to achieve stability for oral delivery and controlled release in the lower GI tract. We are currently focusing on a mucoadhesive polymeric system based on poly(fumaric-co-sebacic) (pFASA) anhydride (231). In principle these polymers with large surface area, alterable pore size, and desirable biocompatibility, also have surface properties for further functionalization and differential absorptivity along the gastrointestinal tract leading to targeted binding and controlled release. The above properties make it amiable for our peptide formulation. Initially mouse models/ mouse ileal loop assays will be used understand

**Table 3. 3 Examples of epoxide containing therapeutic agents are FDA approved or in advanced clinical trails**

| Drug | Approval | Disease | Route of administration |
|---|---|---|---|
| Carfilzomib | FDA approved | myeloma | Intravenous |
| Fosfomycine | FDA approved | Urinary tract infection | Oral |
| Beloranib | Phase I clinical trial | Obesity | Subcutaneous |
| Scopolomine | FDA approved | Motion sickness | Cutaneous |
| Ixabepilone | FDA approved | Metastatic breast cancer | Intravenous |

the therapeutic relevance such as bioavailability, stability, toxicity etc. Although are still several steps to be fulfilled to attain clinical value of our peptide inhibitors, overall agents like these could be potentially used prophylactically to avoid extensive cellular damage during treatment with broad spectrum antibiotics or in populations prone to CDI.

### 3.4 Conclusions

In this study, we rationally designed an epoxide-containing peptide that acts as an irreversible inhibitor of the clostridial-glucosylating toxins sufficiently potent to protect cultured cells from intoxication. Mass spectrometry studies showed that the peptide covalently cross-linked within the active site of TcdA exactly where the parent peptides were computationally predicted to bind. While there are still several steps required to further explore in terms of the stability of these compounds that could withstand harsh gastrointestinal environments, formulation, administration etc, before these candidates can be taken to the clinic, our results can be viewed in a broader perspective. They show for the first time a pathway towards the systematic selection and design. Therefore toxin inhibitors can, if appropriately designed, irreversibly inactivate bacterial virulence factors and prevent cellular damage during infections.

### 3.5 Materials and Methods

#### 3.5.1 *C. difficile* toxin purification

All procedures with TcdA and rTcdA$^{540}$ DNA was carried out in Biosafety Level 2 lab (BL2) following standard operating procedures. The proteins were removed from BL2 only after lysate were sterile filtered and DNAase treated.

TcdA holotoxin purification

The *Bacillus magaterium* Protein Expression System (MoBiTec) was used for the expression of TcdA holotoxin. Expression was induced by addition of 1% xylose to 1L culture at $OD_{600}$~ 0.3-0.4. Cells were harvested after 4 hours growth at room temperature and lysed by sonication in 50 mM sodium phosphate, 300 mM NaCl, 10 mM imidazole, at pH 8.0, supplemented with EDTA-free complete protease inhibitor cocktail (Roche). The cell lysate was clarified by centrifugation and sterile filtered (0.22µm filter). The protein was purified using a nickel-chelated HiTrap column (GE Healthcare) and eluted with 250 mM imidazole. It was further purified over a HiLoad 16/60 Superdex 200 gel filtration column (GE Healthcare). Size exclusion column fractions were reapplied to the nickel-chelated HiTrap column to concentrate the protein and eluted in a small volume of buffer containing 250 mM imidazole. The purified protein was dialyzed into storage buffer (50 mM Sodium phosphate and 300 mM NaCl at pH 7.5 and stored at 4°C.

rTcdA$^{540}$ purification

Cloning and expression of the N-terminal minimal catalytic domain of TcdA comprising residues 1-540 (rTcdA$^{540}$) was previously reported (160). In brief, cells were lysed by sonication in 50 mM sodium phosphate, 300 mM NaCl, 10 mM imidazole, at pH 8.0, supplemented with EDTA-free complete protease inhibitor cocktail (Roche). The cell lysate was clarified by centrifugation and sterile filtered (0.22µm filter). The protein was purified using a nickel-chelated HiTrap column (GE Healthcare) and eluted with 250 mM imidazole. It was further purified over a HiLoad 16/60 Superdex 200 gel filtration column (GE Healthcare). Size exclusion column

fractions were reapplied to the nickel-chelated HiTrap column to concentrate the protein and eluted in a small volume of buffer containing 250 mM imidazole. The purified protein was dialyzed into storage buffer (50 mM sodium phosphate and 300 mM NaCl at pH 7.5 and stored at 4°C.

### 3.5.2 Crosslinking of rTcdA and peptide with benzophenone-4- iodoacetamide (BPIA) and cellular protection assay

The C-terminal Cysteine was reduced with DTT (25 mM) for 54°C for 30 minutes, and excess DTT was removed by microdialysis against water. BPIA [in 0.05 mM stock in DMSO] in 2 fold excess was added and gently stirred at 4 ºC for 1.45 hr in the dark (206). Excess BPIA was quenched with 4 fold excess 2-mercaptoethanol for 10 min in the dark. The sample was dialyzed at 4 ºC for 3 hr in $rTcdA^{540}$ storage buffer. An equimolar mixture of BP-Peptide and rTcdA were incubated at room temperature for 5 min and transferred to a petri dish. The petri dish was kept on ice and positioned underneath a hand-held UV lamp (Spectroline, Model ENF-240C) with a 5 cm distance. The solution was irradiated with UV light at 365 nm for 10 min. As a control rTcdA without any peptide was subjected to UV exposure. The samples were microdialyzed using 10 K cut off dialyzer to remove excess uncrosslinked peptides. The toxin concentrations were determined using a UV spectrometer.

Vero cells (African green monkey kidney cells) were plated in 96 well plates ($1x10^5$ cells/well) in Essential Minimal Eagles Media (EMEM,ATCC) with 10% fetal bovine serum (FBS, USA Scientific) and 1x Antibiotic-Antimycotic and then incubated 24 hrs at 37°C, 5% $CO_2$. Serum containing media was removed and exchanged with 200 µl serum free EMEM and incubated at 37°C, 5% $CO_2$ briefly while the samples were prepared. From each well, Serum free EMEM was removed and replaced with 50 µl serum free EMEM containing 0.2 nM rTcdA or

0.2 nM rTcdA-EGWHAHTGGGC cross-liked sample. [The toxin concentration was selected after titrating the activity (cell death/4 hours)]. Images were collected prior to the assay and after incubation period of 2 hrs (30 min, 60 min, 90 min, 120 min and 240 min) using a 10x objective on a Nikon Eclipse TS100-F microscope, Photometrics CCD camera and NIS-Elements Software.

### 3.5.3 Modeling of toxin catalytic domain and docking studies

Molecular models of selected peptides were built using Spartan '02 (Wave function, Irvine, California), minimizing at the AM1 level of theory. Models were saved in Sybyl mol2 format and catenated into a library for docking. Flexible docking was performed using LeadIT 2. Crystal structure 2BVL was retrieved from the RCSB database for use as the docking receptor. Crystallographic phasing markers and counter ions were removed, retaining crystallographic water molecules. The active site for docking was defined by 20Å spheres around each atom of the crystallographically observed UDP. The crystallographic catalytic manganese was replaced with a magnesium ion for ease of calculation. A docking pharmacophore with two optional constraints was constructed utilizing the two octahedral coordination sites of the magnesium occupied by the crystallographic UDP molecule. Water molecules within the active site were included in the docking, designated as fully rotatable and displaceable. Dockings were ranked an internal scoring protocol(195). Results were viewed and all images were generated using the UCSF Chimera visualization program version1.5.3. The docked structures were then simulated for 10ns to determine the stability of the docked conformation. The complete protein/peptide complex was solvated and ionized to 0.5mM NaCl and simulated using the CHARMM27 force field under NAMD on the WSU Grid Rocks cluster. A timestep of one femtosecond was used, periodic boundary conditions applied, and Langevin dynamics were utilized to maintain constant

temperature at 300K. A scaled cutoff was employed in the calculation of the long-range electrostatics.

After docking studies were performed, amino acid contributions to the binding interaction were further assessed by computational alanine scanning (CAS). In this process, a single amino acid in the peptide is replaced with an alanine and the binding energy recalculated (Table 1). The difference between the original binding energy of the peptide to the toxin and the new alanine-containing binding energy provides the contribution to binding of that side chain. From these calculations one can select amino acid sites in the peptide for derivatization based on the lowest contribution to binding energy. Additionally, each position in the peptide was replaced with an R- or S-epoxide derivative of allylglycine and subjected to docking as described above, each with the original parent peptide included in the docking library. As the docking algorithm is quite computationally demanding, the calculations were split into packets to facilitate processing. The wild type docked structure score is presented with each set. This allows determination of possible steric interference from epoxidation of the inhibitory peptides. Docked epoxide structures were ranked as described above (Table 3.1).

**3.5.4 Peptide derivatization**

C-terminally amidated, allylglycine-incorporated peptides were purchased from American Peptide Company (Sunnyvale, California) and purified. Peptides were dissolved in 0.1 M $(NH_4)_2CO_3$ buffer (pH 8.0), and the reaction vial was flushed with $N_2$. An equimolar (1:1) ratio of freshly prepared DTT was added and incubated at 54°C for 30 minutes. To the reaction mix, a 10-fold molar excess of iodoacetamide solid (Sigma) was added under $N_2$ and incubated in the dark at room temperature with continuous stirring for two hours. Iodoacetamide-labeled peptides were purified by reverse-phase HPLC over a C18 column (Beckman Coulter) using a

gradient of 0 to 100% acetonitrile containing 0.1% trifluoroacetic acid and monitored by UV absorption. After purification, the peptide was lyophilized and redissolved. The identity of each product was confirmed by ESI mass spectrometry.

To a stirred solution of $CH_2Cl_2$:0.01 M $Na_2HPO_4/NaH_2PO_4$ buffer (pH 8.0) (ratio of organic to aqueous phase, 2:1), peptide and a 10-fold molar excess of p-chloroperbenzoic acid (PCBA) was added. The reaction was kept under $N_2$ and incubated at room temperature with stirring for five hours. Reaction progress was monitored by TLC: a 34% propanol:water mix was made, then using that as a solvent a solution was made of 70% $NH_4OH$:30% of the propanol:water. After completion of the reaction, the epoxide derivative was precipitated by addition of diethyl ether and the precipitate was washed several times with ether (199,213). The peptide was dried in a lyophilizer and redissolved in water, desalted and purified by reverse-phase HPLC over a $C_{18}$ column, using a gradient of 0 to 100% acetonitrile containing 0.1% trifluoroacetic acid and monitored by UV absorption. After purification, the peptide was lyophilized and stored at -20°C until used. Purity of the epoxide-derivatized peptides was evaluated by analytical HPLC and LC-ESI. The calculated monoisotopic mass of the HQSPGallylHHGGGC peptide, after cysteine protection with acetamide $C_{47}H_{68}N_{20}O_{14}S$: 1,168.4944; found positive mass spectrum: $[M+H]^+$ m/z 1,169.5023. For final epoxized HQSPGepoxyHHGGGC peptide (H-epoxy-5) with acetamidated cysteine, calculated monoisotopic mass of $C_{47}H_{68}N_{20}O_{15}S$: 1,184.4893; found positive mass spectrum: $[M+H]^+$ m/z 1,185.5494. HQSPWHGallylGGGC peptide after cysteine protection with acetamide calculated monoisotopic mass of $C_{52}H_{71}N_{19}O_{14}S$: 1,217.51481; found positive mass spectrum: $[M+H]^+$ m/z 1,217.4238. For final epoxydized HQSPGepoxyHHGGGC peptide (H-epoxy-7) with

acetamidated cysteine, calculated monoisotopic mass of $C_{52}H_{71}N_{19}O_{15}S$: 1,233.5093; found positive mass spectrum: $[M+H]^+$ m/z 1,233.3894 and $[M+H]^{2+}$ m/z 618.9166.

### 3.5.5 Cell protection assay

Vero cells (African green monkey kidney cells) were plated in 96 well plates ($1x10^5$ cells/well) in Essential Minimal Eagles Media (EMEM,ATCC) with 10% fetal bovine serum (FBS, USA Scientific) and 1x Antibiotic-Antimycotic and then incubated 24 hrs at 37°C, 5% $CO_2$. Serum containing media was removed and exchanged with 200 µl serum free EMEM and incubated at 37°C, 5% $CO_2$ briefly while the samples were prepared. From each well, Serum free EMEM was removed and replaced with 50 µl serum free EMEM containing 0.4 nM TcdA or 0.4 nM TcdA and inhibitor [The toxin concentration were selected after titrating the activity (cell death/48 hours)]. Cells were incubated for 48 hrs at 37°C, 5% $CO_2$. Cell viability was measured using CellTiter-GLO assay (Promega), a luminescent ATP-based assay. CellTiter-GLO reagent was thawed to room temperature from -20°C. Cells were exchanged into 50µl fresh serum free EMEM at room temperature. Plates were maintained at room temperature for 45 minutes, after which 50 µl of the CellTiter-Glo reagent was added to each well. Plates were shaken on an orbital shaker for 2 minutes at moderate speed and maintained at room temperature for an additional 10 minutes before luminescence measurements were taken (Tecan GENios Plus multi label reader). Luminescence readings were compared to their corresponding negative control to obtain % cell protection using equation (1) where; $B_0$ is the luminescence intensity of cell treated with PBS, $P_0$ is the luminescence intensity of cells treated with peptide-TcdA mix and $T_0$ luminescence intensity of cells treated with TcdA. Data were collected from three independent experiments and errors were estimated based on standard propagation. Images were collected

prior to the assay and after incubation period of 28 hrs using a 10x objective on a Nikon Eclipse TS100-F microscope, Photometrics CCD camera and NIS-Elements Software.

$$\left[1-\left(B_0 - P_0 \middle/ B_0 - T_0\right)\right]\times 100 \qquad (1)$$

### 3.5.6 In-gel trypsin digestion

H-epoxy-5 and TcdA$^{540}$ were incubated together at room temperature for 20 min at a 10:1 molar ratio of peptide to toxin in phosphate buffer [50 mM Sodium phosphate and 300 mM NaCl (pH 7.5)]. Toxin samples with and without peptide were boiled at 95°C for 12 min in the presence of 4x SDS-PAGE gels loading buffer. The samples were resolved on 4-12 % gradient SDS-PAGE gel and stained with Coomasie blue. Sections of the gel containing the toxin were cut into 1 mm thick pieces and washed twice with 50 mM ammonium bicarbonate/acetonitrile (1:1) at 37°C for 30 min. After incubation, the buffer was removed and 100 µl acetonitrile was added. Once the gel plugs had shrunk, the acetonitrile was removed. The gel pieces were rehydrated in 50 mM ammonium bicarbonate for 15 min. An equal volume of acetonitrile was added and incubated for another 15 min. The ammonium bicarbonate/acetonitrile mixture was removed and 100% acetonitrile was added to cover the gel fragments. Acetonitrile was removed after the gel pieces had shrunk and samples were dried in a speedvac for 45 min to remove any excess solvent [Proteomic protocols for mass spectrometry-Bruker Daltonic Manual (version 1.0, 6.12.2000)]. Lyophilized trypsin (SIGMA- Trypsin proteomic grade) was reconstituted according to the manufacturer's protocol and 40 µl of the resulting trypsin solution was added to the gel and incubated at RT for 15 min. Then, 100 µl of 40 mM ammonium bicarbonate in 9% acetonitrile solution was added and incubated at 37°C for 6 hrs. Supernatant from the digestion containing the fragmented protein was removed and stored. Further extraction of the peptides

was accomplished by adding 50 µl of 0.1% TFA in 50% acetonitrile solution to gel pieces and incubating at 37°C for 30 min. After the final extraction the solutions were pooled with the initial digestion supernatant and the peptide digests were stored at -20°C until the mass spectrometry experiments could be completed.

### 3.5.7 Nano-HPLC/Nano-ESI-FTICR mass spectrometry

Tryptic digests were separated on a reverse phase separation column (Pep Map, C4, 75µm*150 mm, 3 µm, and 300° A, Dionex) equilibrated with 95% solvent A (0.1% formic acid in water) and 5% B (0.1% formic acid in acetonitrile). Using a Dionex nano-HPLC system, the peptides were separated with a flow rate of 30 nL/min and a 65 min gradient (0-50 min: 4-50% solvent B, 50-55 min:50-95% solvent B, 55-65 min, wash with 95% solvent B). The peptides were detected based on their UV absorption at 214 and 280 nm. For the LC/MS data acquisition, Hystar software (Bruker Daltonics) was used. Nano-HPLC system was coupled on-line to a FTICR mass spectrometer (SOLARIX, Bruker Daltonics) using a nano-electrospray ionization source (Bruker Daltonics). The capillary voltage was set to -1,500 V. Mass spectral data were acquired at estimated resolving power of 9,900 at 400 m/z over a m/z range of 150-2,000 with 1 MW data size. Averages of 10 scans were accumulated per spectra. Data were acquired over 70 min time. Data acquisition, data processing and data analysis were performed using Data Analysis version 4.0 (Bruker Daltonics) and Biotools 3.2 (Bruker Daltonics). After deconvolution of the ESI mass spectra, manually created monoisotropic masses peak lists were used for calculating masses of cross-linked products.

# CHAPTER 4

## Characterizing the regulatory roles of a putative negative regulator TcdC in *C. difficile* toxin gene expression

### 4.1 Abstract

*C. difficile* toxin production has been known to differ greatly among strains and is influenced by a range of environmental factors. High toxin producing epidemic strains carry a common mutation in a putative negative regulator (TcdC). Various correlations were made between the truncated forms of TcdC and increased disease severity as a result of higher levels of toxin expression. However the exact mechanism of TcdC-mediated regulation is not fully understood. Here we employed genetic and biochemical approaches to further elucidate the role of TcdC on the pathogenesis of *C. difficile* using *E. coli* as a surrogate host. This study reveals that TcdC is not a repressor as it was proposed, but rather acts as an anti-sigma factor and negatively regulates *tox* gene expression via a direct interaction with RNA polymerase. GFP (green fluorescent protein)-based fusion studies clarified the fact that the truncated form of TcdC derepress the *tcdA* promoter activity. Our study provides evidence that the hampered activity of the truncated form of TcdC is mainly due to the loss of a ~50 amino acid region that constitutes a putative N-terminal signal peptide.

### 4.2 Introduction

Epidemiology of *C. difficile* associated diseases (CDAD) has changed dramatically over the past decade, predominantly due to the emergence of hyper-virulent strains that have grater antibiotic resistance and changes in virulence properties (232,233). Disease severity with above strains has been proposed to associate with significantly higher levels of expression of toxins, higher sporulation rates and secretion of an actin-ADP-ribosylating toxin known as the binary

toxin (CDT) (234). PaLoc genes are regulated in a highly complex manner by multiple regulatory networks (45). Under normal growth conditions, toxin synthesis increases as cells enter stationary phase and is stimulated by addition of certain amino acids, antibiotics, biotin and is inhibited by rapidly metabolizable carbon sources, etc (43-45). Both *tcdA* and *tcdB* encode for major *C. difficile* virulence factors that are located within a 19.6 kb pathogenicity locus (PaLoc) together with three accessory genes *tcdR*, *tcdE* and *tcdC* (Figure 4.1) (37) which encodes an alternative σ factor, a proposed toxin releasing protein (the definite role of TcdE is controversial in the field) (42,235) and a negative regulator respectively.

TcdR plays a crucial role in specific transcriptional activation of *tcdA*, *tcdB* promoters as well as its own promoter during stationary phase (38,47) which implicates that even a very low level of TcdR accumulation will amplify its regulatory role. Therefore, very tight regulation of *tcdR* is essential for successful invasion of host by *C. difficile*. Based on this scenario, several other regulatory circuits have been identified to act upon TcdR expression. CodY the global negative regulator of gram positive bacteria has been shown to mediate growth dependent toxin gene regulation by repressing toxin genes during the exponential phase via binding to the *tcdR* promoter (43). The catabolic control protein CcpA, a regulatory protein mediates catabolic repression based on rapidly catabolizable carbon sugars, was found to bind to both *tcdA* and *tcdB* promoter regions (45) as well as *tcdR* and *tcdC* regulatory regions . TcdE has been shown to facilitate the release of *C. difficile* toxins to the extracellular environment (42), however another recent study based on insertionaly inactivated PaLoc *tcdE* has questioned this role (235).

The putative negative regulator TcdC is a highly charged acidic protein (37,236). Bioinformatics analyses suggest that TcdC does not have sequence or structural homology to any known regulatory proteins. PsiBLAST alignments did identify several proteins with putative

evolutionary relationships to TcdC; however, none of them were funcationally characterized. Growth dependent transcriptional analysis shows that *tcdC* expression is maximal during the exponential phase and greatly reduced when cells enter stationary phase, in contrast to other genes encoded within the PaLoc. (37). The negative regulatory role of TcdC was first characterized *in vivo* by a reporter fusion study (237). To date, the actual mechanism by which TcdC negatively regulates *toxin* gene expression in not clearly understood. It has been reported that upstream genes of PaLoc (*tcdR, tcdB, tcdE, tcdA*) are transcribed from their own promoter, as well as by read-through transcription from the promoter *tcdR* (Figure 4.1) (37,46). Moreover, transcription of gene-specific promoters are repressed during the exponential growth phase but induced when cells enter stationary phase, leading to speculation that there should be a common regulatory node which represses *tox* gene-specific promoters during exponential phase. Expression of TcdC has been shown to interfere with the interaction between TcdR and RNA polymerase holoenzyme based on a *in vitro* run-off transcription assay (237). However, direct binding between TcdC with TcdR/RNA polymerase core enzyme has not been shown. The above observations prompted us to test the hypothesis that TcdC can act as a repressor by binding to promoter regions and interfering with transcription initiation. On the other hand TcdC may act as an anti-sigma factor and down regulate gene expression by interfering with the activity of its cognate sigma factor TcdR or with RNA polymerase.

High toxin producing epidemic strains including NAP1/027 carry either a common 18 base pair deletion or a frame shift mutation in *tcdC* resulting in the production of a truncated form of TcdC [Explained in detail in Figure 4.6 and Section 4.3.4] (33). This mutation leads to the proposal that high levels of toxin expression in epidemic strains may be associated with the presence of a truncated, non-functional form of TcdC. However, due to lack of experimental

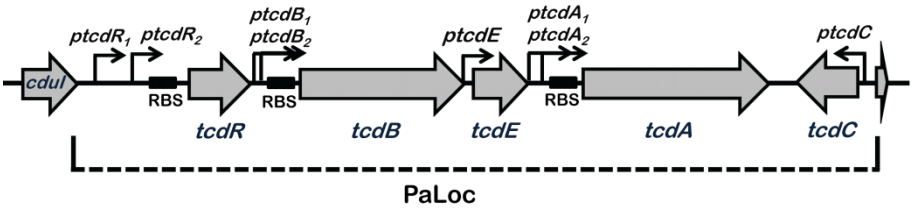


**Figure 4.1 Genetic organization of the *C. difficile* 19.6 kb pathogenicity locus (PaLoc)**. PaLoc consists of 5 coding regions, including genes that encode for two cytotoxins TcdA (*tcdA*), TcdB (*tcdB*) attributed to disease symptoms and the other three proteins TcdR (*tcdR* ), TcdE (*tcdE) and TcbC (tcdC)* are shown to be functional in gene regulation and toxin release. All five coding regions have their own putative promoter regions [Modified based on (238)].

evidence, the exact regulatory network of TcdC and its association with high toxin production remains controversial in the field (239,240). Therefore understanding the regulatory mechanism of toxin gene expression is crucial for exploring the pathogenesis of *C. difficile*. Moreover this knowledge can be utilized in the development of new strategies for treating/preventing *C. difficile* infections.

### 4.3 Results and Discussion

#### 4.3.1 TcdC undergoes N-terminal cleavage *in trans*

TcdC is a membrane associated protein with 3 predicted functional regions that comprise an N-terminal membrane spanning region, a highly charged mid-helical coil-coil domain and a C-terminal region postulated to be involved in its negative regulatory role (Figure 4.2A) (237). We designed two different recombinant TcdC constructs, one bearing a $His_6$ tag at the N-terminus and the other with the tag on C-terminus. We selected this approach because it was unclear whether one or both termini would be functionally affected by the extra amino acids.

A previous study reported that the N-terminal region may be involved in dimerization (236). If dimerization is essential for its function, introducing a $His_6$-tag at the N-terminus may disturb its activity. In this case, using a C-terminal $His_6$-tag TcdC in binding studies would be more appropriate. On the other hand if the C-terminal region of TcdC is essential for its regulatory role, introducing an N-terminal $His_6$-tag will be more relevant. Both constructs were cloned and expressed in *E. coli* BL21 (DE3) expression cells and proteins were purified using IMAC (Immobilized metal ion affinity chromatography) and an imidazole step gradient for elution. Interestingly, the SDS-PAGE analysis of purified TcdC exhibited two very closely spaced bands (< 5 kDa difference) (Figure 4.2B). The overall yield (mg/L culture) of purified TcdC obtained from N-terminal $His_6$-tag was significantly lower than that of the C-terminal

$His_6$-tag. Even though we used protease inhibitors during lysis and purification we explored the possibility that TcdC undergoes proteolytic processing *in vivo* or during purification steps. The above observation was consistent with a recent study that monitored TcdC expression levels in *C. difficile* strain VPI10463 by western blot analysis over time (239). They too observed two TcdC isoforms but interpreted their data in light of the potential that the existence of two protein bands in gels are due to cross-reactivity of their TcdC-specific antibody with another protein of slightly different molecular weight. In our case, we were using an anti-$His_6$ antibody rather than a TcdC antibody, so the cross reactivity pattern should not have been the same. Thus, we hypothesized that TcdC may be undergoing proteolytic cleavage *in vivo* and questioned the potential relevance of this cleavage to its function.

In order to identify the processing site, we first utilized purified TcdC harboring either N or C-terminal $His_6$-tags. Western blot analysis was performed with HisProbe-HRP (Thermo scientific), a nickel ($Ni^{2+}$) activated derivative of horseradish peroxidase (HRP) used for the detection of proteins with poly-histidine-tags. If TcdC undergoes an N-terminal cleavage, the product would lack a poly-histidine tag. As a result, the majority of TcdC would be present without a poly-histidine tag. Accordingly, western blot analysis reveal, purified N-terminally $His_6$-tagged TcdC lacks corresponding signal for poly-histidine tag (Figure 4.2B). On the other hand, C-terminal $His_6$-tagged TcdC retains poly-histidine tags on both closely spaced bands (Figure 4.2B). The above observation provides a clue that TcdC may undergo N-terminal cleavage (Figure 4.2B).

To further understand the identity of the cleavage product we performed bioinformatic-based search using several software packages [ Expasy SignalP V2.0.b2

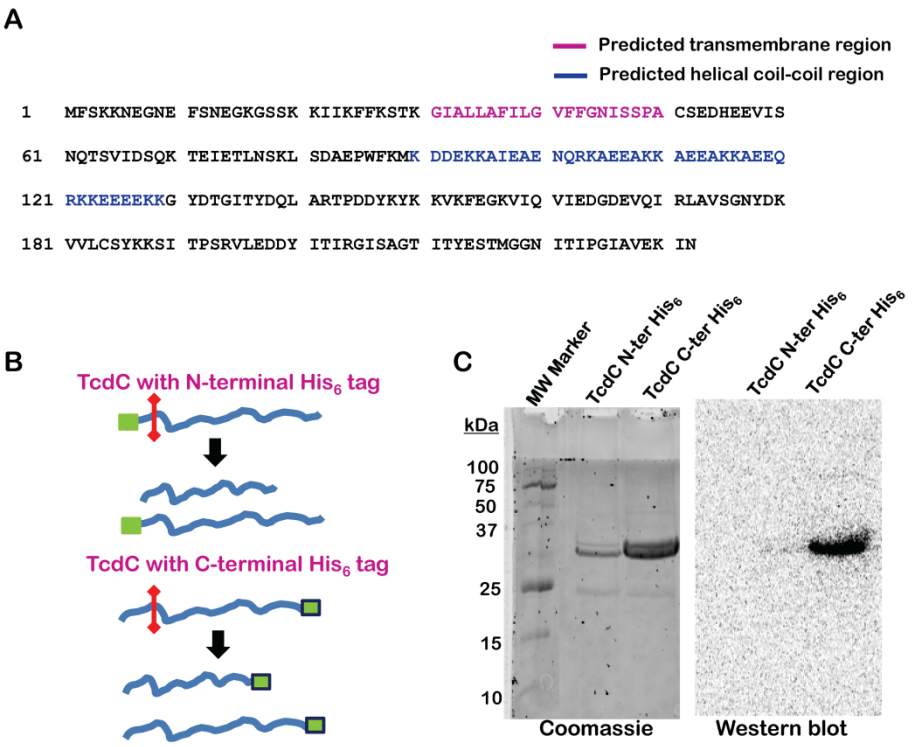


**Figure 4.2 Amino acid sequence of TcdC and proteolytic cleavage pattern of purified TcdC.** (A) Amino acid sequence of TcdC [*C. difficile* 630] with predicted functional regions. An N-terminal transmembrane region (magenta) highly charged helical coil-coil region with alternative acidic and basic residues followed by the C-terminal functional region. (B) Proposed N-terminal cleavage pattern of both recombinant N-terminal $His_6$-tagged and C-terminal $His_6$-tagged TcdC. Blunt end arrow (red) denotes the cleavage and green boxes represents the poly-histidine-tags. (C) Coomassie and western blot analysis of purified N-terminal His6-tagged and C-terminal $His_6$-tagged TcdC. Coomassie stain analysis of denaturation SDS-PAGE indicates barely separated two protein bands (~34 kDa). Corresponding western blot is indicated in far left. Where in the case of C-terminal His6-tagged TcdC, an intense chemiluminescence signal includes both full length and cleaved TcdC with poly-histidine-tag. However in N-terminal $His_6$-tagged TcdC, the lack of corresponding chemiluminescence signals signifies the absence of the poly histidine tag.

(http://www.cbs.dtu.dk/services/SignalP-2.0/) (18,19) (Figure 4.3B), PredSi (http://www.predisi.de/) , Phobius perdiction (http://phobius.sbc.su.se/) ] to classify possible signal peptide sequence within the TcdC sequence that might be removed by subsequent processing. Interestingly, all of the algorithms predicted a putative N-terminal ~ 52 amino acid length signal peptide with a predicted serine protease cleavage site between amino acid Ser52 and Glu53 (Figure 4.3A and 4.3B). The above observation led us to ask a series of questions regarding the physiological roles of signal peptides in toxin gene regulation (discussed in section 4.3.4), an exploration of the exact site of cleavage and what proteases might be involved in cleavage.

To probe the site of cleavage, we performed MALDI-TOF analysis on purified C-terminally $His_6$-tagged TcdC. According to the mass spectrum (Figure 4.3C and Table 4.1), the m/z at 53,911.01 can be assigned to intact C-terminally $His_6$-tagged TcdC dimers, whereas the corresponding monomer was observed at m/Z of 27,172.54. Peak at 42, 548.334 m/z can be assigned to dimer of a processed C-terminal hexa-His tagged TcdC with a theoretical mass of 42,937.68 m/z (~ 289 Da deviations, Table 4.1). However we were not able to obtain a peak corresponding to the signal peptide deleted TcdC monomer (21,468.840 m/z). This could be due to the observed base-line shift of spectra in the related m/z region. The base-line shift (high noise) may associate with the protein storage conditions (high concentration of glycerol and Triton X-100). The above observation suggests that TcdC exists predominantly as dimers and supports that TcdC undergoes cleavage near the predicted signal peptide region. In future bottom-up proteomic profiling/ N-terminal sequencing approaches can be employed to obtain the precise identity on the origin of cleavage.

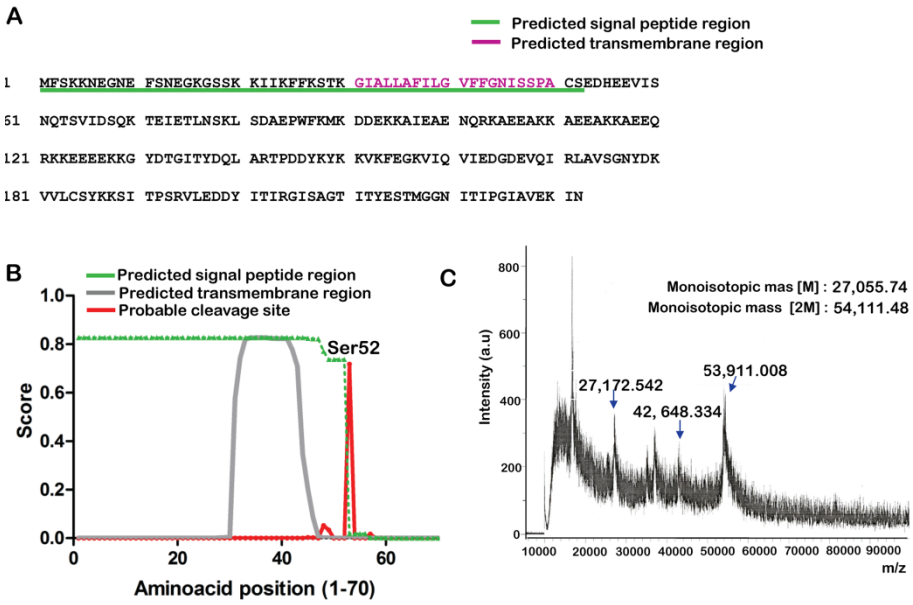


**Figure 4.3 N-terminal signal peptide region prediction and MALDI-TOF analysis of purified TcdC.** (A) TcdC amino acid sequence showing the predicted N-terminal signal peptide region with putative cleavage site between Ser 52 and Glu 53. Plot indicates the SignalP-HMM prediction scores of gram-positive model obtained from Expasy SignalP V2.0.b2 software. Signal peptide probability: 0.828 and maximum cleavage site probability: 0.718 between position 52 and 53. (C) MALDI-TOF spectra of purified TcdC with C-terminal $His_6$ tag. Sinapinic acid was used as matrix. Above spectra reveals TcdC predominantly exists as dimmers.

### 4.3.2 TcdC does not directly interact with upstream PaLoc promoters

Secondary structure predictions of TcdC sequence revealed that it lacks a conserved (helix-turn-helix) DNA binding motif and could exists as a homo-tetramer or homo-dimer (13). Such organization would be consistent with an oligonucleotide binding fold (OB fold) common among DNA binding proteins (20) or a zinc finger-like DNA binding protein (21). Based on this concept we proposed oligomeric form of TcdC may form potential DNA binding motifs and acts as a repressor by binding to promoters regions.

Gel mobility shift assays were used to probe the interaction between TcdC and upstream promoter regions of TcdC. Both N- terminal and C-terminal $His_6$-tag TcdC were tested for DNA binding activity. As a potential DNA target, we initially selected the full length promoter *tcdR* region (246 bp) (Figure 4.4 A and 4.4B). The 5' UTR of *tcdR* contains two short putative promoter segments and a putative operator (Figure 4.1A, 4.4A and 4.4B). But regulatory factors that are involved in tuning of these promoter regions are poorly understood. Therefore to begin with, we analyzed the binding of TcdC with a longer DNA segment harboring both $ptcdR_1$/$ptcdR_2$ regions (246 bp) (Figure 4.4A) (43) and with individual shorter DNA segments (~ 60 bp) containing putative $ptcdR_1$ and $ptcdR_2$ regions (Figure 4.4A and 4.4B) (37). Based on these experiments neither N- nor C terminal tagged TcdC showed any significant binding with *ptcdR* (Figure 4.4C) promoter DNA regions. Although TcdC failed to bind the *tcdR* promoter, it does not overrule the possibility of TcdC having a potential binding preference to other promoter regions of PaLoc (Figure 4.1A). Due to the fact that the transcription of gene-specific promoters is repressed during the exponential growth phase, we hypothesized (46) that TcdC may repress the transcription of gene specific promoters (*ptcdB, ptcdE, ptcdA*) in PaLoc. Consequently we extended our gel mobility shift assays to putative *tcdA* and *tcdB* promoter regions (Figure 4.4D).

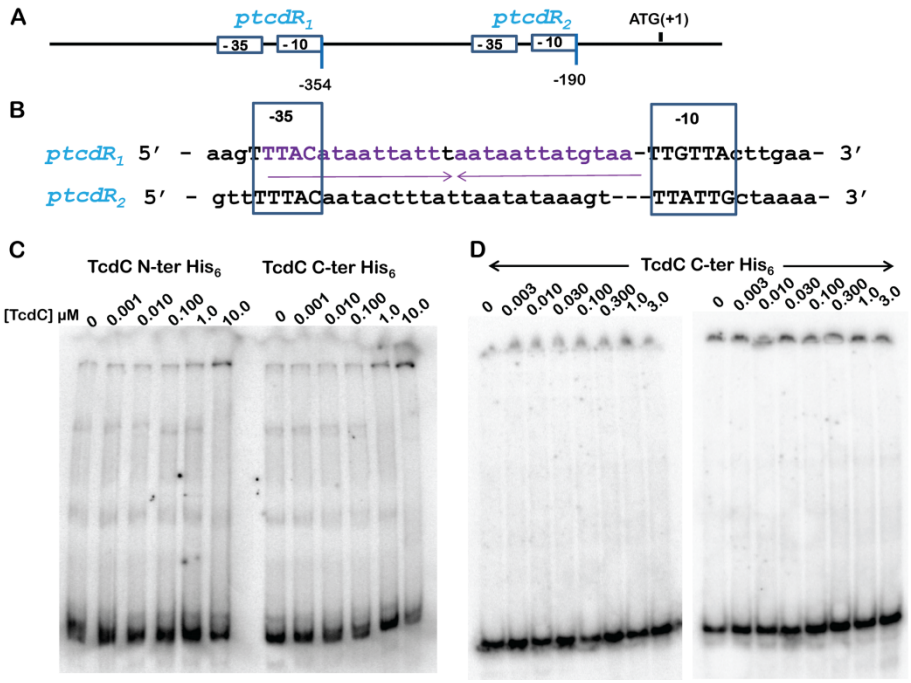


**Figure 4.4 Functional characterization of TcdC as a DNA binding protein.** (A) Schematic of promoter *tcdR* region. (B) Sequence of individual short promoter elements *ptcdR'* and *ptcdR.* Vertical bars represent the -35 and -10 boxes of gram positive bacteria. Purple arrows indicate a sequence with twofold symmetry which presumably functions as an operator region. (C) Analysis of both N-termianl and C-termianl $his_6$ tagged TcdC interaction with *tcdR* (246 bp) promoter region. $^{32}P$ labeled *ptcdR* was titrated with varying concentrations of TcdC. Showing no interaction of TcdC with promoter tcdR . (D) Electromobility shift assay of C-terminal $his_6$ tagged TcdC with individual short promoter segments *ptcdB1* (51bp) and *ptcdB2* (54 bp) accordingly.

**Table 4.1 m/z observed for TcdC-C-terminal $His_6$ by MALDI-TOF analysis**

| | Theoretical mass (m/z) | Experimental mass (m/z) | Deviation (±Da) |
|---|---|---|---|
| TcdC-C-terminal $His_6$ tag monomer | 27,055.74 | 27,172.542 | -116.802 |
| TcdC-C-terminal $His_6$ tag dimer | 54,111.48 | 53,911.008 | 200.472 |
| Signal peptide deleted TcdC-C-terminal $His_6$ tag monomer | 21,468.84 | Not found | - |
| Signal peptide deleted TcdC-C-terminal $His_6$ tag dimer | 42,937.68 | 42, 648.334 | 289.346 |

Consistent with promoter *tcdR* binding studies, TcdC showed no significant binding interactions with *ptcdA* or *ptcdB*.

While this was a negative result, we envisioned the lack of interactions could be due to a mechanism in which a co-factor was required to stimulate DNA binding. Several such cases are known in gram positive bacteria including: a mechanism by which pathogenic gram positive bacteria sense nutrients using small molecules such as GTP, cyclic nucleotides (cGMP), branched amino acids, metal ions ($Fe^{2+}$) etc (43,245) where molecules can act as co-repressors by increasing the affinity of repressors to target DNA in which TcdC-*ptcdR* interaction may require other small molecules for efficient DNA binding. To test this phenomenon, gel mobility shift assays were performed in the presence of small molecules such as GTP and $Mn^{2+}$. None of the co-factors we tested affected the binding and we still failed to observe any interaction between TcdC and ptcdR DNA.

The collection of negative results led us to ask whether it was possible that TcdC repress PaLoc genes through a mechanism other than direct DNA binding. However we cannot exclude the possibility that TcdC acts in conjunction with other proteins/small molecules to bind DNA and perform growth dependent *tox* gene repression. Despite this, as an alternative mechanism, TcdC may destabilize the interaction of TcdR-RNA polymerase core enzyme and function as an anti-sigma factor (246).

### 4.3.2 The *ptcdA*-GFP expression system for analysis of TcdC mediated gene regulation *in trans*

To understand the functional role of TcdC as an anti-sigma factor and to elucidate the activity of truncated forms of TcdC found in hyper virulent strains and signal peptide deleted version of TcdC, we designed an Emerald green fluorescent protein (EmGFP)-based three-

plasmid system (Figure 4.5A) which can be expressed in *E. coli*. Although *E. coli* is not an ideal heterologous host, the fact that *E. coli* lacks any homologous protein sequences to TcdC or TcdR helps its use as an adequate surrogate host and further confirming this, *E. coli* was successfully employed in TcdR mediated *tox* gene regulation studied by Scott et al.,(39). To allow the expression of *tcdR*, *tcdC* and promoter-*tcdA* in *trans*, we sub-cloned the toxin promoter *ptcdA* in frame with EmGFP into a low-copy number plasmid (247), which can co-exist with the pT7-*tcdR* and pBAD-*tcdC* vectors (Figure 4.5A**)**.

In order to validate our plasmid system, GFP expression levels were monitored in the presence and absence of both TcdR and TcdC over a 13-hour time course spanning exponential to early stationary phase. At 7hrs (late exponential phase) time point, cells were withdrawn and GFP levels were measured in cell lysates. The strains harboring 2 plasmids were also used as a control to monitor the tightness of *pT7* and *pBAD* promoters. GFP expression rose significantly when TcdR was co-expressed *in trans* (Figure 4.5B). The above data validates that TcdR activates promoter *tcdA in vivo*. Furthermore the ability to up-regulate promoter *tcdA* by TcdR was diminished when TcdC was co-expressed (Figure 4.5B). Consequently the above observations reveal the presence of a negative regulatory role of TcdC on *ptcdA*-EmGFP expression in our system just as it would in context of the PaLoc. Our initial data are nicely in line with previous findings pertaining to this mode of regulation in gram-positive bacterial models and are indicative of the proper functionality of our GFP-based fusion system in *E. coli* (39).

### 4.3.3 Truncated TcdC modulates tox gene expression

The main phenotypic differences found in epidemic strains include, enhanced toxin production, faster sporulation rates, secretion of binary toxin and increased antibiotic resistance

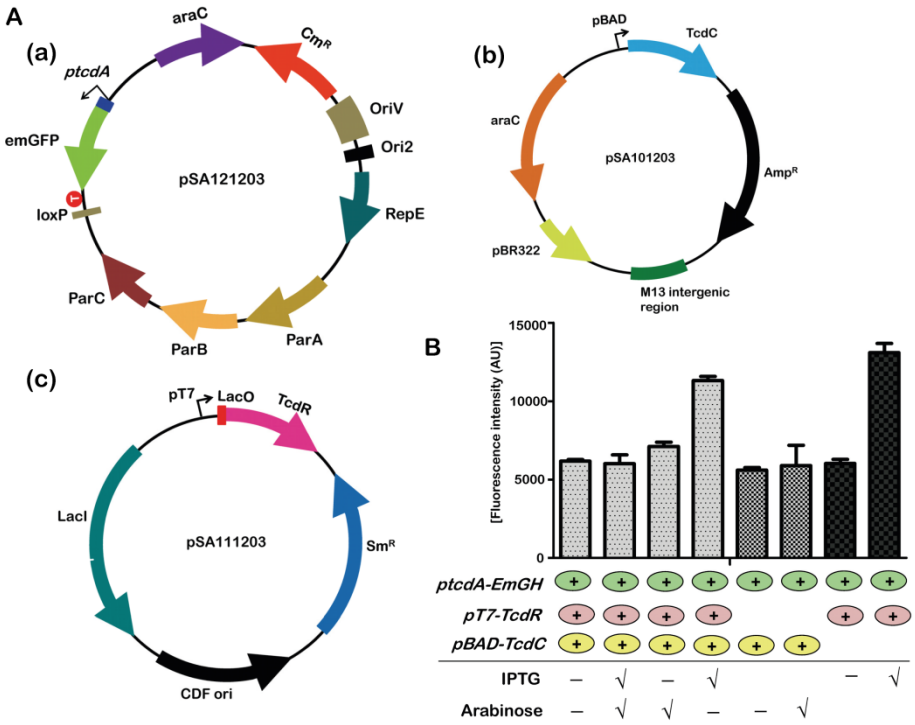


**Figure 4.5 GFP fusion system designed to measure the transcriptional regulation of promoter *tcdA* in the presence of other regulatory proteins TcdR and TcdC.** (A) Representative image showing the three-plasmid systems (a) 5' UTR of *tcdA* fused in frame with GFP (*ptcdA-EmGFP*). The fusion plasmid maintains a low copy number in cells (b) *tcdC* was cloned under the control of a *pBAD* promoter (*pBAD-tcdC*) and expression of TcdC is induced by L-arabinose. (c) *tcdR* was clone under control of a *pT7* promoter (pT7-TcdR). TcdR expression can be induced by IPTG. (B) Fluorescence measurements respective to *ptcdA-EmGH* expression system at 7 hrs. Cells were co-transformed with either two plasmids or all 3 plasmid constructs. Bacterial cell cultures were generated from overnight cultures and after 3 hrs of growth ($OD_{600}$ ~ 0.4 to 0.5) positive controls were induced with either L-arabinose or IPTG or both. Fluorescence measurements were obtained from cell lysates. All fluorescence measurements were at least triplicated using independent inoculations. In cells harboring plasmids *ptcdA-EmGFP* and *pT7-tcdR*, GFP levels were significantly high (~2 fold) when TcdR is co-expressed confirming the functionality of fusion system *in vivo*.

(26). The epidemic strains bear two common mutations in the *tcdC* gene, an 18 base pair deletion and a frame shift mutation at position 117 that consequently leads to the production of an 88 amino acid N-terminal truncated form of TcdC (Figure 4.6A) (248,249). In order to address questions regarding the function of the truncated versions of TcdC and high toxin production, as well as to discover the functional role of the proposed signal peptide region (Section 4.3A), we used our GFP-based fusion system *in trans*. TcdC with an 88 N-terminal amino acids deleted mutant ($TcdC_{frame\text{-}shift}$) and a mutant lacking the 52 amino acids signal peptide ($TcdC_{\Delta signal\ peptide}$) were cloned in frame with a *pBAD* promoter. The functional role of $TcdC_{\Delta signal\ peptide}$/ $TcdC_{frame\text{-}shift}$ mutants on promoter *tcdR* was monitored in the presence of the activator TcdR. Relative repression levels of each forms of TcdC (wild type and mutants) were calculated by comparing the GFP levels in both TcdR, TcdC co-expressed cells with corresponding TcdR only expressed cells. As seen in Figure 4.6B, ~85% repression was observed in cells expressing wild type TcdC. Interestingly, in the presence of either $TcdC_{\Delta signal\ peptide}$ or $TcdC_{frame\text{-}shift}$ mutants, significant reduction in repression was observed, 50% and 30% correspondingly (Figure 4.6). Therefore the loss of negative regulatory functions of the mutants may lead to enhanced promoter *tcdA* mediated GFP expression. As well as the data further reveals the signal peptide region indeed plays a crucial role in regulatory activity of TcdC. Consistent with a recent study (239), our data provides more evidence that the truncated TcdC found in epidemic strain may be an important determinant in its association with high toxin production. In addition to that, the loss of function of the signal peptide deleted mutant leads to the postulation that the lack of activity of truncated mutations found in epidemic strains may be a result of deletion of signal peptide bearing region. Furthermore due to presence of the functional

role of the putative signal peptide region predict the likelihood of TcdC being an ECF (Extra Cytoplasmic Functions) anti-σ-factor (Section 4.3.5 and Section 4.3.6).

**4.3.4 TcdC may act as an anti-sigma factor**

One mechanism for regulating transcription utilizes interaction between a sigma factor and a second protein known as an anti-sigma factor (38,250-252). TcdR, an alternative sigma factor used to express *tox* genes shows similarities to the ECF (Extra Cytoplasmic Functions) subfamily σ factors, that regulate a wide variety of functions by sensing growth conditions in the membrane, periplasm or extracellular environments (246,253,254). These σ factors are often regulated by cognate anti- σ factors. ECF subfamily anti-sigma factors typically have a sensor domain in the periplasm and a regulatory domain in the cytoplasm (246,251,255). Due to the fact that TcdC has a putative single pass trans-membrane domain and a putative signal peptide region we postulate that TcdC may be a member of the ECF class anti-σ factors (236). By definition, all anti-σ factors act by binding to cognate σ factors and prevent the interaction with RNA polymerase. However, to date there is no evidence showing a direct interaction between TcdR and TcdC.

In *C. difficile*, expression of TcdC occurs predominantly during exponential phase (239), whereas TcdR is expressed during stationary phase. Presumably, depending on the cytoplasmic concentrations of TcdC and TcdR, TcdC may compete with TcdR for core RNA polymerase instead of actively promoting the dissociation of TcdR from the pre-formed RNA polymerase holoenzyme. Therefore in order for TcdC to act as a negative regulator during exponential phase, it needs to directly interact with the RNA polymerase core enzyme instead of TcdR.

Many biochemical methods such as co-immunoprecipiation (256), blue native PAGE (257), *in vitro* binding [Surface plasma resonance (SPR) (258), isothermal titration calorimetry

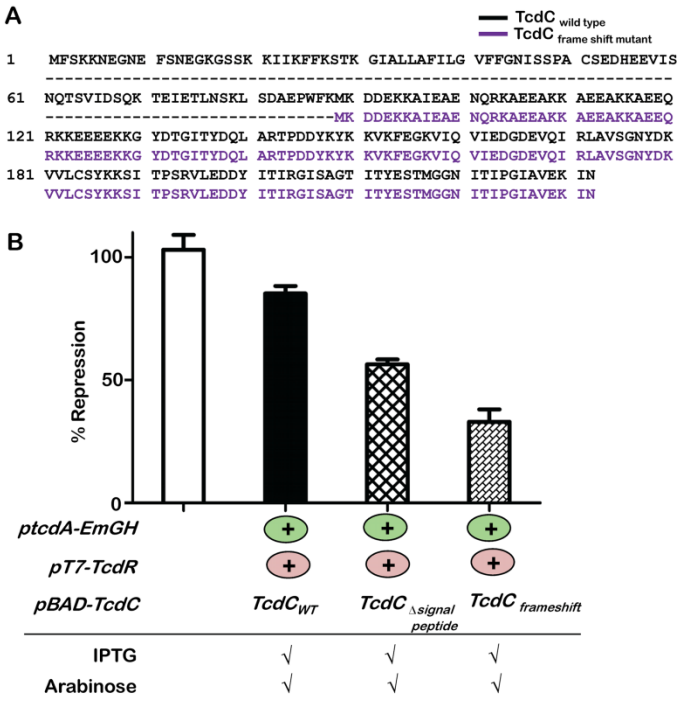


**Figure 4.6 Functional characterization of signal peptide and truncation mutation of TcdC.** (A) Sequence alignment of TcdC wild type with truncated form of TcdC obtained from single frame shift mutation. The epidemic hypervilulence strains harbors an 88 amino acids deleted truncated form of TcdC. (B) In order to probe the physiological role of truncated forms of TcdC, *ptcdA-GFP* expression levels were monitored in the presence of $TcdC_{\Delta signalpepetide}$, $TcdC_{frameshift}$ mutants and TcdR. % repression was compared with average of GFP expression level in the presence of $TcdC_{WT}$, $TcdC_{\Delta signal\ pepetide}$ and $TcdC_{frameshift}$ (white bar). There is a significant reduction in repression levels in the presence of $TcdC_{\Delta signal\ pepetide}$ and $TcdC_{frameshift}$ mutants.

(ITC) etc], chemical cross-linking (259-261), rate-zonal sedimentation (262) can be used to characterize protein-protein interactions. In a cell, proteins can take part in a highly complex network of interactions, which can be characterized as transient to weak interactions or highly stable multiple protein interactions. A method of analysis to study these interactions is selected depending on the nature of interactions and purpose of analysis etc. We used a combination of chemical cross-linking and co-immunoprecipitation to probe TcdC-RNA polymerase interaction *in vivo*. Chemical cross-linking provides a direct means of probing both transient and stable protein interactions *in vivo* and *in vitro*. We opted for chemical cross-linking to preserve any transient interaction *in vivo* and co-immunoprecipitation to separate and identify specific proteins of interest. In our study para-formaldehyde was chosen as the cross-linking agent, since it is a membrane permeable, small molecule having reactivity by means of adjacent Lysine residues. Although it has an interaction distance of just of 2Å, it is considered as a "zero length" cross-linker, meaning it cross-links protein interactions which are in very close proximity, consequently avoiding many non-specific protein-protein interactions *in vivo* (263).

We utilized a GFP-based fusion system to gain more evidence on the TcdC-RNA polymerase interaction *in vivo*. For the pull down and detection purposes TcdC with a C-terminal $His_6$ tag was cloned under the control of *pBAD* promoter. Cells were grown in identical conditions similar to the GFP-based fusion study (Materials and Methods) and harvested after 7 hrs of growth. Next, 1% paraformaldehyde in PBS was used to cross-link any protein interactions *in vivo* (Materials and Methods) (264-266), followed by mild enzyme-based cell lysis in the presence of 1% Triton X-100 to maintain optimal conditions for solubilizing membrane bound proteins and to ensure release of membrane-bound TcdC. Two immunoprecipitation strategies were used to pull down TcdC-RNA polymerase. First, an

immnunoaffinity pull down using *E. coli* RNA polymerase monoclonal antibody specific for β subunit was carried out and probed for the presence of TcdC C-ter $His_6$ tag via a nickel ($Ni^{2+}$) activated derivative of horseradish peroxidase (HRP) used for the detection of proteins with poly-histidine-tag (Figure 4.7A). Secondly, a complimentary reverse pull down of TcdC C-ter $His_6$ tag by Ni-NTA affinity beads was performed and probed for the presence of RNA polymerase by western blot analysis with *E. coli* RNA polymerase β monoclonal antibody (Figure 4.7B). In both approaches paraformaldehyde cross-link was released by heating with SDS-PAGE gel loading dye for 15 min at 95°C before SDS-PAGE and western blot analysis. Accordingly, [Figure 4.6Aand 4.6B] western bolt analysis reveals, RNA polymerase β antibodies precipitated TcdC (Figure 4.7A, Lane 4) in its immunocomplex, which was confirmed by loading affinity purified TcdC with poly-histidine-tag (Figure 4.7A, Lane 5). On the other hand in the Ni-NTA pull down of poly-histidine-tagged TcdC, precipitated RNA polymerase (Figure 4.7B, Lane 4). Both blots lack corresponding bands in washing steps (Figure 4.7A, Lane 3 and Figure 4.7B Lane 3 ), indicating that the washing conditions are sufficient enough to eliminate non-specific binding interactions and the observed corresponding immuno-eluted bands (Figure 4.7A, Lane 4 and Figure 4.7B, Lane 4) were due to specific protein-protein interactions. Both approaches confirmed for the first time a direct TcdC/RNA polymerase interaction *in vivo*. Moreover binding of TcdC to RNA polymerase suggests it may act via a complex layer of negative regulation as seen in other well characterized anti-sigma factors such as the bacteriophage T4 anti-sigma factor AsiA (253,267,268). These observations leads to the postulation that TcdC may trap RNA polymerase core enzyme/TcdR in a ternary complex and prevents direct interaction of TcdR with the RNA polymerase core during exponential phase (Figure 4.7C).

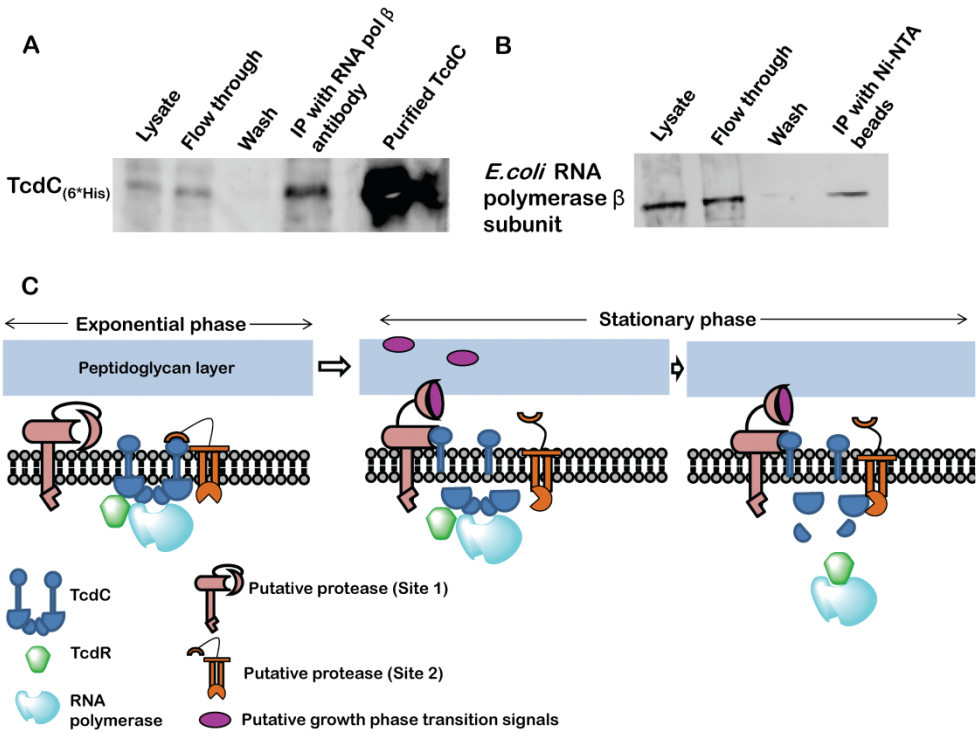


**Figure 4.7 Co-immunoprecipitation of TcdC associated proteins and proposed model for TcdC-mediated negative gene regulation.** (A), (B) Western blot analysis of immunoprecipitation experiments performed on TcdR/TcdC/*ptcdA-EmGFP* expressing cells. Showing direct interaction between TcdC and RNA polymerase (A) Indicates immunoprecipitation carried out using *Ecoli* RNA polymerase mono clonal antibody specific for β subunit. Lane 1; lyaste, Lane 2; follow-through after separation of immunocomplex by Protein A/G Agarose beads, Lane 3; fraction form 4$^{th}$ wash by lysate buffer, Lane 4; immunoeluted sample, Lane 5; purified C-terminal $His_6$ tag TcdC.(B) Indicates pull-down experiment carried out using. Ni-NTA Agarose beads, Lane 1; lyaste, Lane 2; follow-through after separation of TcdC associated proteins with Ni-NTA beads, Lane 3; fraction from 3$^{rd}$ 50 mM imidazole buffer wash; Lane 4; Immunoeluted sample. (C) TcdC may functions as ECF class anti-sigma factors, following regulated transmembrane proteolysis (RIP) pathway. During exponential phase TcdC/RNA polymerase/TcdR ternary complex prevents transcriptional activation. Putative proteases are held in inactive conformations. However, direct interactions of TcdC with putative proteases during this phase were pictured for simplicity. During exponential to stationary phase transition, periplasmic signals leads to activation of putative site 1 protease and cleaves TcdC in site 1 cleavage site (cleavage at putative signal peptide region) initiates TcdC degradation, followed by activation of putative site 2 proteases leading to complete degradation of TcdC and there by releasing RNA polymerase and TcdR. Consequently TcdR bind to RNA polymerase forming RNA polymerase holoenzyme and subsequent transcriptional activation of *tox* genes.[Figure adopted from (52)]

### 4.3.5 Proposed model for TcdC mediated gene regulation

A number of previous studies have revealed ECF class-σ-factors, their cognate anti- σ-factors and the proteases that regulate them play significant roles in pathogenesis of several gram-negative and gram-positive pathogens such as *Vibrio cholerae* (270), *Mycobacterium tuberculosis* (271) , *Staphylococcus aureus* (272) and *Clostridium difficile* (273). The above signal transduction regulatory pathway is known as regulated transmembrane proteolysis (RIP). Proteolytic degradation of membrane bound anti- σ-factor leads to release of sigma factor and transcriptional activation. RIP pathway utilizes two intra-membrane proteases. Site-1 proteases receive the extracellular signals and cleave at the site one of anti-sigma factor. After Site-1 cleavage, Site-2 proteases further degrade the anti-sigma factors and follow-on activation of sigma factor. One of the well studied systems is *E. coli* $\sigma^E$ (251,269) , its cognate ECF class anti-σ-factor RseA and inner membrane proteases DegS and YaeL (274). In the absence of stress conditions RseA binds $\sigma^E$ and prevents its association with RNA polymerase inhibiting transcription of sigma-E dependent genes. Upon receiving stress, the periplasmic serine protease DegS, cleaves RseA at site 1, which is subsequently cleaved by a membrane-embedded metalloprotease YaeL at site 2. The result of this cascade is that $\sigma^E$ released from its association with RseA and can initiate $\sigma^E$ dependtent transcription with the help of RNAP (274,275).

The work described above lead us to conclude that TcdC is in fact an ECF-class anti-sigma factor. It is a membrane bound dimeric protein; it lacks the ability to bind DNA but still negatively regulates *tox* gene expression; it harbors an N-terminal signal peptide which undergoes proteolytic cleavage at a canonical serine protease cleavage site and loses function upon processing; and finally it interacts directly with RNA polymerase. Thus, it has all of the hallmarks of a RIP pathway (Fig. 4.7C). However, an additional layer of interaction needs to be

considered in this case is the possible incidence of a direct association with RNA polymerase. The ternary TcdR/TcdC/RNA polymerase complex could result in the proteolytic destabilization of TcdC and TcdR-RNA polymerase association followed by transcriptional activation. A recent study identified three ECF class sigma factors CsfT, CsfU, and CsfV and their cognate anti-sigma factors RsiT, RsiU, and RsiV, respectively in *C. difficile* (273). CsfT-RsiT regulation was mediated by a putative site 1 protease PrsW and the above interactions play important roles in antimicrobial resistance and colonization. Accordingly, TcdC may function through the RIP pathway for the regulation of *tox* gene expression.

Further biochemical and genetic studies are required to definitively prove the occurrence of TcdR/TcdC/RNA polymerase complex *in vivo,* putative proteases associated with the cleavage and extracellular recognition signals associated with pathway etc. In this case the role of anti-sigma may expand to include pathogenesis and development of hypervirulent strains.

**4.4 Conclusions**

Finely tuned expression of virulence factors is critical for the success of a pathogenic organism. Here we identified that the negative regulator TcdC is not a DNA binding protein and rather it could act as an anti-sigma factor. We have provided evidence that TcdC harbors a putative N-terminal signal peptide region and it undergoes cleavage. *In vivo* fusion studies further confirmed that an N-terminal signal peptide region could have a functional role and removal of signal peptide that significantly reduces its negative regulatory role. Co-immunoprecipitation experiments provided evidence of a direct interaction between TcdC and RNA polymerase *in vivo*. The above observations based on biochemical and genetic studies lead us to propose that TcdC may function as a ECF class anti-sigma factor with the regulated transmembrane proteolysis (RIP) pathway. Consistent with previous findings (239) our data

further verified that the truncated mutation leads to the activation of toxin promoters and thus TcdC in an important factor in development of high toxin producing epidemic strains. Since there is much less known about the PaLoc regulatory network, having a functional GFP fusion in hand can be an advantages in future to identify promoter specificities of major PaLoc regulatory proteins, etc. Ultimately understanding the mechanism of regulation of toxin gene expression may open up new therapeutic strategies in controlling *C. difficile* infections.

### 4.5 Materials and Methods

All procedures involving *C.difficile* genomic DNA were carried out in a Biosafety level 2 lab following standard operation conditions.

#### 4.5.1 DNA oligonucleotides

The complete lists of DNA oligonucleotides used in the study for cloning and electromobility shift assay are provided in Table 4.2. and Table 4.3.

#### 4.5.2 Bacterial strains, media and growth conditions

The *E.coli* strains XL-10 (Stratagene) or Top 10 (Invtrogen) were used for cloning purposes and *E.coli* BL21 (DE3) cells were used for protein expression and for *in vivo* fusion studies. All constructs made carrying genes of interests in this study were confirmed by DNA sequencing. Growth in Luria-Bertani (LB) broth or LB Agar plates were carried out in 37°C unless specified. Antibiotics were used in following concentrations when appropriate; Kanamycin (34 µg/ml), Ampicillin (100 µg/ml), Chloramphenicol (30 µg/ml) and Spectinomycin (100 µg/ml).

### 4.5.3 Purification of TcdC

To construct TcdC with both N-terminal and C-terminal polyhistidine tag, the *tcdC* from chromosomal DNA of *C.difficile* strain ATCC 9689 was amplified [Primer pairs (SA001and SA002), (SA003 and SA004)] and cloned within Nde1 and Xho 1 sites of pET30-b (Novagen). The resulting plasmid was expressed in *E.coli* Rosetta2 (DE3) (Invitrogen) cells, a 1-liter culture was grown at room temperature for 16 hrs ($OD_{600}$ ~ 3.0) till stationary phase (237). Cells were induced by 1mM IPTG and continued to grow for another 3 hrs and harvested by centrifuging at 5,000 rpm for 15 min. Cells were lysed by sonication in 50 mM Tris.HCl, 300 mM NaCl, 10 mM imidazole, 10% glycerol at pH 7.5, supplemented with EDTA-free complete protease inhibitor cocktail (Roche). The cell lysate was clarified by centrifugation, supernatant was incubated with 1% Triton X-100, DNAase (100 U/ml) for 1hr at 4°C and sterile filtered (0.22µm filter). Proteins were purified using an imidazole step gradient from a nickel-chelated HiTrap column using FPLC ($AKTA_{FPLC}$, Amersham Pharmacia Biotech**)**. The purified $His_6$-tagged protein were dialyzed into storage buffer (50 mM Tris.HCl pH 7.5, 300 mM NaCl, 1mM DTT and 10% glycerol) and stored at 4 °C in the presence of 40% glycerol.

### 4.5.4 Gel mobility shift assays

A 246 bp DNA fragment containing the promoter *tcdR* region was amplified form chromosomal DNA using primers (SA005 and SA006), purified and radio labeled with [$\gamma$-$^{32}$P]-ATP. To obtain short putative promoters, individual single stranded DNA fragments were purchased (IDT-Integrated DNA Technologies), single strand is radio labeled and annealed with corresponding complementary strand by heating at 95°C for 3 min and cooled to room temperature for 15 min in annealing buffer (10 mM Tris.HCl pH 7.5, 20 mM NaCl). List of oligonucleotides used in the gel mobility shift assays were indicated in Table 4.2. Labeled DNAs

(10 kcpm final count) were mixed with increasing concentration of purified recombinant TcdC and binding reactions were performed in binding buffer [25 mM Tris.HCl pH 7.5, 75 mM NaCl, 50 mM Potassium glutamate, 10 mM $MgCl_2$, 0.1 mM EDTA, 12% glycerol, 0.3 mM DTT, 0.005 mg/ml BSA (where indicated 2mM GTP/ 125 M $MnCl_2$ added as co-repressors] at room temperature for 30 min. For all reactions 15 µl aliquots were loaded after mixing with loading buffer (4% w/v sucrose, 1 mM Tris.HCl pH 7.5, 0.001% bromophenol blue) on to a 5 or 8 % native polyacrylamide (37:1) gel. Electrophoresis was carried out at 7W in Tris-glycine buffer. Dried gels were phosphorimaged, scanned by a Typhoon 9210 imaging system (GE Lifer Scieneces) and quantification was performed using ImageQuant 5.1(Molecular Dynamics).

**4.5.5 *In vivo* fusion study plasmid constructs**

Parent plasmids were selected with compatible origins of replications and independent antibiotic selection for co-expression and maintenance. The GFP fusion plasmid was constructed starting from the plasmid pBAC-EmGH [gift from Cunningham Lab] (247,276). The *pBAD* promoter form the plasmid was removed by MluI and BamH1 restriction digestions. Promoter *tcdA* region (521 bp) was amplified from *C.difficile* ATCC 9689 genomic DNA using primers SA0017, SA0018 and inserted in-frame with reporter gene *Em-gfp* to generate pSA121201 (*ptcdA-EmGH)* (Figure 4.5A(a)). pSA111202 (*pT7-TcdR)* was based on plasmid pJLM016 [a pCDF-1b derivative, gift from Tamara L. Hendrickson lab]. A 555 bp length *tcdR* coding region was amplified using primers (SA025 and SA026) and cloned in-frame with *T*7 promoter within NcoI and XhoI sites (Figure 4.5A(c)). pSA101203 (*pBAD-TcdC)*, $TcdC_{wt}$ (wild type) was amplified using SA021 and SA022 primers from *C.difficile* ATCC 9689. Cloned in-frame with *pBAD* promoter using MscI and EcoRI restriction sites of parent plasmid pNM12 (Figure 4.5A (b)) (277,278). pSA101204, $TcdC_{farme\text{-}shift}$ mutant was generated using SA029 and SA030 primers

from pSA101203. Cloned in-frame with *pBAD* promoter using MscI and EcoRI restriction sites of pNM12. pSA101205, $TcdC_{\Delta\ signal\ peptide}$ mutant was generated using SA029 and SA031 primers from pSA101203. Cloned in-frame with *pBAD* promoter using MscI and EcoRI restriction sites of pNM12. pSA101206, TcdC-C-terminal $His_6$ tag was amplified using SA032 and SA022 primers from pSA101203. Cloned in-frame with *pBAD* promoter using MscI and EcoRI restriction sites of pNM12.

**4.5.6 *In vivo* GFP-reporter assay**

Bacterial start up cell cultures with $OD_{600nm}$ of 0.02 were obtained by diluting overnight cultures with LB. Cells were induced after 3 hrs ($OD_{600nm}$ of ~0.4-0.5) with 0.2% L-arabinose (Sigma) or 0.1 mM IPTG accordingly and allowed to grow until early stationary phase for 13 hrs. At (3hrs, 7hrs, 11hrs, 13hrs) indicated time points, cells were withdrawn, absorbance were measured, 2 ml cultures were harvested at13,000 rpm for 1 min and stored at -80°C until lysis. For lysis and GFP measurements, cell pellets were re-suspended in 200 µl lysis buffer (50 mM Tris.Cl pH 7.5, 25 mM NaCl, 2 mM EDTA). In order to lyse the cells, 20 µl of lysozyme (25 mg/mL, freshly prepared), 30 µl of protease inhibitor (one tablet per 8 mL ultrapure water, complete EDTA-free protease inhibitor cocktail, Roche) and 25 µl of 10 % TritonX-100 were added and incubated at 37°C for 45 min with continuous shaking. Followed a freeze thaw cycle by incubating in ethanol/dry ice bath for 10 min and thawed at room temperature for 10 min. For the complete lysis, cells were further incubated at 37°C for another 30 min with continuous shaking. Lysed cells were centrifuged at 13 000 rpm for 2 min to separate the membrane components and 200 µl supernatant was transferred into a 96-well flat bottom black plate (Coaster®). The fluorescence measurements were made at an excitation wavelength of 485 nm and at an emission wavelength of 535 nm (Tecan GENios Plus multi label reader). Individual

fluorescence measurements were normalized by corresponding $OD_{600}$ measurements. The fluorescence gain values were consistently set between 95 and 103. All measurements were triplicated and error values were based on the standard deviation between independent trials.

### 4.5.7 *In vivo* cross-linking

Bacterial cells carrying 3 plasmids *ptcdA-EmGH*, *pBAD-TcdC*, *pT7-TcdR* or 2 plasmids *ptcdA-EmGH*, *pBAD-TcdC* were used. Cells were grown in identical conditions as described in GFP-reporter assy. Bacterial start up cell cultures (500 mL) with $OD_{600nm}$ of 0.02 were generated by diluting overnight cultures with LB. Cells harboring 3 plasmids were induce with 0.2% L-arabinose (Sigma), 0.1 mM IPTG and cells with 2 plasmids were induced with 0.2% L-arabinose. At the 7 hrs time point ($OD_{600nm}$~ 1.2), cells were harvested at 5,000 rpm for 15 min, and separated in to 100 mg cells (wet weight) aliquots and washed twice with 1×PBS (pH 7.4, Calbiochem). Cell pellets were suspended in 1% (w/v) paraformaldehyde in PBS (pH 7.4) (Sigma) and incubated at room temperature for 45 min without shaking. Cells were harvested, remaining paraformaldehyde solution was removed, washed once with 1×PBS and twice with TcdC lysis buffer (50 mM Tris.HCl, 300 mM NaCl). The washed cell pellets were used for immunoprecipitation.

### 4.5.8 Co-immunoprecipitation and western blot analysis

Cells were lysed by B-PER® Direct Bacterial Protein Extraction Kit (Thermo Scientific), 800 µL B-PER Direct reagent, 8 µL Lysozyme (50 mg/mL stock), 8 µL DNAase I (2,500 U/mL stock), 80 µl 10 % Triton X-100, 50 µl of protease inhibitor (complete EDTA-free, Roche) 80 µl 80 % Glycerol were added and incubated at 37°C for 30 min with shaking. Briefly centrifuged to remove not lysed cells and supernatant was proceeded for immunoprecipitation experiments.

### 4.5.9 Immunoprecipitation with *E.coli* RNA pol β mouse monoclonal antibody

To cell lysate 4 µg of *E.coli* RNA polymerase β subunit mouse monoclonal antibody (Santa Cruz Biotechnology, Inc) was added and incubated overnight at 4°C with rotation. Immunocomplex was captured by adding pre-washed 50 µL (packed beads) Pierce® Protein A/G Agarose (Thermo Scientific) and incubation for 2 hrs at 4°C with rotation. Beads were collected by centrifugation at 700*g for 3 min and washed 4 times with ice cold TcdC lysis buffer (400 µL wash each time). Beads were re-suspended in 100 µL TcdC lysis buffer, 25 µL of 4X SDS gel loading buffer and boiled at 95°C for 15 min to dissociate immunocomplexes from beads and to reverse paraformaldehyde cross-linking. Samples were next loaded with appropriate controls, separated on 4-10% denaturation polyacrylamide gel and electroblotted to a PVDF membrane. Presence of C-terminally poly-histidine tagged TcdC was probed by HisProbe-HRP (Thermo scientific), a nickel ($Ni^{2+}$) activated derivative of horseradish peroxidase (HRP) (1:5000) and visualized by chemiluminescence signal obtained from Super Signal West Pico Chemiluminescence Substrate kit (Thermo scientific). Images were obtained from CCD camera.

### 4.5.10 Pull-down experiments using poly-histidine tagged TcdC

To cell lysate, imidazole was added to final concentration of 10 mM, followed by addition of 60 µL (packed beads) pre-washed HisPur™ Ni-NTA resin (Thermo Scientific). Samples were incubated overnight at 4°C with rotation. Beads were collected by centrifugation at 700*g for 3 min and washed once with lysis buffer with 10 mM Imidazole and followed by three washes with 50 mM imidazole containing lysis buffer (400 µL wash each time). Bound proteins were eluted, electrophoresed and electroblotted to a PVDF membrane as indicated in RNA pol β pull down experiments. The presence of RNA polymerase from the pull-down was probed by *E.coli* RNA pol β mouse monoclonal antibody (Santa Cruz Biotechnology, Inc)

(1:200) and Goat anti-mouse IgG H&L (Cy5 ®) secondary antibody (abcam) (1: 1000). Membrane was scanned by a Typhoon 9210 imaging system (GE Lifer Scieneces) and analyzed by ImageQuant 5.1(Molecular Dynamics).

**Table 4.2 List of oligonucleotides used in gel mobility shift assays and expression of recombinant TcdC with N-terminal $His_6$ tag and C-terminal $His_6$ tag**

| Code | DNA primer name | Sequence |
|---|---|---|
| SA001 | TcdC N-terminal his Fw primer | CCGAGCCTCGAGTTAATTAATTTTCTCTACAGC |
| SA002 | TcdC N-terminal his Rev primer | GGAACCCATATGCACCATCATCACCACGGTTCTATGTTTTCTAAA AAAAATGATG |
| SA003 | TcdC C-terminal his Fw primer | CCGAGCCTCGAGATTAATTTTCTCTACAGCTATC |
| SA004 | TcdC C-terminal his Rev primer | GGAACCCATATGTTTTCTAAAAAAAATGATG |
| SA005 | PtcdR Fw primer | CCGAGCGCATGCATGTTATTATTTTTATTACAATTTAG |
| SA006 | PtcdR Rev primer | GGAACCGAATTCTCATAAAAAGACTTTTGC |
| SA007 | PtcdR a | GACTAAATTATAAAGTTTACATAATTATTTAATAATTATGTAATT GTTACTTGAAAATTGATCT |
| SA008 | PtcdR b | AGATCAATTTTCAAGTAACAATTACATAATTATTAAATAATTATG TAAACTTTATAATTTAGTC |
| SA009 | PtcdR' I | ATAAAATGATTTGTTTTTACAATACTTTATTAATATAAAGTTTATT GCTAAAATACTTTATT |
| SA010 | PtcdR' II | ATAAAGTATTTTAGCAATAAACTTTATATTAATAAAGTATTGTAA AAACAAATCATTTTAT |
| SA011 | PtcdA upper strand | AATATAAGATATGTTTACAAATTACTATCAGACAATCTCCTTATC TAATAGAAGAGTCAA |
| SA012 | PtcdA lower strand | TTGACTCTTCTATTAGATAAGGAGATTGTCTGATAGTAATTTGTA AACATATCTTATATT |
| SA013 | PtcdB 1 upper strand | TAGAACAAAGTTTACATATTTATTTCAGACAACGTCTTTATTCAA TCGAAG |
| SA014 | PtcdB 1 lower strand | CTTCGATTGAATAAAGACGTTGTCTGAAATAAATATGTAAACTTT GTTCTA |
| SA015 | PtcdB 2 upper sd | CAATAACTTAATCTAAGAATATCTTAATTTTTATATTTTATATAGA ACAAAGTT |
| SA016 | PtcdB 2 lower sd | AACTTTGTTCTATATAAAATATAAAAATTAAGATATTCTTAGATT AAGTTATTG |

**Table 4.3 List of oligonucleotides used in gel mobility shift assays and expression of recombinant TcdC with N-terminal $His_6$ tag and C-terminal $His_6$ tag**

| Code | DNA primer name | Sequence |
|---|---|---|
| SA017 | ptcdA forward primer | CCGAGCACGCGTAGTTGGTAAAATCTATTAAG |
| SA018 | ptcdA reverse primer | GGAACCGGATCCAGATATTAAAGACATAAAAACC |
| SA019 | ptcdA-EmGH Fw seq primer | CTTATTAAAAGCATTCTGTAAC |
| SA020 | ptcdA-EmGH Rev seq primer | CTTATTAAAAGCATTCTGTAAC |
| SA021 | TcdC Fw primer | CCGAGCGAATTCTTAATTAATTTTCTCTACAGC |
| SA022 | TcdC Rev primer | GGAACCTGGCCAATGTTTTCTAAAAAAAATGATG |
| SA023 | pNM12 Fw seq primer | TATCCATAAGATTAGCGGATC |
| SA024 | pNM12 Rev seq primer | TGTATCAGGCTGAAAATC |
| SA025 | TcdR Fw primer | CCGAGCCCATGGATGCAAAAGTCTTTTTATG |
| SA026 | TcdR Rev primer | GGAACCCTCGAGTTACAAGTTAAAATAATTTTC |
| SA027 | pJLMO16 Fw seq primer | GAATTGTGAGCGGATAAC |
| SA028 | pJLMO16 Rev seq primer | AGCAGCGGTTTCTTTAC |
| SA029 | TcdC frame shift mutation Fw | CCGAGCGAATTCTTAATTAATTTTCTCTACAGCTATC |
| SA030 | TcdC frame shift mutation Rev | GGAACCTGGCCAATGAAAGACGACGAAAAG |
| SA031 | TcdC signal peptide deleted Rev Primer | GGAACCTGGCCAATGTGTTCTGAAGACCATGAG |
| SA032 | TcdC-Cter 6*His tag Fw primer | CGAGCGAATTCTTAGTGGTGGTGGTGGTGGTGCTCGAGATTAATTTTCTCTACAGCTATC |

# REFERENCES


1. Cloud, J. and Kelly, C.P. (2007) Update on Clostridium difficile associated disease. *Current opinion in gastroenterology*, **23**, 4-9.
2. Rupnik, M., Wilcox, M.H. and Gerding, D.N. (2009) Clostridium difficile infection: new developments in epidemiology and pathogenesis. *Nature reviews. Microbiology*, **7**, 526-536.
3. Madan, R. and Jr, W.A. (2012) Immune responses to Clostridium difficile infection. *Trends in molecular medicine*, **18**, 658-666.
4. Wilson, K.H., Sheagren, J.N. and Freter, R. (1985) Population dynamics of ingested Clostridium difficile in the gastrointestinal tract of the Syrian hamster. *The Journal of infectious diseases*, **151**, 355-361.
5. Cunningham, R. and Dial, S. (2008) Is over-use of proton pump inhibitors fuelling the current epidemic of Clostridium difficile-associated diarrhoea? *The Journal of hospital infection*, **70**, 1-6.
6. Burns, D.A., Heap, J.T. and Minton, N.P. (2010) Clostridium difficile spore germination: an update. *Research in microbiology*, **161**, 730-734.
7. Rousseau, C., Levenez, F., Fouqueray, C., Dore, J., Collignon, A. and Lepage, P. (2011) Clostridium difficile colonization in early infancy is accompanied by changes in intestinal microbiota composition. *Journal of clinical microbiology*, **49**, 858-865.
8. Deneve, C., Delomenie, C., Barc, M.C., Collignon, A. and Janoir, C. (2008) Antibiotics involved in Clostridium difficile-associated disease increase colonization factor gene expression. *Journal of medical microbiology*, **57**, 732-738.

9. Blondeau, J.M. (2009) What have we learned about antimicrobial use and the risks for Clostridium difficile-associated diarrhoea? *The Journal of antimicrobial chemotherapy*, **63**, 238-242.

10. Owens, R.C., Jr., Donskey, C.J., Gaynes, R.P., Loo, V.G. and Muto, C.A. (2008) Antimicrobial-associated risk factors for Clostridium difficile infection. *Clinical infectious diseases : an official publication of the Infectious Diseases Society of America*, **46 Suppl 1**, S19-31.

11. Trinh, C. and Prabhakar, K. (2007) Diarrheal diseases in the elderly. *Clinics in geriatric medicine*, **23**, 833-856, vii.

12. Zerey, M., Paton, B.L., Lincourt, A.E., Gersin, K.S., Kercher, K.W. and Heniford, B.T. (2007) The burden of Clostridium difficile in surgical patients in the United States. *Surgical infections*, **8**, 557-566.

13. Cho, S.M., Lee, J.J. and Yoon, H.J. (2012) Clinical risk factors for Clostridium difficile-associated diseases. *The Brazilian journal of infectious diseases : an official publication of the Brazilian Society of Infectious Diseases*, **16**, 256-261.

14. Weese, J.S. (2010) Clostridium difficile in food--innocent bystander or serious threat? *Clin Microbiol Infect*, **16**, 3-10.

15. Hensgens, M.P., Keessen, E.C., Squire, M.M., Riley, T.V., Koene, M.G., de Boer, E., Lipman, L.J., Kuijper, E.J., European Society of Clinical, M. and Infectious Diseases Study Group for Clostridium, d. (2012) Clostridium difficile infection in the community: a zoonotic disease? *Clin Microbiol Infect*, **18**, 635-645.

16. Britton, R.A. and Young, V.B. (2012) Interaction between the intestinal microbiota and host in Clostridium difficile colonization resistance. *Trends in microbiology*, **20**, 313-319.

17. Pruitt, R.N., Chagot, B., Cover, M., Chazin, W.J., Spiller, B. and Lacy, D.B. (2009) Structure-function analysis of inositol hexakisphosphate-induced autoprocessing in Clostridium difficile toxin A. *J Biol Chem*, **284**, 21934-21940.

18. Just, I., Selzer, J., Wilm, M., von Eichel-Streiber, C., Mann, M. and Aktories, K. (1995) Glucosylation of Rho proteins by Clostridium difficile toxin B. *Nature*, **375**, 500-503.

19. Ng, J., Hirota, S.A., Gross, O., Li, Y., Ulke-Lemee, A., Potentier, M.S., Schenck, L.P., Vilaysane, A., Seamone, M.E., Feng, H. *et al.* (2010) Clostridium difficile toxin-induced inflammation and intestinal injury are mediated by the inflammasome. *Gastroenterology*, **139**, 542-552, 552 e541-543.

20. Voth, D.E. and Ballard, J.D. (2005) Clostridium difficile toxins: mechanism of action and role in disease. *Clin Microbiol Rev*, **18**, 247-263.

21. Kelly, C.P. and Kyne, L. (2011) The host immune response to Clostridium difficile. *Journal of medical microbiology*, **60**, 1070-1079.

22. Dallal, R.M., Harbrecht, B.G., Boujoukas, A.J., Sirio, C.A., Farkas, L.M., Lee, K.K. and Simmons, R.L. (2002) Fulminant Clostridium difficile: an underappreciated and increasing cause of death and complications. *Annals of surgery*, **235**, 363-372.

23. Pepin, J., Valiquette, L., Alary, M.E., Villemure, P., Pelletier, A., Forget, K., Pepin, K. and Chouinard, D. (2004) Clostridium difficile-associated diarrhea in a region of Quebec from 1991 to 2003: a changing pattern of disease severity. *CMAJ : Canadian Medical Association journal = journal de l'Association medicale canadienne*, **171**, 466-472.

24. Labbe, A.C., Poirier, L., Maccannell, D., Louie, T., Savoie, M., Beliveau, C., Laverdiere, M. and Pepin, J. (2008) Clostridium difficile infections in a Canadian tertiary care

hospital before and during a regional epidemic associated with the BI/NAP1/027 strain. *Antimicrobial agents and chemotherapy*, **52**, 3180-3187.

25. Aktories, K. (2007) Self-cutting to kill: new insights into the processing of Clostridium difficile toxins. *ACS chemical biology*, **2**, 228-230.

26. Aly, M. and Balkhy, H.H. (2012) The prevalence of antimicrobial resistance in clinical isolates from Gulf Corporation Council countries. *Antimicrobial resistance and infection control*, **1**, 26.

27. Khan, F.Y., Abu-Khattab, M., Anand, D., Baager, K., Alaini, A., Siddique, M.A., Mohamed, S.F., Ali, M.I., Al Bedawi, M.M. and Naser, M.S. (2012) Epidemiological features of Clostridium difficile infection among inpatients at Hamad General Hospital in the state of Qatar, 2006-2009. *Travel medicine and infectious disease*, **10**, 179-185.

28. Lessa, F.C., Gould, C.V. and McDonald, L.C. (2012) Current status of Clostridium difficile infection epidemiology. *Clinical infectious diseases : an official publication of the Infectious Diseases Society of America*, **55 Suppl 2**, S65-70.

29. Kim, J., Kang, J.O., Pai, H. and Choi, T.Y. (2012) Association between PCR ribotypes and antimicrobial susceptibility among Clostridium difficile isolates from healthcare-associated infections in South Korea. *International journal of antimicrobial agents*, **40**, 24-29.

30. Vaishnavi, C. and Singh, M. (2012) Preliminary investigation of environmental prevalence of Clostridium difficile affecting inpatients in a north Indian hospital. *Indian journal of medical microbiology*, **30**, 89-92.

31. Kallen, A.J., Thompson, A., Ristaino, P., Chapman, L., Nicholson, A., Sim, B.T., Lessa, F., Sharapov, U., Fadden, E., Boehler, R. *et al.* (2009) Complete restriction of

fluoroquinolone use to control an outbreak of Clostridium difficile infection at a community hospital. *Infection control and hospital epidemiology : the official journal of the Society of Hospital Epidemiologists of America*, **30**, 264-272.

32. Leffler, D.A. and Lamont, J.T. (2009) Treatment of Clostridium difficile-associated disease. *Gastroenterology*, **136**, 1899-1912.

33. Warny, M., Pepin, J., Fang, A., Killgore, G., Thompson, A., Brazier, J., Frost, E. and McDonald, L.C. (2005) Toxin production by an emerging strain of Clostridium difficile associated with outbreaks of severe disease in North America and Europe. *Lancet*, **366**, 1079-1084.

34. Centers for Disease, C. and Prevention. (2005) Severe Clostridium difficile-associated disease in populations previously at low risk--four states, 2005. *MMWR. Morbidity and mortality weekly report*, **54**, 1201-1205.

35. McFarland, L.V. (2008) Update on the changing epidemiology of Clostridium difficile-associated disease. *Nature clinical practice. Gastroenterology & hepatology*, **5**, 40-48.

36. Jhung, M.A., Thompson, A.D., Killgore, G.E., Zukowski, W.E., Songer, G., Warny, M., Johnson, S., Gerding, D.N., McDonald, L.C. and Limbago, B.M. (2008) Toxinotype V Clostridium difficile in humans and food animals. *Emerging infectious diseases*, **14**, 1039-1045.

37. Hundsberger, T., Braun, V., Weidmann, M., Leukel, P., Sauerborn, M. and von Eichel-Streiber, C. (1997) Transcription analysis of the genes tcdA-E of the pathogenicity locus of Clostridium difficile. *European journal of biochemistry / FEBS*, **244**, 735-742.

38. Mani, N. and Dupuy, B. (2001) Regulation of toxin synthesis in Clostridium difficile by an alternative RNA polymerase sigma factor. *Proceedings of the National Academy of Sciences of the United States of America*, **98**, 5844-5849.

39. Moncrief, J.S., Barroso, L.A. and Wilkins, T.D. (1997) Positive regulation of Clostridium difficile toxins. *Infection and immunity*, **65**, 1105-1108.

40. Tan, K.S., Wee, B.Y. and Song, K.P. (2001) Evidence for holin function of tcdE gene in the pathogenicity of Clostridium difficile. *J Med Microbiol*, **50**, 613-619.

41. Wang, I.N., Smith, D.L. and Young, R. (2000) Holins: the protein clocks of bacteriophage infections. *Annual review of microbiology*, **54**, 799-825.

42. Govind, R. and Dupuy, B. (2012) Secretion of Clostridium difficile toxins A and B requires the holin-like protein TcdE. *PLoS pathogens*, **8**, e1002727.

43. Dineen, S.S., Villapakkam, A.C., Nordman, J.T. and Sonenshein, A.L. (2007) Repression of Clostridium difficile toxin gene expression by CodY. *Molecular microbiology*, **66**, 206-219.

44. Dupuy, B. and Sonenshein, A.L. (1998) Regulated transcription of Clostridium difficile toxin genes. *Molecular microbiology*, **27**, 107-120.

45. Antunes, A., Martin-Verstraete, I. and Dupuy, B. (2011) CcpA-mediated repression of Clostridium difficile toxin gene expression. *Molecular microbiology*, **79**, 882-899.

46. Hammond, G.A., Lyerly, D.M. and Johnson, J.L. (1997) Transcriptional analysis of the toxigenic element of Clostridium difficile. *Microbial pathogenesis*, **22**, 143-154.

47. Mani, N., Lyras, D., Barroso, L., Howarth, P., Wilkins, T., Rood, J.I., Sonenshein, A.L. and Dupuy, B. (2002) Environmental response and autoregulation of Clostridium difficile TxeR, a sigma factor for toxin gene expression. *Journal of bacteriology*, **184**, 5971-5978.

48. Pruitt, R.N., Chambers, M.G., Ng, K.K., Ohi, M.D. and Lacy, D.B. (2010) Structural organization of the functional domains of Clostridium difficile toxins A and B. *Proceedings of the National Academy of Sciences of the United States of America*, **107**, 13467-13472.

49. Schwan, C., Stecher, B., Tzivelekidis, T., van Ham, M., Rohde, M., Hardt, W.D., Wehland, J. and Aktories, K. (2009) Clostridium difficile toxin CDT induces formation of microtubule-based protrusions and increases adherence of bacteria. *PLoS pathogens*, **5**, e1000626.

50. Papatheodorou, P., Carette, J.E., Bell, G.W., Schwan, C., Guttenberg, G., Brummelkamp, T.R. and Aktories, K. (2011) Lipolysis-stimulated lipoprotein receptor (LSR) is the host receptor for the binary toxin Clostridium difficile transferase (CDT). *Proceedings of the National Academy of Sciences of the United States of America*, **108**, 16422-16427.

51. Calabi, E., Calabi, F., Phillips, A.D. and Fairweather, N.F. (2002) Binding of Clostridium difficile surface layer proteins to gastrointestinal tissues. *Infection and immunity*, **70**, 5770-5778.

52. Fagan, R.P., Albesa-Jove, D., Qazi, O., Svergun, D.I., Brown, K.A. and Fairweather, N.F. (2009) Structural insights into the molecular organization of the S-layer from Clostridium difficile. *Molecular microbiology*, **71**, 1308-1322.

53. Tasteyre, A., Barc, M.C., Collignon, A., Boureau, H. and Karjalainen, T. (2001) Role of FliC and FliD flagellar proteins of Clostridium difficile in adherence and gut colonization. *Infection and immunity*, **69**, 7937-7940.

54. Hennequin, C., Janoir, C., Barc, M.C., Collignon, A. and Karjalainen, T. (2003) Identification and characterization of a fibronectin-binding protein from Clostridium difficile. *Microbiology*, **149**, 2779-2787.

55. Waligora, A.J., Hennequin, C., Mullany, P., Bourlioux, P., Collignon, A. and Karjalainen, T. (2001) Characterization of a cell surface protein of Clostridium difficile with adhesive properties. *Infection and immunity*, **69**, 2144-2153.

56. Just, I. and Gerhard, R. (2004) Large clostridial cytotoxins. *Rev Physiol Biochem Pharmacol*, **152**, 23-47.

57. Schirmer, J. and Aktories, K. (2004) Large clostridial cytotoxins: cellular biology of Rho/Ras-glucosylating toxins. *Biochimica et biophysica acta*, **1673**, 66-74.

58. Gould, C.V. and McDonald, L.C. (2008) Bench-to-bedside review: Clostridium difficile colitis. *Crit Care*, **12**, 203.

59. von Eichel-Streiber, C., Laufenberg-Feldmann, R., Sartingen, S., Schulze, J. and Sauerborn, M. (1990) Cloning of Clostridium difficile toxin B gene and demonstration of high N-terminal homology between toxin A and B. *Medical microbiology and immunology*, **179**, 271-279.

60. Chaves-Olarte, E., Weidmann, M., Eichel-Streiber, C. and Thelestam, M. (1997) Toxins A and B from Clostridium difficile differ with respect to enzymatic potencies, cellular substrate specificities, and surface binding to cultured cells. *The Journal of clinical investigation*, **100**, 1734-1741.

61. Lyerly, D.M., Saum, K.E., MacDonald, D.K. and Wilkins, T.D. (1985) Effects of Clostridium difficile toxins given intragastrically to animals. *Infection and immunity*, **47**, 349-352.

62. Alfa, M.J., Kabani, A., Lyerly, D., Moncrief, S., Neville, L.M., Al-Barrak, A., Harding, G.K., Dyck, B., Olekson, K. and Embil, J.M. (2000) Characterization of a toxin A-negative, toxin B-positive strain of Clostridium difficile responsible for a nosocomial outbreak of Clostridium difficile-associated diarrhea. *Journal of clinical microbiology*, **38**, 2706-2714.

63. Drudy, D., Fanning, S. and Kyne, L. (2007) Toxin A-negative, toxin B-positive Clostridium difficile. *International journal of infectious diseases : IJID : official publication of the International Society for Infectious Diseases*, **11**, 5-10.

64. Kuehne, S.A., Cartman, S.T., Heap, J.T., Kelly, M.L., Cockayne, A. and Minton, N.P. (2010) The role of toxin A and toxin B in Clostridium difficile infection. *Nature*, **467**, 711-713.

65. Kuehne, S.A., Cartman, S.T. and Minton, N.P. (2011) Both, toxin A and toxin B, are important in Clostridium difficile infection. *Gut microbes*, **2**, 252-255.

66. von Eichel-Streiber, C., Laufenberg-Feldmann, R., Sartingen, S., Schulze, J. and Sauerborn, M. (1992) Comparative sequence analysis of the Clostridium difficile toxins A and B. *Mol Gen Genet*, **233**, 260-268.

67. Ho, J.G., Greco, A., Rupnik, M. and Ng, K.K. (2005) Crystal structure of receptor-binding C-terminal repeats from Clostridium difficile toxin A. *Proceedings of the National Academy of Sciences of the United States of America*, **102**, 18373-18378.

68. Krivan, H.C., Clark, G.F., Smith, D.F. and Wilkins, T.D. (1986) Cell surface binding site for Clostridium difficile enterotoxin: evidence for a glycoconjugate containing the sequence Gal alpha 1-3Gal beta 1-4GlcNAc. *Infection and immunity*, **53**, 573-581.

69. Tucker, K.D. and Wilkins, T.D. (1991) Toxin A of Clostridium difficile binds to the human carbohydrate antigens I, X, and Y. *Infection and immunity*, **59**, 73-78.

70. Pothoulakis, C., Gilbert, R.J., Cladaras, C., Castagliuolo, I., Semenza, G., Hitti, Y., Montcrief, J.S., Linevsky, J., Kelly, C.P., Nikulasson, S. *et al.* (1996) Rabbit sucrase-isomaltase contains a functional intestinal receptor for Clostridium difficile toxin A. *The Journal of clinical investigation*, **98**, 641-649.

71. Na, X., Kim, H., Moyer, M.P., Pothoulakis, C. and LaMont, J.T. (2008) gp96 is a human colonocyte plasma membrane binding protein for Clostridium difficile toxin A. *Infection and immunity*, **76**, 2862-2871.

72. Pruitt, R.N. and Lacy, D.B. (2012) Toward a structural understanding of Clostridium difficile toxins A and B. *Frontiers in cellular and infection microbiology*, **2**, 28.

73. Swett, R., Cisneros, G.A. and Feig, A.L. (2012) Conformational analysis of Clostridium difficile toxin B and its implications for substrate recognition. *PloS one*, **7**, e41518.

74. Olling, A., Goy, S., Hoffmann, F., Tatge, H., Just, I. and Gerhard, R. (2011) The repetitive oligopeptide sequences modulate cytopathic potency but are not crucial for cellular uptake of Clostridium difficile toxin A. *PloS one*, **6**, e17623.

75. Genisyuerek, S., Papatheodorou, P., Guttenberg, G., Schubert, R., Benz, R. and Aktories, K. (2011) Structural determinants for membrane insertion, pore formation and translocation of Clostridium difficile toxin B. *Molecular microbiology*, **79**, 1643-1654.

76. Torres, J.F., Lyerly, D.M., Hill, J.E. and Monath, T.P. (1995) Evaluation of formalin-inactivated Clostridium difficile vaccines administered by parenteral and mucosal routes of immunization in hamsters. *Infection and immunity*, **63**, 4619-4627.

77. Aboudola, S., Kotloff, K.L., Kyne, L., Warny, M., Kelly, E.C., Sougioultzis, S., Giannasca, P.J., Monath, T.P. and Kelly, C.P. (2003) Clostridium difficile vaccine and serum immunoglobulin G antibody response to toxin A. *Infection and immunity*, **71**, 1608-1610.

78. Tian, J.H., Fuhrmann, S.R., Kluepfel-Stahl, S., Carman, R.J., Ellingsworth, L. and Flyer, D.C. (2012) A novel fusion protein containing the receptor binding domains of C. difficile toxin A and toxin B elicits protective immunity against lethal toxin and spore challenge in preclinical efficacy models. *Vaccine*, **30**, 4249-4258.

79. Papatheodorou, P., Zamboglou, C., Genisyuerek, S., Guttenberg, G. and Aktories, K. (2010) Clostridial glucosylating toxins enter cells via clathrin-mediated endocytosis. *PloS one*, **5**, e10673.

80. Dove, C.H., Wang, S.Z., Price, S.B., Phelps, C.J., Lyerly, D.M., Wilkins, T.D. and Johnson, J.L. (1990) Molecular characterization of the Clostridium difficile toxin A gene. *Infection and immunity*, **58**, 480-488.

81. Barth, H., Pfeifer, G., Hofmann, F., Maier, E., Benz, R. and Aktories, K. (2001) Low pH-induced formation of ion channels by clostridium difficile toxin B in target cells. *J Biol Chem*, **276**, 10670-10676.

82. Giesemann, T., Jank, T., Gerhard, R., Maier, E., Just, I., Benz, R. and Aktories, K. (2006) Cholesterol-dependent pore formation of Clostridium difficile toxin A. *J Biol Chem*, **281**, 10808-10815.

83. Ziegler, M.O., Jank, T., Aktories, K. and Schulz, G.E. (2008) Conformational changes and reaction of clostridial glycosylating toxins. *Journal of molecular biology*, **377**, 1346-1356.

84. Egerer, M., Giesemann, T., Jank, T., Satchell, K.J. and Aktories, K. (2007) Auto-catalytic cleavage of Clostridium difficile toxins A and B depends on cysteine protease activity. *J Biol Chem*, **282**, 25314-25321.

85. Reineke, J., Tenzer, S., Rupnik, M., Koschinski, A., Hasselmayer, O., Schrattenholz, A., Schild, H. and von Eichel-Streiber, C. (2007) Autocatalytic cleavage of Clostridium difficile toxin B. *Nature*, **446**, 415-419.

86. Shen, A., Lupardus, P.J., Gersch, M.M., Puri, A.W., Albrow, V.E., Garcia, K.C. and Bogyo, M. (2011) Defining an allosteric circuit in the cysteine protease domain of Clostridium difficile toxins. *Nature structural & molecular biology*, **18**, 364-371.

87. Puri, A.W., Lupardus, P.J., Deu, E., Albrow, V.E., Garcia, K.C., Bogyo, M. and Shen, A. (2010) Rational design of inhibitors and activity-based probes targeting Clostridium difficile virulence factor TcdB. *Chemistry & biology*, **17**, 1201-1211.

88. Pothoulakis, C. (2000) Effects of Clostridium difficile toxins on epithelial cell barrier. *Annals of the New York Academy of Sciences*, **915**, 347-356.

89. Pruitt, R.N., Chumbler, N.M., Rutherford, S.A., Farrow, M.A., Friedman, D.B., Spiller, B. and Lacy, D.B. (2012) Structural determinants of Clostridium difficile toxin A glucosyltransferase activity. *J Biol Chem*, **287**, 8013-8020.

90. Geissler, B., Tungekar, R. and Satchell, K.J. (2010) Identification of a conserved membrane localization domain within numerous large bacterial protein toxins. *Proceedings of the National Academy of Sciences of the United States of America*, **107**, 5581-5586.

91. Busch, C., Hofmann, F., Selzer, J., Munro, S., Jeckel, D. and Aktories, K. (1998) A common motif of eukaryotic glycosyltransferases is essential for the enzyme activity of large clostridial cytotoxins. *J Biol Chem*, **273**, 19566-19572.

92. Jank, T., Giesemann, T. and Aktories, K. (2007) Clostridium difficile glucosyltransferase toxin B-essential amino acids for substrate binding. *J Biol Chem*, **282**, 35222-35231.

93. Raaijmakers, J.H. and Bos, J.L. (2009) Specificity in Ras and Rap signaling. *J Biol Chem*, **284**, 10995-10999.

94. Bishop, A.L. and Hall, A. (2000) Rho GTPases and their effector proteins. *The Biochemical journal*, **348 Pt 2**, 241-255.

95. Ihara, K., Muraguchi, S., Kato, M., Shimizu, T., Shirakawa, M., Kuroda, S., Kaibuchi, K. and Hakoshima, T. (1998) Crystal structure of human RhoA in a dominantly active form complexed with a GTP analogue. *J Biol Chem*, **273**, 9656-9666.

96. Reinert, D.J., Jank, T., Aktories, K. and Schulz, G.E. (2005) Structural basis for the function of Clostridium difficile toxin B. *Journal of molecular biology*, **351**, 973-981.

97. Jank, T., Giesemann, T. and Aktories, K. (2007) Rho-glucosylating Clostridium difficile toxins A and B: new insights into structure and function. *Glycobiology*, **17**, 15R-22R.

98. Stubbs, S., Rupnik, M., Gibert, M., Brazier, J., Duerden, B. and Popoff, M. (2000) Production of actin-specific ADP-ribosyltransferase (binary toxin) by strains of Clostridium difficile. *FEMS microbiology letters*, **186**, 307-312.

99. Perelle, S., Gibert, M., Bourlioux, P., Corthier, G. and Popoff, M.R. (1997) Production of a complete binary toxin (actin-specific ADP-ribosyltransferase) by Clostridium difficile CD196. *Infection and immunity*, **65**, 1402-1407.

100. Carter, G.P., Lyras, D., Allen, D.L., Mackin, K.E., Howarth, P.M., O'Connor, J.R. and Rood, J.I. (2007) Binary toxin production in Clostridium difficile is regulated by CdtR, a LytTR family response regulator. *Journal of bacteriology*, **189**, 7290-7301.

101. Wegner, A. and Aktories, K. (1988) ADP-ribosylated actin caps the barbed ends of actin filaments. *J Biol Chem*, **263**, 13739-13742.

102. Sundriyal, A., Roberts, A.K., Shone, C.C. and Acharya, K.R. (2009) Structural basis for substrate recognition in the enzymatic component of ADP-ribosyltransferase toxin CDTa from Clostridium difficile. *J Biol Chem*, **284**, 28713-28719.

103. Geric, B., Carman, R.J., Rupnik, M., Genheimer, C.W., Sambol, S.P., Lyerly, D.M., Gerding, D.N. and Johnson, S. (2006) Binary toxin-producing, large clostridial toxin-negative Clostridium difficile strains are enterotoxic but do not cause disease in hamsters. *The Journal of infectious diseases*, **193**, 1143-1150.

104. Johnson, S. (2009) Recurrent Clostridium difficile infection: causality and therapeutic approaches. *International journal of antimicrobial agents*, **33 Suppl 1**, S33-36.

105. O'Neill, G.L., Beaman, M.H. and Riley, T.V. (1991) Relapse versus reinfection with Clostridium difficile. *Epidemiology and infection*, **107**, 627-635.

106. Johnson, S., Adelmann, A., Clabots, C.R., Peterson, L.R. and Gerding, D.N. (1989) Recurrences of Clostridium difficile diarrhea not caused by the original infecting organism. *The Journal of infectious diseases*, **159**, 340-343.

107. Lamontagne, F., Labbe, A.C., Haeck, O., Lesur, O., Lalancette, M., Patino, C., Leblanc, M., Laverdiere, M. and Pepin, J. (2007) Impact of emergency colectomy on survival of patients with fulminant Clostridium difficile colitis during an epidemic caused by a hypervirulent strain. *Annals of surgery*, **245**, 267-272.

108. Cherifi, S., Delmee, M., Van Broeck, J., Beyer, I., Byl, B. and Mascart, G. (2006) Management of an outbreak of Clostridium difficile-associated disease among geriatric patients. *Infection control and hospital epidemiology : the official journal of the Society of Hospital Epidemiologists of America*, **27**, 1200-1205.

109. Johnson, S., Gerding, D.N., Olson, M.M., Weiler, M.D., Hughes, R.A., Clabots, C.R. and Peterson, L.R. (1990) Prospective, controlled study of vinyl glove use to interrupt Clostridium difficile nosocomial transmission. *The American journal of medicine*, **88**, 137-140.

110. Cecil, J.A. (2012) Clostridium difficile: Changing Epidemiology, Treatment and Infection Prevention Measures. *Current infectious disease reports*, **14**, 612-619.

111. Badger, V.O., Ledeboer, N.A., Graham, M.B. and Edmiston, C.E., Jr. (2012) Clostridium difficile: Epidemiology, Pathogenesis, Management, and Prevention of a Recalcitrant Healthcare-Associated Pathogen. *JPEN. Journal of parenteral and enteral nutrition*, **36**, 645-662.

112. Samore, M.H., Venkataraman, L., DeGirolami, P.C., Arbeit, R.D. and Karchmer, A.W. (1996) Clinical and molecular epidemiology of sporadic and clustered cases of nosocomial Clostridium difficile diarrhea. *The American journal of medicine*, **100**, 32-40.

113. Fawley, W.N., Underwood, S., Freeman, J., Baines, S.D., Saxton, K., Stephenson, K., Owens, R.C., Jr. and Wilcox, M.H. (2007) Efficacy of hospital cleaning agents and germicides against epidemic Clostridium difficile strains. *Infection control and hospital epidemiology : the official journal of the Society of Hospital Epidemiologists of America*, **28**, 920-925.

114. Wilcox, M.H. and Fawley, W.N. (2000) Hospital disinfectants and spore formation by Clostridium difficile. *Lancet*, **356**, 1324.

115. Wilcox, M.H., Fawley, W.N., Wigglesworth, N., Parnell, P., Verity, P. and Freeman, J. (2003) Comparison of the effect of detergent versus hypochlorite cleaning on environmental contamination and incidence of Clostridium difficile infection. *The Journal of hospital infection*, **54**, 109-114.

116. Rea, M.C., Dobson, A., O'Sullivan, O., Crispie, F., Fouhy, F., Cotter, P.D., Shanahan, F., Kiely, B., Hill, C. and Ross, R.P. (2011) Effect of broad- and narrow-spectrum antimicrobials on Clostridium difficile and microbial diversity in a model of the distal colon. *Proceedings of the National Academy of Sciences of the United States of America*, **108 Suppl 1**, 4639-4644.

117. Miyachi, Y., Imamura, S. and Niwa, Y. (1986) Anti-oxidant action of metronidazole: a possible mechanism of action in rosacea. *The British journal of dermatology*, **114**, 231-234.

118. Wong, S.S., Woo, P.C., Luk, W.K. and Yuen, K.Y. (1999) Susceptibility testing of Clostridium difficile against metronidazole and vancomycin by disk diffusion and Etest. *Diagnostic microbiology and infectious disease*, **34**, 1-6.

119. Johnson, S., Sanchez, J.L. and Gerding, D.N. (2000) Metronidazole resistance in Clostridium difficile. *Clinical infectious diseases : an official publication of the Infectious Diseases Society of America*, **31**, 625-626.

120. Pelaez, T., Cercenado, E., Alcala, L., Marin, M., Martin-Lopez, A., Martinez-Alarcon, J., Catalan, P., Sanchez-Somolinos, M. and Bouza, E. (2008) Metronidazole resistance in Clostridium difficile is heterogeneous. *Journal of clinical microbiology*, **46**, 3028-3032.

121. Zar, F.A., Bakkanagari, S.R., Moorthi, K.M. and Davis, M.B. (2007) A comparison of vancomycin and metronidazole for the treatment of Clostridium difficile-associated diarrhea, stratified by disease severity. *Clinical infectious diseases : an official publication of the Infectious Diseases Society of America*, **45**, 302-307.

122. Moellering, R.C., Jr. (2006) Vancomycin: a 50-year reassessment. *Clinical infectious diseases : an official publication of the Infectious Diseases Society of America*, **42 Suppl 1**, S3-4.

123. Dworczynski, A., Sokol, B. and Meisel-Mikolajczyk, F. (1991) Antibiotic resistance of Clostridium difficile isolates. *Cytobios*, **65**, 149-153.

124. Louie, T.J., Miller, M.A., Mullane, K.M., Weiss, K., Lentnek, A., Golan, Y., Gorbach, S., Sears, P., Shue, Y.K. and Group, O.P.T.C.S. (2011) Fidaxomicin versus vancomycin for Clostridium difficile infection. *The New England journal of medicine*, **364**, 422-431.

125. Tannock, G.W., Munro, K., Taylor, C., Lawley, B., Young, W., Byrne, B., Emery, J. and Louie, T. (2010) A new macrocyclic antibiotic, fidaxomicin (OPT-80), causes less alteration to the bowel microbiota of Clostridium difficile-infected patients than does vancomycin. *Microbiology*, **156**, 3354-3359.

126. Bartlett, J.G. (2010) Clostridium difficile: progress and challenges. *Annals of the New York Academy of Sciences*, **1213**, 62-69.

127. Bartlett, J.G. (2002) Clinical practice. Antibiotic-associated diarrhea. *The New England journal of medicine*, **346**, 334-339.

128. Merrigan, M.M., Sambol, S.P., Johnson, S. and Gerding, D.N. (2009) New approach to the management of Clostridium difficile infection: colonisation with non-toxigenic C.

difficile during daily ampicillin or ceftriaxone administration. *International journal of antimicrobial agents*, **33 Suppl 1**, S46-50.

129. Gevers, D., Knight, R., Petrosino, J.F., Huang, K., McGuire, A.L., Birren, B.W., Nelson, K.E., White, O., Methe, B.A. and Huttenhower, C. (2012) The human microbiome project: a community resource for the healthy human microbiome. *PLoS biology*, **10**, e1001377.

130. Pham, M., Lemberg, D.A. and Day, A.S. (2008) Probiotics: sorting the evidence from the myths. *The Medical journal of Australia*, **188**, 304-308.

131. Quigley, E.M. (2010) Prebiotics and probiotics; modifying and mining the microbiota. *Pharmacological research : the official journal of the Italian Pharmacological Society*, **61**, 213-218.

132. Miller, M. (2009) The fascination with probiotics for Clostridium difficile infection: lack of evidence for prophylactic or therapeutic efficacy. *Anaerobe*, **15**, 281-284.

133. Dendukuri, N., Costa, V., McGregor, M. and Brophy, J.M. (2005) Probiotic therapy for the prevention and treatment of Clostridium difficile-associated diarrhea: a systematic review. *CMAJ : Canadian Medical Association journal = journal de l'Association medicale canadienne*, **173**, 167-170.

134. Suwantarat, N. and Bobak, D.A. (2011) Current Status of Nonantibiotic and Adjunct Therapies for Clostridium difficile Infection. *Current infectious disease reports*, **13**, 21-27.

135. Thompson, I. (2008) Clostridium difficile-associated disease: update and focus on non-antibiotic strategies. *Age and ageing*, **37**, 14-18.

136. Aas, J., Gessert, C.E. and Bakken, J.S. (2003) Recurrent Clostridium difficile colitis: case series involving 18 patients treated with donor stool administered via a nasogastric tube. *Clinical infectious diseases : an official publication of the Infectious Diseases Society of America*, **36**, 580-585.

137. Rohlke, F., Surawicz, C.M. and Stollman, N. (2010) Fecal flora reconstitution for recurrent Clostridium difficile infection: results and methodology. *Journal of clinical gastroenterology*, **44**, 567-570.

138. Kelly, C.P., Pothoulakis, C., Orellana, J. and LaMont, J.T. (1992) Human colonic aspirates containing immunoglobulin A antibody to Clostridium difficile toxin A inhibit toxin A-receptor binding. *Gastroenterology*, **102**, 35-40.

139. Sanchez-Hurtado, K., Corretge, M., Mutlu, E., McIlhagger, R., Starr, J.M. and Poxton, I.R. (2008) Systemic antibody response to Clostridium difficile in colonized patients with and without symptoms and matched controls. *Journal of medical microbiology*, **57**, 717-724.

140. Warny, M., Vaerman, J.P., Avesani, V. and Delmee, M. (1994) Human antibody response to Clostridium difficile toxin A in relation to clinical course of infection. *Infection and immunity*, **62**, 384-389.

141. Kyne, L., Warny, M., Qamar, A. and Kelly, C.P. (2000) Asymptomatic carriage of Clostridium difficile and serum levels of IgG antibody against toxin A. *The New England journal of medicine*, **342**, 390-397.

142. Sougioultzis, S., Kyne, L., Drudy, D., Keates, S., Maroo, S., Pothoulakis, C., Giannasca, P.J., Lee, C.K., Warny, M., Monath, T.P. *et al.* (2005) Clostridium difficile toxoid vaccine in recurrent C. difficile-associated diarrhea. *Gastroenterology*, **128**, 764-770.

143. Wang, H., Sun, X., Zhang, Y., Li, S., Chen, K., Shi, L., Nie, W., Kumar, R., Tzipori, S., Wang, J. *et al.* (2012) A chimeric toxin vaccine protects against primary and recurrent Clostridium difficile infection. *Infection and immunity*, **80**, 2678-2688.

144. Hussack, G. and Tanha, J. (2010) Toxin-Specific Antibodies for the Treatment of Clostridium difficile: Current Status and Future Perspectives. *Toxins*, **2**, 998-1018.

145. Leung, D.Y., Kelly, C.P., Boguniewicz, M., Pothoulakis, C., LaMont, J.T. and Flores, A. (1991) Treatment with intravenously administered gamma globulin of chronic relapsing colitis induced by Clostridium difficile toxin. *The Journal of pediatrics*, **118**, 633-637.

146. Babcock, G.J., Broering, T.J., Hernandez, H.J., Mandell, R.B., Donahue, K., Boatright, N., Stack, A.M., Lowy, I., Graziano, R., Molrine, D. *et al.* (2006) Human monoclonal antibodies directed against toxins A and B prevent Clostridium difficile-induced mortality in hamsters. *Infection and immunity*, **74**, 6339-6347.

147. Taylor, C.P., Tummala, S., Molrine, D., Davidson, L., Farrell, R.J., Lembo, A., Hibberd, P.L., Lowy, I. and Kelly, C.P. (2008) Open-label, dose escalation phase I study in healthy volunteers to evaluate the safety and pharmacokinetics of a human monoclonal antibody to Clostridium difficile toxin A. *Vaccine*, **26**, 3404-3409.

148. Ivarsson, M.E., Leroux, J.C. and Castagner, B. (2012) Targeting bacterial toxins. *Angew Chem Int Ed Engl*, **51**, 4024-4045.

149. Barczak, A.K. and Hung, D.T. (2009) Productive steps toward an antimicrobial targeting virulence. *Current opinion in microbiology*, **12**, 490-496.

150. Taylor, N.S. and Bartlett, J.G. (1980) Binding of Clostridium difficile cytotoxin and vancomycin by anion-exchange resins. *The Journal of infectious diseases*, **141**, 92-97.

151. Weiss, K. (2009) Toxin-binding treatment for Clostridium difficile: a review including reports of studies with tolevamer. *International journal of antimicrobial agents*, **33**, 4-7.

152. Kurtz, C.B., Cannon, E.P., Brezzani, A., Pitruzzello, M., Dinardo, C., Rinard, E., Acheson, D.W., Fitzpatrick, R., Kelly, P., Shackett, K. *et al.* (2001) GT160-246, a toxin binding polymer for treatment of Clostridium difficile colitis. *Antimicrobial agents and chemotherapy*, **45**, 2340-2347.

153. Braunlin, W., Xu, Q., Hook, P., Fitzpatrick, R., Klinger, J.D., Burrier, R. and Kurtz, C.B. (2004) Toxin binding of tolevamer, a polyanionic drug that protects against antibiotic-associated diarrhea. *Biophysical journal*, **87**, 534-539.

154. Castagliuolo, I., LaMont, J.T., Qiu, B., Nikulasson, S.T. and Pothoulakis, C. (1996) A receptor decoy inhibits the enterotoxic effects of Clostridium difficile toxin A in rat ileum. *Gastroenterology*, **111**, 433-438.

155. Savidge, T.C., Urvil, P., Oezguen, N., Ali, K., Choudhury, A., Acharya, V., Pinchuk, I., Torres, A.G., English, R.D., Wiktorowicz, J.E. *et al.* (2011) Host S-nitrosylation inhibits clostridial small molecule-activated glucosylating toxins. *Nature medicine*, **17**, 1136-1141.

156. Gloster, T.M., Meloncelli, P., Stick, R.V., Zechel, D., Vasella, A. and Davies, G.J. (2007) Glycosidase inhibition: an assessment of the binding of 18 putative transition-state mimics. *J Am Chem Soc*, **129**, 2345-2354.

157. Jank, T., Ziegler, M.O., Schulz, G.E. and Aktories, K. (2008) Inhibition of the glucosyltransferase activity of clostridial Rho/Ras-glucosylating toxins by castanospermine. *FEBS Lett*, **582**, 2277-2282.

158. Sorg, J.A. and Sonenshein, A.L. (2010) Inhibiting the initiation of Clostridium difficile spore germination using analogs of chenodeoxycholic acid, a bile acid. *Journal of bacteriology*, **192**, 4983-4990.

159. Tam Dang, T.H., Fagan, R.P., Fairweather, N.F. and Tate, E.W. (2012) Novel inhibitors of surface layer processing in Clostridium difficile. *Bioorganic & medicinal chemistry*, **20**, 614-621.

160. Abdeen, S.J., Swett, R.J. and Feig, A.L. (2010) Peptide inhibitors targeting Clostridium difficile toxins A and B. *ACS chemical biology*, **5**, 1097-1103.

161. Koo, H.L., Garey, K.W. and Dupont, H.L. (2010) Future novel therapeutic agents for Clostridium difficile infection. *Expert Opin Investig Drugs*, **19**, 825-836.

162. Tschudin-Sutter, S., Widmer, A.F. and Perl, T.M. (2012) Clostridium difficile: novel insights on an incessantly challenging disease. *Current opinion in infectious diseases*, **25**, 405-411.

163. Kim, J., Smathers, S.A., Prasad, P., Leckerman, K.H., Coffin, S. and Zaoutis, T. (2008) Epidemiological features of Clostridium difficile-associated disease among inpatients at children's hospitals in the United States, 2001-2006. *Pediatrics*, **122**, 1266-1270.

164. Rouphael, N.G., O'Donnell, J.A., Bhatnagar, J., Lewis, F., Polgreen, P.M., Beekmann, S., Guarner, J., Killgore, G.E., Coffman, B., Campbell, J. *et al.* (2008) Clostridium difficile-associated diarrhea: an emerging threat to pregnant women. *American journal of obstetrics and gynecology*, **198**, 635 e631-636.

165. Drekonja, D.M., Butler, M., MacDonald, R., Bliss, D., Filice, G.A., Rector, T.S. and Wilt, T.J. (2011) Comparative effectiveness of Clostridium difficile treatments: a systematic review. *Annals of internal medicine*, **155**, 839-847.

166. Traynor, K. (2011) Fidaxomicin approved for C. difficile infections. *American journal of health-system pharmacy : AJHP : official journal of the American Society of Health-System Pharmacists*, **68**, 1276.

167. Davies, A.H., Roberts, A.K., Shone, C.C. and Acharya, K.R. (2011) Super toxins from a super bug: structure and function of Clostridium difficile toxins. *Biochem J*, **436**, 517-526.

168. Hussack, G., Arbabi-Ghahroudi, M., van Faassen, H., Songer, J.G., Ng, K.K., MacKenzie, R. and Tanha, J. (2011) Neutralization of Clostridium difficile toxin A with single-domain antibodies targeting the cell receptor binding domain. *J Biol Chem*, **286**, 8961-8976.

169. Kehoe, J.W. and Kay, B.K. (2005) Filamentous phage display in the new millennium. *Chem Rev*, **105**, 4056-4072.

170. Sidhu, S.S., Fairbrother, W.J. and Deshayes, K. (2003) Exploring protein-protein interactions with phage display. *Chembiochem*, **4**, 14-25.

171. Efimov, V.P., Nepluev, I.V. and Mesyanzhinov, V.V. (1995) Bacteriophage T4 as a surface display vector. *Virus Genes*, **10**, 173-177.

172. Smith, G.P. (1985) Filamentous fusion phage: novel expression vectors that display cloned antigens on the virion surface. *Science*, **228**, 1315-1317.

173. Smith, G.P. and Petrenko, V.A. (1997) Phage Display. *Chem Rev*, **97**, 391-410.

174. Beer, M. and Liu, C.Q. (2012) Panning of a Phage Display Library against a Synthetic Capsule for Peptide Ligands That Bind to the Native Capsule of Bacillus anthracis. *PLoS One*, **7**, e45472.

175. Mandal, K., Uppalapati, M., Ault-Riche, D., Kenney, J., Lowitz, J., Sidhu, S.S. and Kent, S.B. (2012) Chemical synthesis and X-ray structure of a heterochiral {D-protein antagonist plus vascular endothelial growth factor} protein complex by racemic crystallography. *Proc Natl Acad Sci U S A*, **109**, 14779-14784.

176. Domenech, R., Martinez-Rodriguez, S., Velazquez-Campoy, A. and Neira, J.L. (2012) Peptides as Inhibitors of the First Phosphorylation Step of the Streptomyces coelicolor Phosphoenolpyruvate: Sugar Phosphotransferase System. *Biochemistry*, **51**, 7393-7402.

177. Geyer, C.R., McCafferty, J., Dubel, S., Bradbury, A.R. and Sidhu, S.S. (2012) Recombinant antibodies and in vitro selection technologies. *Methods Mol Biol*, **901**, 11-32.

178. Fukuda, M.N. (2012) Peptide-displaying phage technology in glycobiology. *Glycobiology*, **22**, 318-325.

179. Castel, G., Chteoui, M., Heyd, B. and Tordo, N. (2011) Phage display of combinatorial peptide libraries: application to antiviral research. *Molecules*, **16**, 3499-3518.

180. Basha, S., Rai, P., Poon, V., Saraph, A., Gujraty, K., Go, M.Y., Sadacharan, S., Frost, M., Mogridge, J. and Kane, R.S. (2006) Polyvalent inhibitors of anthrax toxin that target host receptors. *Proc Natl Acad Sci U S A*, **103**, 13509-13513.

181. Houshmand, H., Froman, G. and Magnusson, G. (1999) Use of bacteriophage T7 displayed peptides for determination of monoclonal antibody specificity and biosensor analysis of the binding reaction. *Anal Biochem*, **268**, 363-370.

182. Paschke, M. (2006) Phage display systems and their applications. *Appl Microbiol Biotechnol*, **70**, 2-11.

183. Rakonjac, J., Bennett, N.J., Spagnuolo, J., Gagic, D. and Russel, M. (2011) Filamentous bacteriophage: biology, phage display and nanotechnology applications. *Current issues in molecular biology*, **13**, 51-76.

184. Kerzmann, A. (2009), Indiana University, Bloomington, IN.

185. Laughlin, M.R., Petit, W.A., Jr., Dizon, J.M., Shulman, R.G. and Barrett, E.J. (1988) NMR measurements of in vivo myocardial glycogen metabolism. *J Biol Chem*, **263**, 2285-2291.

186. Belyi, Y. and Aktories, K. (2010) Bacterial toxin and effector glycosyltransferases. *Biochim Biophys Acta*, **1800**, 134-143.

187. Gujraty, K., Sadacharan, S., Frost, M., Poon, V., Kane, R.S. and Mogridge, J. (2005) Functional characterization of peptide-based anthrax toxin inhibitors. *Mol Pharm*, **2**, 367-372.

188. Abedi, M.R., Caponigro, G. and Kamb, A. (1998) Green fluorescent protein as a scaffold for intracellular presentation of peptides. *Nucleic Acids Res*, **26**, 623-630.

189. Kobayashi, T., Morone, N., Kashiyama, T., Oyamada, H., Kurebayashi, N. and Murayama, T. (2008) Engineering a novel multifunctional green fluorescent protein tag for a wide variety of protein research. *PLoS ONE*, **3**, e3822.

190. Hart, M.J., Eva, A., Zangrilli, D., Aaronson, S.A., Evans, T., Cerione, R.A. and Zheng, Y. (1994) Cellular transformation and guanine nucleotide exchange activity are catalyzed by a common domain on the dbl oncogene product. *J Biol Chem*, **269**, 62-65.

191. Narindrasorasak, S., Lowery, D., Gonzalez-DeWhitt, P., Poorman, R.A., Greenberg, B. and Kisilevsky, R. (1991) High affinity interactions between the Alzheimer's beta-

amyloid precursor proteins and the basement membrane form of heparan sulfate proteoglycan. *J Biol Chem*, **266**, 12878-12883.

192. Yang, G., Zhou, B., Wang, J., He, X., Sun, X., Nie, W., Tzipori, S. and Feng, H. (2008) Expression of recombinant Clostridium difficile toxin A and B in Bacillus megaterium. *BMC Microbiol*, **8**, 192.

193. Gosselin, S., Alhussaini, M., Streiff, M.B., Takabayashi, K. and Palcic, M.M. (1994) A continuous spectrophotometric assay for glycosyltransferases. *Anal Biochem*, **220**, 92-97.

194. Schellhammer, I. and Rarey, M. (2004) FlexX-Scan: fast, structure-based virtual screening. *Proteins*, **57**, 504-517.

195. Gohlke, H., Hendlich, M. and Klebe, G. (2000) Knowledge-based scoring function to predict protein-ligand interactions. *Journal of molecular biology*, **295**, 337-356.

196. Pettersen, E.F., Goddard, T.D., Huang, C.C., Couch, G.S., Greenblatt, D.M., Meng, E.C. and Ferrin, T.E. (2004) UCSF Chimera--a visualization system for exploratory research and analysis. *J Comput Chem*, **25**, 1605-1612.

197. Wagner, B.M., Smith, R.A., Coles, P.J., Copp, L.J., Ernest, M.J. and Krantz, A. (1994) In vivo inhibition of cathepsin B by peptidyl (acyloxy)methyl ketones. *Journal of medicinal chemistry*, **37**, 1833-1840.

198. Wyrembak, P.N., Babaoglu, K., Pelto, R.B., Shoichet, B.K. and Pratt, R.F. (2007) O-aryloxycarbonyl hydroxamates: new beta-lactamase inhibitors that cross-link the active site. *J Am Chem Soc*, **129**, 9548-9549.

199. Bause, E. (1983) Active-site-directed inhibition of asparagine N-glycosyltransferases with epoxy-peptide derivatives. *Biochem J*, **209**, 323-330.

200. Cohen, M.S., Zhang, C., Shokat, K.M. and Taunton, J. (2005) Structural bioinformatics-based design of selective, irreversible kinase inhibitors. *Science*, **308**, 1318-1321.

201. Lynas, J.F., Martin, S.L. and Walker, B. (2001) Synthesis and kinetic evaluation of peptide alpha-keto-beta-aldehyde-based inhibitors of trypsin-like serine proteases. *The Journal of pharmacy and pharmacology*, **53**, 473-480.

202. Tipparaju, S.K., Joyasawal, S., Forrester, S., Mulhearn, D.C., Pegan, S., Johnson, M.E., Mesecar, A.D. and Kozikowski, A.P. (2008) Design and synthesis of 2-pyridones as novel inhibitors of the Bacillus anthracis enoyl-ACP reductase. *Bioorg Med Chem Lett*, **18**, 3565-3569.

203. Kisselev, A.F., van der Linden, W.A. and Overkleeft, H.S. (2012) Proteasome inhibitors: an expanding army attacking a unique target. *Chemistry & biology*, **19**, 99-115.

204. Lu, R.C., Moo, L. and Wong, A.G. (1986) Both the 25-kDa and 50-kDa domains in myosin subfragment 1 are close to the reactive thiols. *Proc Natl Acad Sci U S A*, **83**, 6392-6396.

205. Hassan, A.Q. and Stubbe, J. (2008) Mapping the subunit interface of ribonucleotide reductase (RNR) using photo cross-linking. *Bioorg Med Chem Lett*, **18**, 5923-5925.

206. Laufen, T., Mayer, M.P., Beisel, C., Klostermeier, D., Mogk, A., Reinstein, J. and Bukau, B. (1999) Mechanism of regulation of hsp70 chaperones by DnaJ cochaperones. *Proc Natl Acad Sci U S A*, **96**, 5452-5457.

207. Dorman, G. and Prestwich, G.D. (1994) Benzophenone photophores in biochemistry. *Biochemistry*, **33**, 5661-5673.

208. Leach, A.R. and Hann, M.M. (2000) The in silico world of virtual libraries. *Drug discovery today*, **5**, 326-336.

209. Kitchen, D.B., Decornez, H., Furr, J.R. and Bajorath, J. (2004) Docking and scoring in virtual screening for drug discovery: methods and applications. *Nature reviews. Drug discovery*, **3**, 935-949.

210. Rutenber, E., Fauman, E.B., Keenan, R.J., Fong, S., Furth, P.S., Ortiz de Montellano, P.R., Meng, E., Kuntz, I.D., DeCamp, D.L., Salto, R. *et al.* (1993) Structure of a non-peptide inhibitor complexed with HIV-1 protease. Developing a cycle of structure-based drug design. *J Biol Chem*, **268**, 15343-15346.

211. Bodian, D.L., Yamasaki, R.B., Buswell, R.L., Stearns, J.F., White, J.M. and Kuntz, I.D. (1993) Inhibition of the fusion-inducing conformational change of influenza hemagglutinin by benzoquinones and hydroquinones. *Biochemistry*, **32**, 2967-2978.

212. Chen, D., Misra, M., Sower, L., Peterson, J.W., Kellogg, G.E. and Schein, C.H. (2008) Novel inhibitors of anthrax edema factor. *Bioorg Med Chem*, **16**, 7225-7233.

213. Bause, E., Wesemann, M., Bartoschek, A. and Breuer, W. (1997) Epoxyethylglycyl peptides as inhibitors of oligosaccharyltransferase: double-labelling of the active site. *Biochem J*, **322 ( Pt 1)**, 95-102.

214. Sinz, A. (2006) Chemical cross-linking and mass spectrometry to map three-dimensional protein structures and protein-protein interactions. *Mass Spectrom Rev*, **25**, 663-682.

215. Trakselis, M.A., Alley, S.C. and Ishmael, F.T. (2005) Identification and mapping of protein-protein interactions by a combination of cross-linking, cleavage, and proteomics. *Bioconjugate chemistry*, **16**, 741-750.

216. Jin Lee, Y. (2008) Mass spectrometric analysis of cross-linking sites for the structure of proteins and protein complexes. *Mol Biosyst*, **4**, 816-823.

217. Marshall, A.G. and Hendrickson, C.L. (2008) High-resolution mass spectrometers. *Annual review of analytical chemistry*, **1**, 579-599.

218. Bogdanov, B. and Smith, R.D. (2005) Proteomics by FTICR mass spectrometry: top down and bottom up. *Mass Spectrom Rev*, **24**, 168-200.

219. Park, Y. and Lebrilla, C.B. (2005) Application of Fourier transform ion cyclotron resonance mass spectrometry to oligosaccharides. *Mass Spectrom Rev*, **24**, 232-264.

220. Almeida, A.J. and Souto, E. (2007) Solid lipid nanoparticles as a drug delivery system for peptides and proteins. *Advanced drug delivery reviews*, **59**, 478-490.

221. Gallarate, M., Trotta, M., Battaglia, L. and Chirio, D. (2009) Preparation of solid lipid nanoparticles from W/O/W emulsions: preliminary studies on insulin encapsulation. *Journal of microencapsulation*, **26**, 394-402.

222. Eiamtrakarn, S., Itoh, Y., Kishimoto, J., Yoshikawa, Y., Shibata, N., Murakami, M. and Takada, K. (2002) Gastrointestinal mucoadhesive patch system (GI-MAPS) for oral administration of G-CSF, a model protein. *Biomaterials*, **23**, 145-152.

223. Sakuma, S., Hayashi, M. and Akashi, M. (2001) Design of nanoparticles composed of graft copolymers for oral peptide delivery. *Advanced drug delivery reviews*, **47**, 21-37.

224. Lowman, A.M., Morishita, M., Kajita, M., Nagai, T. and Peppas, N.A. (1999) Oral delivery of insulin using pH-responsive complexation gels. *Journal of pharmaceutical sciences*, **88**, 933-937.

225. Saffran, M., Kumar, G.S., Savariar, C., Burnham, J.C., Williams, F. and Neckers, D.C. (1986) A new approach to the oral administration of insulin and other peptide drugs. *Science*, **233**, 1081-1084.

226. Van den Mooter, G., Maris, B., Samyn, C., Augustijns, P. and Kinget, R. (1997) Use of azo polymers for colon-specific drug delivery. *Journal of pharmaceutical sciences*, **86**, 1321-1327.

227. Alves-Rosa, F., Stanganelli, C., Cabrera, J., van Rooijen, N., Palermo, M.S. and Isturiz, M.A. (2000) Treatment with liposome-encapsulated clodronate as a new strategic approach in the management of immune thrombocytopenic purpura in a mouse model. *Blood*, **96**, 2834-2840.

228. Pissinati, R. and Oliveira, W.P. (2003) Enteric coating of soft gelatin capsules by spouted bed: effect of operating conditions on coating efficiency and on product quality. *European journal of pharmaceutics and biopharmaceutics : official journal of Arbeitsgemeinschaft fur Pharmazeutische Verfahrenstechnik e.V*, **55**, 313-321.

229. Boddupalli, B.M., Mohammed, Z.N., Nath, R.A. and Banji, D. (2010) Mucoadhesive drug delivery system: An overview. *Journal of advanced pharmaceutical technology & research*, **1**, 381-387.

230. Wani, A., Muthuswamy, E., Savithra, G.H., Mao, G., Brock, S. and Oupicky, D. (2012) Surface functionalization of mesoporous silica nanoparticles controls loading and release behavior of mitoxantrone. *Pharmaceutical research*, **29**, 2407-2418.

231. Thanos, C.G., Liu, Z., Reineke, J., Edwards, E. and Mathiowitz, E. (2003) Improving relative bioavailability of dicumarol by reducing particle size and adding the adhesive poly(fumaric-co-sebacic) anhydride. *Pharmaceutical research*, **20**, 1093-1100.

232. Loo, V.G., Poirier, L., Miller, M.A., Oughton, M., Libman, M.D., Michaud, S., Bourgault, A.M., Nguyen, T., Frenette, C., Kelly, M. *et al.* (2005) A predominantly

clonal multi-institutional outbreak of Clostridium difficile-associated diarrhea with high morbidity and mortality. *The New England journal of medicine*, **353**, 2442-2449.

233. Muto, C.A., Pokrywka, M., Shutt, K., Mendelsohn, A.B., Nouri, K., Posey, K., Roberts, T., Croyle, K., Krystofiak, S., Patel-Brown, S. *et al.* (2005) A large outbreak of Clostridium difficile-associated disease with an unexpected proportion of deaths and colectomies at a teaching hospital following increased fluoroquinolone use. *Infection control and hospital epidemiology : the official journal of the Society of Hospital Epidemiologists of America*, **26**, 273-280.

234. McDonald, L.C., Killgore, G.E., Thompson, A., Owens, R.C., Jr., Kazakova, S.V., Sambol, S.P., Johnson, S. and Gerding, D.N. (2005) An epidemic, toxin gene-variant strain of Clostridium difficile. *The New England journal of medicine*, **353**, 2433-2441.

235. Olling, A., Seehase, S., Minton, N.P., Tatge, H., Schroter, S., Kohlscheen, S., Pich, A., Just, I. and Gerhard, R. (2012) Release of TcdA and TcdB from Clostridium difficile cdi 630 is not affected by functional inactivation of the tcdE gene. *Microbial pathogenesis*, **52**, 92-100.

236. Govind, R., Vediyappan, G., Rolfe, R.D. and Fralick, J.A. (2006) Evidence that Clostridium difficile TcdC is a membrane-associated protein. *Journal of bacteriology*, **188**, 3716-3720.

237. Matamouros, S., England, P. and Dupuy, B. (2007) Clostridium difficile toxin expression is inhibited by the novel regulator TcdC. *Molecular microbiology*, **64**, 1274-1288.

238. Merrigan, M., Venugopal, A., Mallozzi, M., Roxas, B., Viswanathan, V.K., Johnson, S., Gerding, D.N. and Vedantam, G. (2010) Human hypervirulent Clostridium difficile

strains exhibit increased sporulation as well as robust toxin production. *Journal of bacteriology*, **192**, 4904-4911.

239. Carter, G.P., Douce, G.R., Govind, R., Howarth, P.M., Mackin, K.E., Spencer, J., Buckley, A.M., Antunes, A., Kotsanas, D., Jenkin, G.A. *et al.* (2011) The anti-sigma factor TcdC modulates hypervirulence in an epidemic BI/NAP1/027 clinical isolate of Clostridium difficile. *PLoS pathogens*, **7**, e1002317.

240. Bakker, D., Smits, W.K., Kuijper, E.J. and Corver, J. (2012) TcdC Does Not Significantly Repress Toxin Expression in Clostridium difficile 630DeltaErm. *PloS one*, **7**, e43247.

241. Nielsen, H., Engelbrecht, J., Brunak, S. and von Heijne, G. (1997) Identification of prokaryotic and eukaryotic signal peptides and prediction of their cleavage sites. *Protein engineering*, **10**, 1-6.

242. Petersen, T.N., Brunak, S., von Heijne, G. and Nielsen, H. (2011) SignalP 4.0: discriminating signal peptides from transmembrane regions. *Nature methods*, **8**, 785-786.

243. Theobald, D.L., Mitton-Fry, R.M. and Wuttke, D.S. (2003) Nucleic acid recognition by OB-fold proteins. *Annual review of biophysics and biomolecular structure*, **32**, 115-133.

244. O'Shea, E.K., Klemm, J.D., Kim, P.S. and Alber, T. (1991) X-ray structure of the GCN4 leucine zipper, a two-stranded, parallel coiled coil. *Science*, **254**, 539-544.

245. Tao, X., Boyd, J. and Murphy, J.R. (1992) Specific binding of the diphtheria tox regulatory element DtxR to the tox operator requires divalent heavy metal ions and a 9-base-pair interrupted palindromic sequence. *Proceedings of the National Academy of Sciences of the United States of America*, **89**, 5897-5901.

246. Hughes, K.T. and Mathee, K. (1998) The anti-sigma factors. *Annual review of microbiology*, **52**, 231-286.

247. Salim, N.N., Faner, M.A., Philip, J.A. and Feig, A.L. (2012) Requirement of upstream Hfq-binding (ARN)x elements in glmS and the Hfq C-terminal region for GlmS upregulation by sRNAs GlmZ and GlmY. *Nucleic acids research*, **40**, 8021-8032.

248. Goldenberg, S.D. and French, G.L. (2011) Lack of association of tcdC type and binary toxin status with disease severity and outcome in toxigenic Clostridium difficile. *The Journal of infection*, **62**, 355-362.

249. MacCannell, D.R., Louie, T.J., Gregson, D.B., Laverdiere, M., Labbe, A.C., Laing, F. and Henwick, S. (2006) Molecular analysis of Clostridium difficile PCR ribotype 027 isolates from Eastern and Western Canada. *Journal of clinical microbiology*, **44**, 2147-2152.

250. Helmann, J.D. (1999) Anti-sigma factors. *Current opinion in microbiology*, **2**, 135-141.

251. Campbell, E.A., Tupy, J.L., Gruber, T.M., Wang, S., Sharp, M.M., Gross, C.A. and Darst, S.A. (2003) Crystal structure of Escherichia coli sigmaE with the cytoplasmic domain of its anti-sigma RseA. *Molecular cell*, **11**, 1067-1078.

252. Jordan, S., Hutchings, M.I. and Mascher, T. (2008) Cell envelope stress response in Gram-positive bacteria. *FEMS microbiology reviews*, **32**, 107-146.

253. Hofmann, N., Wurm, R. and Wagner, R. (2011) The E. coli anti-sigma factor Rsd: studies on the specificity and regulation of its expression. *PloS one*, **6**, e19235.

254. Helmann, J.D. (2002) The extracytoplasmic function (ECF) sigma factors. *Advances in microbial physiology*, **46**, 47-110.

255. Bashyam, M.D. and Hasnain, S.E. (2004) The extracytoplasmic function sigma factors: role in bacterial pathogenesis. *Infection, genetics and evolution : journal of molecular epidemiology and evolutionary genetics in infectious diseases*, **4**, 301-308.

256. Miernyk, J.A. and Thelen, J.J. (2008) Biochemical approaches for discovering protein-protein interactions. *The Plant journal : for cell and molecular biology*, **53**, 597-609.

257. Heinemeyer, J., Lewejohann, D. and Braun, H.P. (2007) Blue-native gel electrophoresis for the characterization of protein complexes in plants. *Methods in molecular biology*, **355**, 343-352.

258. Drescher, D.G., Ramakrishnan, N.A. and Drescher, M.J. (2009) Surface plasmon resonance (SPR) analysis of binding interactions of proteins in inner-ear sensory epithelia. *Methods in molecular biology*, **493**, 323-343.

259. Tang, X. and Bruce, J.E. (2009) Chemical cross-linking for protein-protein interaction studies. *Methods in molecular biology*, **492**, 283-293.

260. Chavez, J.D., Liu, N.L. and Bruce, J.E. (2011) Quantification of protein-protein interactions with chemical cross-linking and mass spectrometry. *Journal of proteome research*, **10**, 1528-1537.

261. Chacko, A.R., Arifullah, M., Sastri, N.P., Jeyakanthan, J., Ueno, G., Sekar, K., Read, R.J., Dodson, E.J., Rao, D.C. and Suguna, K. (2011) Novel pentameric structure of the diarrhea-inducing region of the rotavirus enterotoxigenic protein NSP4. *Journal of virology*, **85**, 12721-12732.

262. Basi, N.S. and Rebois, R.V. (1997) Rate zonal sedimentation of proteins in one hour or less. *Analytical biochemistry*, **251**, 103-109.

263. Prossnitz, E., Nikaido, K., Ulbrich, S.J. and Ames, G.F. (1988) Formaldehyde and photoactivatable cross-linking of the periplasmic binding protein to a membrane component of the histidine transport system of Salmonella typhimurium. *J Biol Chem*, **263**, 17917-17920.

264. D'Ulisse, V., Fagioli, M., Ghelardini, P. and Paolozzi, L. (2007) Three functional subdomains of the Escherichia coli FtsQ protein are involved in its interaction with the other division proteins. *Microbiology*, **153**, 124-138.

265. Skare, J.T., Ahmer, B.M., Seachord, C.L., Darveau, R.P. and Postle, K. (1993) Energy transduction between membranes. TonB, a cytoplasmic membrane protein, can be chemically cross-linked in vivo to the outer membrane receptor FepA. *J Biol Chem*, **268**, 16302-16308.

266. Layh-Schmitt, G., Podtelejnikov, A. and Mann, M. (2000) Proteins complexed to the P1 adhesin of Mycoplasma pneumoniae. *Microbiology*, **146 ( Pt 3)**, 741-747.

267. Sharma, U.K. and Chatterji, D. (2008) Differential mechanisms of binding of anti-sigma factors Escherichia coli Rsd and bacteriophage T4 AsiA to E. coli RNA polymerase lead to diverse physiological consequences. *Journal of bacteriology*, **190**, 3434-3443.

268. Pineda, M., Gregory, B.D., Szczypinski, B., Baxter, K.R., Hochschild, A., Miller, E.S. and Hinton, D.M. (2004) A family of anti-sigma70 proteins in T4-type phages and bacteria that are similar to AsiA, a Transcription inhibitor and co-activator of bacteriophage T4. *Journal of molecular biology*, **344**, 1183-1197.

269. Ades, S.E. (2004) Control of the alternative sigma factor sigmaE in Escherichia coli. *Current opinion in microbiology*, **7**, 157-162.

270. Kovacikova, G. and Skorupski, K. (2002) The alternative sigma factor sigma(E) plays an important role in intestinal survival and virulence in Vibrio cholerae. *Infection and immunity*, **70**, 5355-5362.

271. Manganelli, R., Voskuil, M.I., Schoolnik, G.K. and Smith, I. (2001) The Mycobacterium tuberculosis ECF sigma factor sigmaE: role in global gene expression and survival in macrophages. *Molecular microbiology*, **41**, 423-437.

272. Shaw, L.N., Lindholm, C., Prajsnar, T.K., Miller, H.K., Brown, M.C., Golonka, E., Stewart, G.C., Tarkowski, A. and Potempa, J. (2008) Identification and characterization of sigma, a novel component of the Staphylococcus aureus stress and virulence responses. *PloS one*, **3**, e3844.

273. Ho, T.D. and Ellermeier, C.D. (2011) PrsW is required for colonization, resistance to antimicrobial peptides, and expression of extracytoplasmic function sigma factors in Clostridium difficile. *Infection and immunity*, **79**, 3229-3238.

274. Alba, B.M., Leeds, J.A., Onufryk, C., Lu, C.Z. and Gross, C.A. (2002) DegS and YaeL participate sequentially in the cleavage of RseA to activate the sigma(E)-dependent extracytoplasmic stress response. *Genes & development*, **16**, 2156-2168.

275. Kanehara, K., Ito, K. and Akiyama, Y. (2002) YaeL (EcfE) activates the sigma(E) pathway of stress response through a site-2 cleavage of anti-sigma(E), RseA. *Genes & development*, **16**, 2147-2155.

276. Lamichhane, T.N., Abeydeera, N.D., Duc, A.C., Cunningham, P.R. and Chow, C.S. (2011) Selection of peptides targeting helix 31 of bacterial 16S ribosomal RNA by screening M13 phage-display libraries. *Molecules*, **16**, 1211-1239.

277. Guzman, L.M., Belin, D., Carson, M.J. and Beckwith, J. (1995) Tight regulation, modulation, and high-level expression by vectors containing the arabinose PBAD promoter. *Journal of bacteriology*, **177**, 4121-4130.

278. Majdalani, N., Cunning, C., Sledjeski, D., Elliott, T. and Gottesman, S. (1998) DsrA RNA regulates translation of RpoS message by an anti-antisense mechanism, independent of its action as an antisilencer of transcription. *Proceedings of the National Academy of Sciences of the United States of America*, **95**, 12462-12467.

# ABSTRACT

## DEVELOPMENT OF PEPTIDE INHIBITORS TARGETING *CLOSTRIDIUM DIFFICILE* TOXINS A/B AND CHARACTERIZING THE REGULATORY ROLE OF A PUTATIVE NEGATIVE REGULATOR TCDC IN *CLOSTRIDIUM DIFFICILE* TOXIN GENE EXPRESSION

by

**SANOFAR J. ABDEEN**

**May 2013**

**Advisor:** Prof. Andrew L. Feig

**Major:** Chemistry (biochemistry)

**Degree:** Doctor of Philosophy

*Clostridium difficile* infections cause one of the most common and vital hospital-acquired diseases often associated with broad-spectrum antibiotic usage. TcdA and TcdB are the key virulence factors involved in major patho-physiology. While standard antibiotics provide some respite, due to the high relapse rates and the emergence of more severe disease presentations, antibiotics alone have often proven to be suboptimal. Therefore there is a desperate need to develop an effective non-antimicrobial therapeutics. Part of this work focuses on identification and further characterization of peptide therapeutic that target the major virulence factor TcdA/TcdB. Towards development of mechanistic-based anti-toxin agent, phage display was used to identify peptides that bind to the catalytic domain of *C. difficile* Toxin A. Characterization of the binding and inhibitory activity revealed that the lack of parent peptide ability to inhibit the cells *in vivo*. Further derivatization of above parent peptides in to irreversible binders

lead to protects cells *in vivo*. Mass spectroscopy approaches revealed the peptide inhibition was mainly due to cross-linking of modified peptide in to key catalytic residues in active site. While there are still several steps required to further explore in terms of the stability of these compounds, agents like these could be potentially used prophylactically to avoid extensive cellular damage during treatment with broad spectrum antibiotics or in populations prone to CDI.

The other area, focused on this thesis, is identification of the functional role of a negative regulator (TcdC) involved in toxin gene expression. In this work, we used a variety of biochemical and genetic approaches and characterized TcdC is not repressor instead acts as an Extra Cytoplasmic Class (ECF) anti-sigma factor and was able to propose a new mechanistic model regarding the regulatory role of TcdC. As well as here we have successfully developed GFP-based reporter system which has a potential to be an adaptable tool for investigating fine details on toxin genes tuning. Being able to adopt in host environment is vital for survival and propagation of a pathogenic bacteria. Thus, exploring the regulatory nodes on PaLoc gene expression can be lead to exploit potential therapeutic opportunities hidden within such systems.

# AUTOBIOGRAPHICAL STATEMENT

## SANOFAR J ABDEEN

**Education**

Ph.D. in Chemistry (Major: Biological chemistry), Dec 2012
Department of Chemistry, Wayne State University, Detroit

Bachelor of Science (B.Sc.), Magna cum Laude in Chemistry, May 2005
University of Colombo, Colombo, Sri Lanka

**Publications:**

1. Abdeen, S. J., Swett, R. J., and Feig, A. L. (2010) Peptide inhibitors targeting *Clostridium difficile* toxins A and B, *ACS Chem Biol 5*, 1097-1103.

2. Manuscript submitted:
(Abdeen, S. J., Kern,S. M., Swett, R. J., and Feig, A. L.) : Rational design of an irreversible inhibitor of *Clostridium difficile* virulence factors TcdA and TcdB

3. Manuscript in preparation:
(Abdeen, S. J. and Feig, A. L.) *Clostridium difficile* toxin gene negative regulator TcdC: a potential candidate for regulated transmembrane proteolysis (RIP) pathway

Provisional patent pending
"Peptide inhibitors for inhibition of *Clostridium difficile* toxins", Feig, A. L. (PI), Abdeen, S. J., Kern, S. M., and Swett, R. J.- 2066728.00075; 11-1069

**Selected Presentations:**

Swett, R.J; Abdeen, S. J; Andrés Cisneros and Feig, A. L. Investigation of peptide inhibitors of *Clostridium difficile* Toxin B: Differentiating between mechanisms by computational methods, functionalizing to irreversibility. Poster presented at the ACS National Meeting & Expo, Philadelphia PA, August 2012

Swett, R.J; Abdeen, S. J; Andrés Cisneros and Feig, A. L. Investigation of peptide inhibitors of *Clostridium difficile* Toxin B: Differentiating between mechanisms by computational methods. Poster presented at the ACS National Meeting & Expo, San Diego CA, March 2012

Abdeen, S. J; Swett, R.J and Feig, A. L.; "Peptide inhibitors targeting *Clostridium difficile* toxins A and B". The 12th Annual Graduate Symposium, Wayne State University, Detroit, MI, 2010 – poster presentation

Abdeen, S. J; Swett, R.J and Feig, A. L.; "Identification of peptide inhibitors for *Clostridium difficile* toxins". The 11th Annual Graduate Symposium, Wayne State University, Detroit, MI, 2009 – poster presentation